SEP
SECRETARÍA DE EDUCACIÓN PÚBLICA

Instituto Politécnico Nacional
"La Técnica al Servicio de la Patria"

ISSN: 1870-4069

RCS

Research in Computing Science

Vol.67

Advances in Computing Science

E. A. Santos Camacho,
J. C. Chimal Eguía,
L. Cabrera Rivera,
E. Castillo Montiel, (Eds.)

Advances in Computing Science

Research in Computing Science

Series Editorial Board

Comité Editorial de la Serie

Editors-in-Chief:

Editores en Jefe

Grigori Sidorov (Mexico)
Gerhard Ritter (USA)
Jean Serra (France)
Ulises Cortés (Spain)

Associate Editors:

Editores Asociados

Jesús Angulo (France)
Jihad El-Sana (Israel)
Jesús Figueroa (Mexico)
Alexander Gelbukh (Russia)
Ioannis Kakadiaris (USA)
Serguei Levachkine (Russia)
Petros Maragos (Greece)
Julian Padget (UK)
Mateo Valero (Spain)

Editorial Coordination:

Coordinación Editorial

Socorro Méndez Lemus

Formatting:

Formación

Evelia Araceli Santos Camacho
Juan Carlos Chimal Eguía
Erandi Castillo Montiel
Imelda Escamilla Bouchan
Julio César Rangel Reyes
Víctor Antonio Ruiz Ibáñez
Rodolfo Navarro Zayas
Daniel Jimenéz Alcantar
Edwin Alan Moedano Cardiel
Luis Cabrera Rivera
Vladimir Luna Soto
Iliac Huerta Trujillo
Blanca Cecilia López Ramírez
Rodrigo Gabino Ramírez Moreno
Miguel Márquez Molina
Juan Francisco Islas Austria
Marco Hugo Reyes Larios

Research in Computing Science es una publicación trimestral, de circulación internacional, editada por el Centro de Investigación en Computación del IPN, para dar a conocer los avances de investigación científica y desarrollo tecnológico de la comunidad científica internacional. **Volumen 67,** Noviembre, 2013. Tiraje: 500 ejemplares. *Certificado de Reserva de Derechos al Uso Exclusivo del Título* No. : 04-2005-121511550100-102, expedido por el Instituto Nacional de Derecho de Autor. *Certificado de Licitud de Título* No. 12897, *Certificado de licitud de Contenido* No. 10470, expedidos por la Comisión Calificadora de Publicaciones y Revistas Ilustradas. El contenido de los artículos es responsabilidad exclusiva de sus respectivos autores.

Queda prohibida la reproducción total o parcial, por cualquier medio, sin el permiso expreso del editor, excepto para uso personal o de estudio haciendo cita explícita en la primera página de cada documento.

Impreso en la Ciudad de México, en los Talleres Gráficos del IPN – Dirección de Publicaciones, Tres Guerras 27, Centro Histórico, México, D.F. Distribuida por el Centro de Investigación en Computación, Av. Juan de Dios Bátiz S/N, Esq. Av. Miguel Othón de Mendizábal, Col. Nueva Industrial Vallejo, C.P. 07738, México, D.F. Tel. 57 29 60 00, ext. 56571.

Editor responsable: *Grigori Sidorov, RFC SIGR651028L69*

Research in Computing Science is published by the Center for Computing Research of IPN. **Volume 67**, November, 2013. Printing 500. The authors are responsible for the contents of their articles.

All rights reserved. No part of this publication may be reproduced, stored in a retrieval system, or transmitted, in any form or by any means, electronic, mechanical, photocopying, recording or otherwise, without prior permission of Centre for Computing Research.

Printed in Mexico City, in the IPN Graphic Workshop – Publication Office.

Volume 67
Volumen 67

Advances in Computing Science

Editores del volumen:
Volume Editors

Evelia Araceli Santos Camacho,
Juan Carlos Chimal Eguía,
Luis Cabrera Rivera,
Erandi Castillo Montiel, (Eds.)

Instituto Politécnico Nacional, Centro de Investigación en Computación
México 2013

ISSN: 1870-4069

Copyright © Instituto Politécnico Nacional 2013

Instituto Politécnico Nacional (IPN)
Centro de Investigación en Computación (CIC)
Av. Juan de Dios Bátiz s/n esq. M. Othón de Mendizábal
Unidad Profesional "Adolfo López Mateos", Zacatenco
07738, México D.F., México

http://www.ipn.mx
http://www.cic.ipn.mx

The editors and the publisher of this journal have made their best effort in preparing this special issue, but make no warranty of any kind, expressed or implied, with regard to the information contained in this volume.

All rights reserved. No part of this publication may be reproduced, stored on a retrieval system or transmitted, in any form or by any means, including electronic, mechanical, photocopying, recording, or otherwise, without prior permission of the Instituto Politécnico Nacional, except for personal or classroom use provided that copies bear the full citation notice provided on the first page of each paper.

Indexed in LATINDEX and Periodica / Indexada en LATINDEX y Periódica

Printing: 500 / Tiraje: 500

Printed in Mexico / Impreso en México

Preface

The purpose of this volume is to present the most recent advance in selected areas of Computer Science, The works included in this volume were carefully selected by the editors on the basis of the blind reviewing process and the main criteria for selection were originality and technical quality. This issue of Research in Computing Science will be useful for researches and students working in the different areas of Computer Science, as well as, for all readers interested in enrich the knowledge of this document.

In total, we received 55 papers that were submitted for evaluation; each submitted paper was reviewed by 2 independent members of the editorial board or additional reviewers and the acceptance rate is 60%. This volume contains revised version of 16 accepted papers, divided into three sections corresponding to the areas: Databases & Software Technology, Robotics & Mechatronics and Simulation & Modeling. The others papers will be published in the volume number 63 of the journal Research in Computing Science.

We would like express our gratitude to all people who help to elaborate this volume. First to the authors of the papers for the technical excellence of their works, that guarantees the quality of this publication. We also want to thanks the members of the editorial board for their hard work in evaluating and selecting the best's papers out of many submissions that we received. We express sincerely our gratitude to the Sociedad Mexicana de Inteligencia Artificial (SMIA) for their collaboration in the elaboration of this publication. Also we want to give special recognition to the Centro de Investigación en Computación of the Instituto Politécnico Nacional (CIC-IPN) for the facilities given to achieve the success in the publication of this volume. The submission, reviewing, and selection process was supported for free by the EasyChair system, www.EasyChair.org. Also we want to give special recognition to ORACLE, for its participation as a sponsor.

November 2013

Evelia Araceli Santos Camacho
Juan Carlos Chimal Eguía
Luis Cabrera Rivera
Erandi Castillo Montiel

Table of Contents

Índice

Databases & software Technology

Robotics and Mechatronics

Simulation & Modeling

Databases & Software Technology

MMIA Improvement and Services for Cloud Computing

Sandra Anízar, Chadwick Carreto

Escuela Superior de Cómputo, Instituto Politécnico Nacional, México, D.F.,
sanizargon@hotmail.com, ccarretoa@ipn.mx

Abstract. In this paper we present the results obtained from the implementation and improvement of the Management Model for Interconnection and Access (MMIA) Services for Cloud Computing, is a mechanism that enables connectivity services provided by a "Public Cloud" are most of the time available to users when they need it.

Keywords: Mobile computing, cloud computing, communications, access, management and networking.

1 Introduction

The Cloud Computing is the convergence and evolution of several concepts related to information technologies, such as virtualization, mobile computing, distributed application design or network design and management and provision of applications, information and data as a service [1].

Thus Cloud Computing efficiently provides access to computer services, regardless of physical systems that use or its actual location, as long as it has access to the Internet [2], and can work together on the same content.

But like all technology that is in its beginnings, Cloud Computing is not without controversy, although availability is an advantage, currently one of the strongest issues facing the growing development of Computer in Cloud is to ensure interconnection and access to services that this technology provides.

This problem is compounded when you take into account that currently the vast majority of computer systems schemes migrate to Cloud Computing, so it is vital to ensure that these systems are interconnected to the network and Computer services in the Cloud as long as possible without interruption.

The structure of this paper consists of eight sections, first discussed the current situation of Cloud Computing in terme s of concept, characteristics and advantages in the second section defines and presents the MMIA, later in the third section defining the architecture that has been developed for the MMIA, in the fourth section discusses the Installing a Public Cloud, followed MMIA Implementation, Testing and Results subsequently obtained, the final conclusions and finally some improvements and work future.

© E. A. Santos, J. C. Chimal, L. Cabrera, E. Castillo.
Advances in Computer Science and Engineering
Research in Computing Science 67, 2013 pp. 3–13
Paper Recived 17-08-2013 and Acepted 21-10-2013

2 Management model for the interconnection and availability (Mmia)

In Figure 1 shows the MMIA has been developed, which is equipped with a standard character, ie it can be implemented in different architectures of "Cloud", to allow optimization services availability, connectivity, recognition and link status monitoring and users.

Fig. 1. Management model for cloud computing.

As can be seen the MMIA comprises five interconnected layers, these layers are:

- Interconnect Layer.
- Layer Validation and Identification.
- Layer Information Management.
- Monitoring Layer Connection.
- Correction Layer Techniques.

Through this MMIA has achieved an improvement in the management and delivery of applications and services that are within the Public Cloud Educational and that users can access and use these services at the time you request.

3 Design and architecture MMIA

In Figure 2 shows the architecture of the MMIA, which is very important because it defines as interacting all elements of the MMIA and how they are supported by some standards, standards, protocols, processes, rules etc.., in order to make it fully functional the MMIA designed.

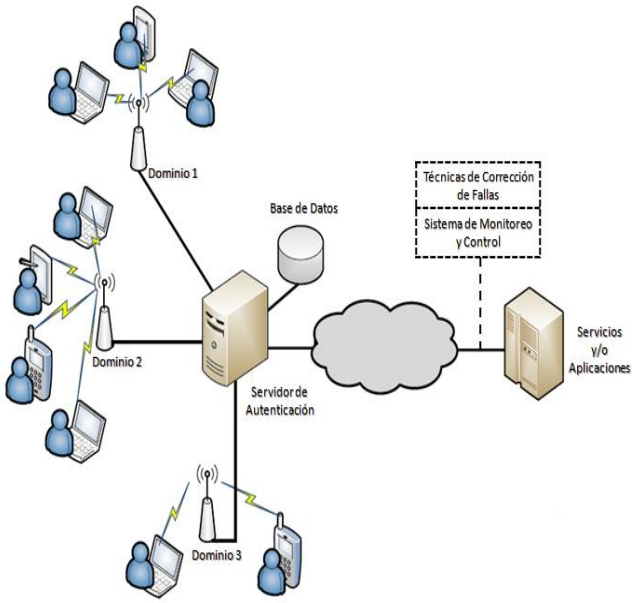

Fig. 2. MMIA architecture in cloud computing.

Then, the architecture of the MMIA has the feature that the user receives immediate attention, as well as total mobility and also, the services offered are managed intelligently [3] depending on the profile with the person who access the "Cloud", will be the type of services to which you have access.

This architecture has allowed users to access their cloud services regardless interconnect various problems such as delays, and intermittent disconnections and several Wireless Technologies to interoperate with each other, so this is not an obstacle in communication, however for our case and for practical purposes has worked with computer Wi - Fi and IEEE 802.11g.

4 MMIA implementation and installation of cloud public education

Both the MMIA and a Computing Cloud Server is implemented within the Mobile Computing Lab School of Computing (ESCOM), since in this are the means and facilities necessary to develop them and to carry out any sufficient evidence to prove operation and functionality.

The software we use to install our Educational Public Cloud is ownCloud, which is based on PHP, SQLite, MySQL or PostgreSQL and can run on all platforms that meet these requirements, it is a free software solution developed that can be downloaded for free and install it on a Server itself and emerges as an alternative to providers of commercial cloud services, in the following table shows the most important features that we installed as Server Cloud.

Table 1. Cloud computing server properties.

Características	Descripción
Configuración	Servidor Cloud
Sistema Operativo	Ubuntu Server 12.04.1 de 32 bits
Computadora	Motherboard Gigabyte Technology Co., Ltd. GA-VM900M
Procesador	Intel Core2 CPU 2300 de 1.80 GHz
Memoria RAM	2 GB DDR3
Disco Duro	320 GB

After installation of the OS on your computer, you must configure the network card to assign a public IP and fixed immediately proceed to install all necessary packages and then download and install the latest version of ownCloud from its official site .

Once ready the Cloud Server, you can proceed to creating users, among the main advantages that the cloud offers us, is that we will have all the space that the server takes on the hard drive and everything staying in he will be only under our control and manage your security, your privacy and ensuring the confidentiality of the information.

The MMIA implemented and is responsible for managing all Cloud Services within an educational environment and the concept of domain, in order to benefit those users (students, teachers, administrative staff, etc..) With mobile equipment are within the coverage area of the point of interconnection to the cloud, to learn more about Cloud Server installation and deployment and configuration of computers that make up the layers of MMIA reader is encouraged to consult some of the previous articles that have been published [4], [5].

5 Tests and results

Thanks to ownCloud package by default in our Cloud Server offers all users the following services: information storage, share files with users and non-users, music playback, image galleries, calendar / address book, file viewer PDF and text editor. In addition to allowing the most common functions such as the Backup and File Synchronization between various devices and the use of the Cloud with WebDAV technology.

At its meeting, the administrator is responsible for providing each user with a name, password and enter them into a workgroup database Cloud Server, which would give them access to their meeting within the cloud and get their services; also assigned each user a certain quota of storage, which in our case is 10 GB of disk space per user, ie according to the size of 320 GB hard disk maximum capacity people in the laboratory that is 30 users. First connection was tested and storing information in the cloud with registered users to date via the Web from your Internet browser to the server in the cloud (see Figure 3 and Figure 4).

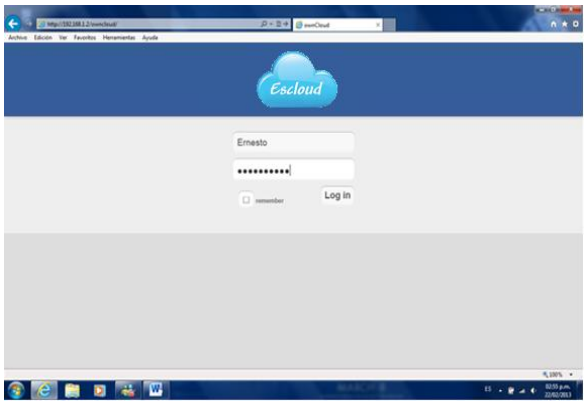

Fig. 3. Access to the cloud from your web browser.

.

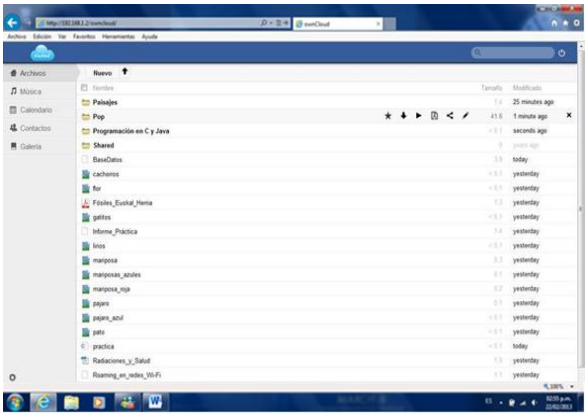

Fig. 4. Session in the cloud via the web.

Also through the file browser of a computer GNU / Linux or Ubuntu using WebDAV, as shown in Figure 5 and Figure 6, respectively.

Fig. 5. Connecting to the cloud using nautilus.

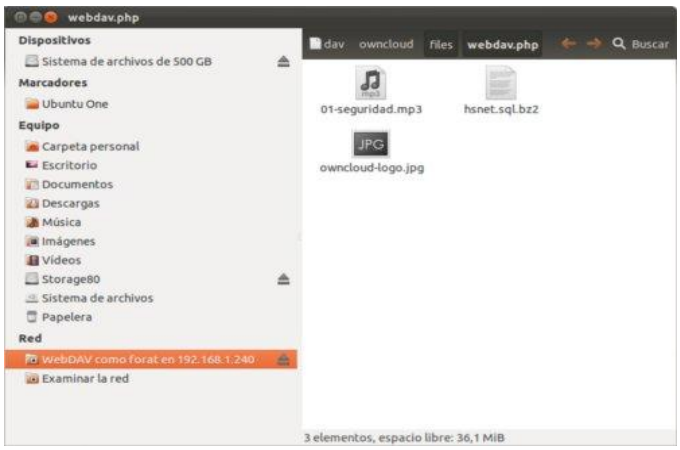

Fig. 6. Session in the cloud as a network drive.

In Figure 7 shows the GUI of an application for mobile devices with Android operating system that was developed, as well as performance tests conducted in order to provide users with a manager that allows access to your information within of the cloud in a much simpler, more flexible and dynamic.

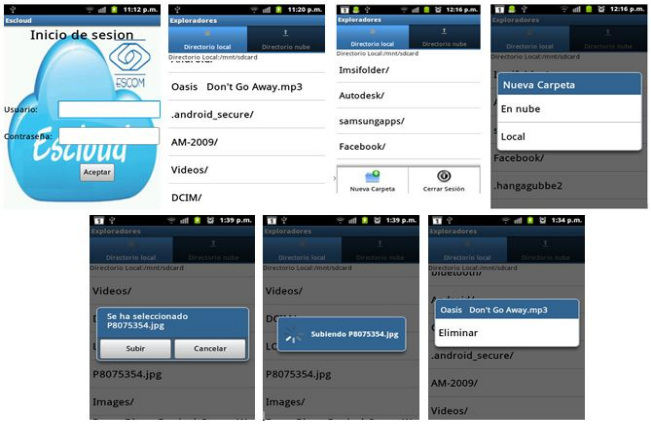

Fig. 7 Evidence of application for android.

Finally for measurements concerning the traffic in the Cloud was used Wireshark Protocol Analyzer, which is also a free software that allows us to capture the packets transmitted and received directly from the wireless network interface of the Cloud.

Using Wireshark Tool can also get valuable information Network Infrastructure (see Figure 8) where the cloud settled and Implement the MMIA, input shows the Host name, the domain to which it is associated, the Directorate IP, MAC Address, the bandwidth consumption, Manufacturer Name, Number of hops to the Domain, Uptime, etc.

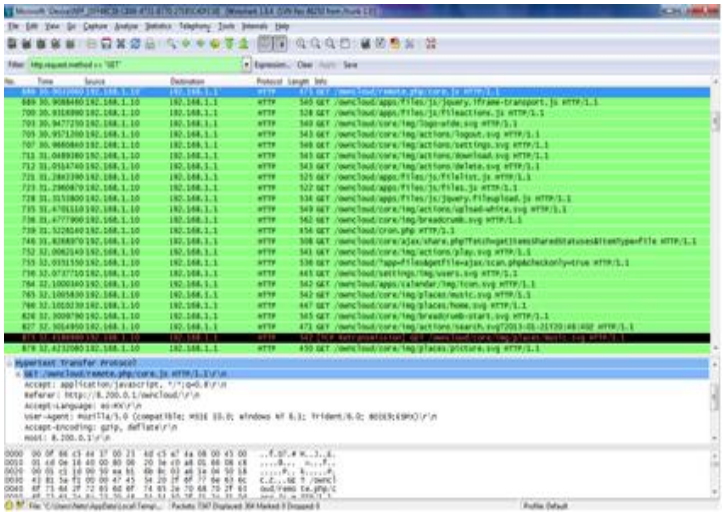

Fig. 8. Recognition cloud network with wireshark.

Now, in Figure 9 are observed Traffic Statistics Packet Interface WLAN, by implementing the Software in the MMIA also been able to classify Packet Flows in traveling on the Cloud.

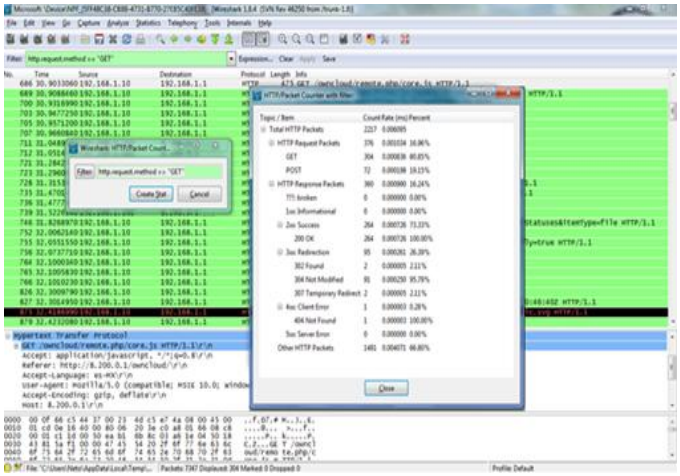

Fig. 9. Recognition of packet traffic in the cloud.

In Figure 10, show that the Packet Traffic Statistics collected and studied over a month on the Cloud environment under study is minimal, the graph shows the average travel data ranging between 10 and 15 Kbps which is within an acceptable range with minimal packet loss.

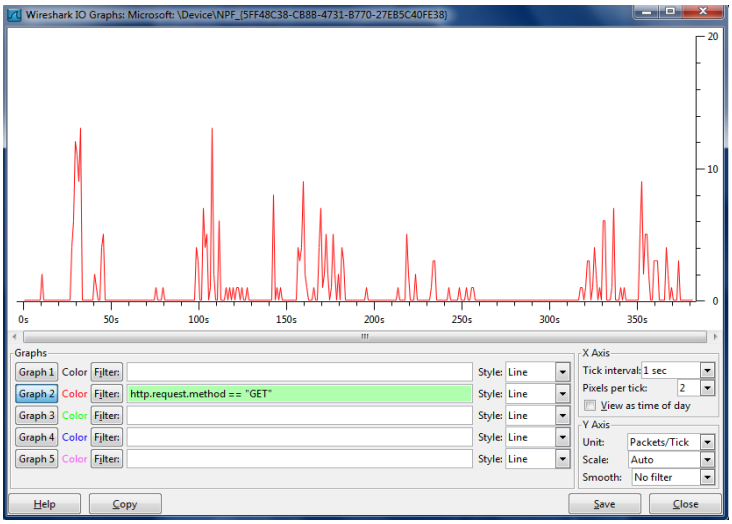

Fig. 10. Traffic Monitoring in the cloud with wireshark.

Below in Figure 11 is a breakdown of the directions in which traffic flows either locally - local, local - remote remote - remote.

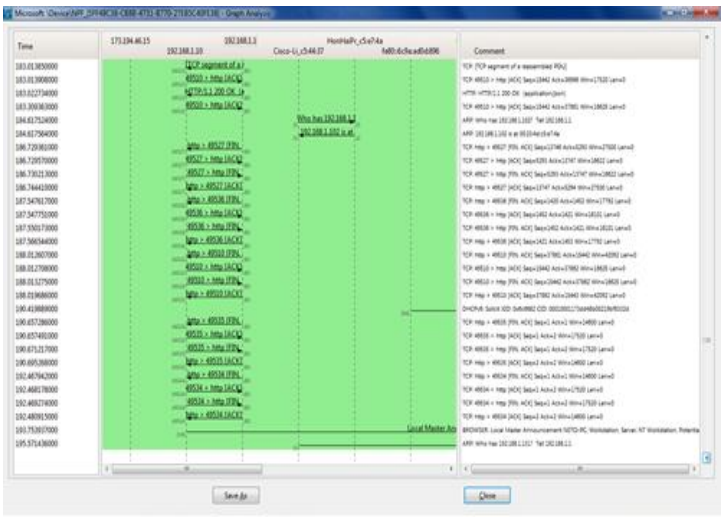

Fig. 11. Breakdown of traffic flow in the cloud.

Another type of result has been obtained in the development of the research is the bandwidth monitoring in the cloud, which is consumed by the registered users to access the Cloud Server and make use of the services offered in this.

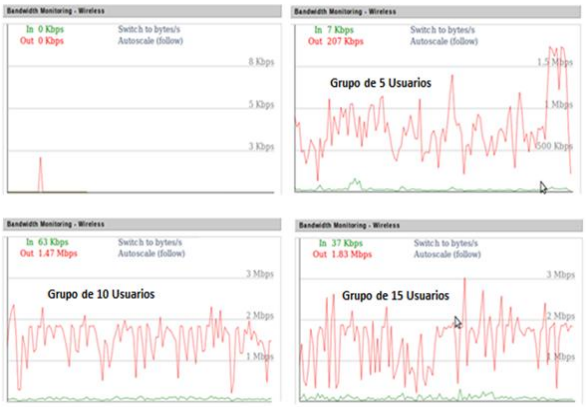

Fig. 12. Bandwidth Monitoring in the cloud.

The tests were conducted to see the bandwidth consumption by the Cloud with different numbers of people in the lab can be seen in Figure 12, observing that with groups of 5, 10 and 15 concurrent users was required bandwidth of 1.55 Mbps, 2.1 Mbps and 3.2 Mbps respectively. However, these needs are fully covered by the interconnection point and IEEE 802.11g standard operates as it can handle a maximum bandwidth of up to 22Mbps. Consumption results Bandwidth Traffic coupled with us "guarantees" that communications have been performing well and that the traffic generated was only the essential, allowing you to have a higher occupancy of the Cloud. In Figure 13, we see the percentage of Success Connections, these tests involved that users came to the lab with his team, will connect to the cloud, will authenticate and receive appropriate services and make use of them, the result was one which 97.78% is considered acceptable for the functionality of the MMIA.

As for the validation and identification layers and management information MMIA, the percentage of successful authentications was 100% as shown in Figure 14, while the results of the information management server within the Cloud can appreciate in Figure 15 and Figure 16. Thus, the average unit tests consisted authentication and management of user information proved successful with a percentage of 98.33% as shown in Figure 17, which shows the reliability, speed and enhanced effectiveness.

Finally after making the calculations was obtained that the Network Infrastructure Public Cloud environment where services are offered filed a 99.97% availability as shown in Figure 18, this indicates an efficient operation MMIA elements that implement and excellent availability of the Services within the Cloud.

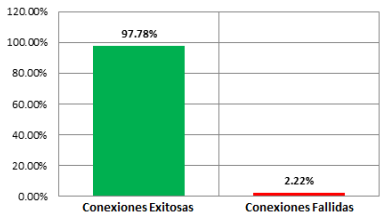

Fig. 13. Testing connection to the cloud.

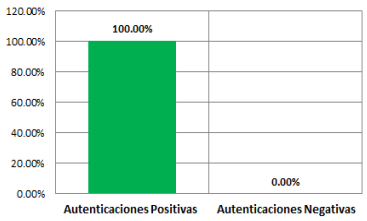

Fig. 14. Test authentication to the cloud.

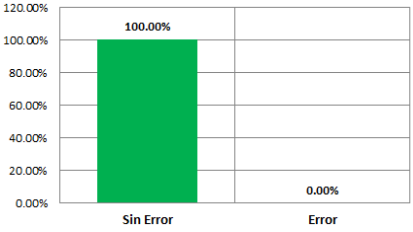

Fig. 15. Testing local management.

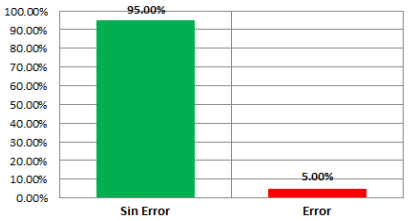

Fig. 16. Tests run in the cloud.

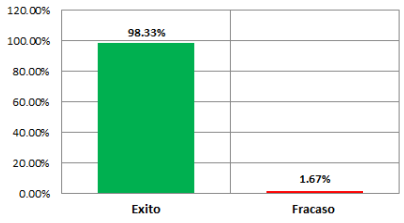

Fig. 17. Result of unit tests.

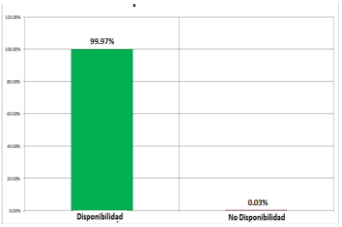

Fig. 18. Percentage of availability of MMIA.

6 Conclusions

The results obtained in this study have proved satisfactory, since it is able to develop and evaluate a MMIA in Cloud Computing for users of a Public Cloud environment could have optimal access to services and applications that this offers. It concludes that the proposed methodology is effective for measuring the availability of the applications according to the results obtained, and the inclusion of Traffic Analysis and Bandwidth consumption as a support tool for as long as the Cloud Server is responsible for responding to requests, process them and provide services to users.

References

1. Oracle Corporation: Architectural Strategies for Cloud Computing. Oracle White Paper in Enterprise Architecture, California, EE.UU. (2009).
2. L. J. Aguilar: The Cloud Computing: The New Paradigm Technological for Business. Quarterly Magazine of the Faculty of Law and Economics and Business., Pontificial University Comillas Madrid., (2009).
3. Oracle Corporation: Architectural Strategies for Cloud Computing. Oracle White Paper in Enterprise Architecture., California EE. UU., [Online]. Available at http://www.oracle.com, August (2010).
4. J. E. Chávez, C. Carreto and S. Álvarez: Implementation of a Management Model Interconnection and access Availability Cloud Computing. Presented at the 1st. International Conference on Robotics and Computer, Los Cabos, BCS., Mexico, May. 23 and 24, (2013).
5. J. E. Chávez, C. Carreto and S. Álvarez: Management Model for Interconnection and Access Availability for Cloud Computing. Presented at the World Congress in Computer Science, Computer Engineering, and Applied Computing (WORLDCOMP'13), Las Vegas, Nevada, USA, (2013).

Análisis Comparativo de Algoritmos de Minería de Datos para Predecir la Deserción Escolar

Maricela Quintana López, Juan Carlos Trinidad Pérez, Saturnino Job Morales Escobar, Víctor M. Landassuri Moreno

Centro Universitario UAEM Valle de México
{mquintanal, sjmoralese, vlandassurim}@uaemex.mx,
jtrinidadp359@alumno.uaemex.mx

Resumen. Un tutor académico, debe dar seguimiento personalizado al alumno para evitar que deserte por cuestiones académicas, por ejemplo, materias que se le dificulten. Sin embargo, la información del seguimiento es bastante, por lo que debe procesarse para extraer patrones que permitan tomar decisiones oportunamente. Este artículo presenta la comparación de algoritmos de clasificación para la predicción de la deserción escolar del Centro Universitario UAEM Valle de México en la carrera de Ingeniería en Sistemas y Comunicaciones. El objetivo fue determinar el mejor algoritmo basándose en la precisión de la clasificación, así como en la utilidad en la información provista al tutor. De los experimentos concluimos que los mejores algoritmos son Naïve Bayes Tree, que tiene el menor error, y J48 que provee información útil para el tutor al indicar las materias que debe cuidar, permitiéndole crear estrategias que apoyen el desempeño académico del alumno en las mismas.

Palabras clave: Minería de datos, clasificación, árboles de decisión, naïve bayes.

1 Introducción

La deserción escolar en las instituciones de nivel superior, es un problema que actualmente las autoridades administrativas enfrentan. Diversos estudios realizados llegan a la conclusión de que el problema existe tanto a nivel local como a nivel global y este continuará si no se atiende de manera adecuada.

Para cada país o estado existen estadísticas que describen el nivel de deserción estudiantil en educación superior, permitiéndonos detectar la situación que se vive para cada una de las carreras profesionales de las instituciones públicas y privadas [18-20]. Sin embargo, es posible utilizar las tecnologías de la información para detectar situaciones de riesgo que pueden llevar a un alumno a abandonar sus estudios. Ésta fue la motivación principal por la cual en la Universidad Autónoma del Estado de México, se diseñó el sistema SITA (Sistema Inteligente para la Tutoría Académica), que permite a los tutores académicos monitorear el desempeño académico y consultar información socioeconómica del alumno [16-17].

© E. A. Santos, J. C. Chimal, L. Cabrera, E. Castillo.
Advances in Computer Science and Engineering
Research in Computing Science 67, 2013 pp. 13–23
Paper Recived 30-08-2013 and Acepted 21-10-2013

A pesar de este gran apoyo, determinar si un alumno desertará o no, requiere de un análisis particular para cada trayectoria y situación, labor que debe realizar el tutor. Por ello, en este trabajo nos enfocamos en generar un modelo clasificador cuyo nivel de fiabilidad y precisión sea aceptable para determinar la posibilidad de que un alumno interrumpa sus estudios. Con la gran ventaja de que la aplicación del modelo sea realizada de manera automática.

Para realizar este trabajo, se tomará como base las calificaciones obtenidas por 193 alumnos de la carrera de Ingeniería en Sistemas y Comunicaciones durante el primer año de estudios, específicamente de las generaciones 2008 (71 alumnos), 2009 (63 alumnos) y 2010 (59 alumnos).

En la figura 1, se muestran las diferentes fases de la metodología utilizada en este trabajo, la cual está basada en el modelo KDD (Knowledge Discovery in Databases) [9,11].

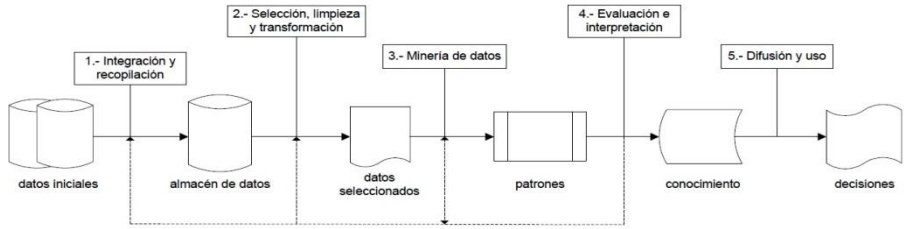

Fig. 1. Fases del proceso KDD

Con esto en mente, en la sección 2 se mostrará la preparación de los datos, seguida de la sección 3 en donde se presentarán las técnicas de minería de datos empleadas en esta investigación. Posteriormente, en la sección 4 se mostrarán los experimentos y resultados obtenidos. Finalmente, en las secciones 5 y 6 se presentarán las conclusiones y trabajo futuro respectivamente.

2 Preparación de los datos

En este trabajo, se utilizaron las trayectorias académicas de todos los alumnos de la carrera de Ingeniería en Sistemas y Comunicaciones, de las generaciones 2008, 2009 y 2010. La información obtenida de las bases de datos de control escolar fue filtrada para utilizar únicamente las calificaciones de las unidades de aprendizaje del primer año de estudios que cursaron los 193 alumnos. En la tabla 1, se muestran los atributos y los posibles valores numéricos y nominales de los mismos. El atributo Número de Cuenta se utiliza únicamente para identificar los registros más no para generar los patrones, mientras que el atributo desertó es la clase a aprender.

Es necesario aclarar que las calificaciones consideradas son únicamente las primeras que obtuvo el alumno en las unidades de aprendizaje, no consideramos las notas obtenidas en evaluaciones extraordinarias. También, fueron eliminados de la muestra

los registros de alumnos que únicamente cursaron el primer semestre, ya que el trabajo considera lo que ocurre en el primer año.

Tabla 1. Datos utilizados con su respectivo tipo de variable

Atributos	Valores Numéricos	Valores Nominales
Número de Cuenta	Matrícula institucional	Matrícula institucional
Introducción a la Computación	0-100	A: Aprobado R: Reprobado NP: No Presentó
Álgebra y Geometría Analítica		
Administración		
Estática y Dinámica		
Introducción a la Ingeniería		
Técnicas de Comunicación		
Álgebra Lineal		
Calculo Diferencial e Integral		
Fundamentos de Programación		
Arquitectura de computadores		
Química		
Desertó	si, no	si, no

Debido a la naturaleza de los algoritmos a aplicar, se transformaron los datos para tenerlos de forma numérica y de forma nominal. Para la versión numérica, las calificaciones NP fueron transformadas a cero. En la tabla 2, se muestra un fragmento de cómo quedaron los datos.

Tabla 2. Muestra de datos a considerar en el análisis con datos numéricos

	Primer Semestre				Segundo Semestre			Clase
Cuenta	**Introducción a la Computación**	**Técnicas de Comunicación**	**Administración**		**Álgebra Lineal**	**Química**	**Arquitectura de Computadores**	**Desertó**
449905	65	47	32		70	81	48	Si
540214	92	100	70	…	92	82	88	No
726037	92	71	100		83	87	90	No
823719	68	100	70		71	67	60	No
823753	73	90	70		60	87	82	Si

Para la versión nominal, las calificaciones mayores o iguales a 60 tienen un valor de A (aprobado), las menores a 60, tienen un valor de R (reprobado) y las evaluaciones no presentadas tienen un valor de NP. En la tabla 3, se muestra un conjunto de datos con la transformación mencionada.

Tabla 3. Muestra de datos a considerar en el análisis con datos nominales

	Primer Semestre				Segundo Semestre			Clase
Cuenta	**Introducción a la Computación**	**Técnicas de Comunicación**	**Administración**		**Álgebra Lineal**	**Química**	**Arquitectura de Computadores**	**Desertó**
449905	A	R	R		A	A	R	Si
540214	A	A	A	…	A	A	A	No
726037	A	A	A		A	A	A	No
823719	A	A	A		A	A	A	No
823753	A	A	A		A	A	A	Si

3 Minería de datos

Existen varios trabajos desarrollados para predecir el desempeño académico de un alumno empleando técnicas de minería de datos. Entre las técnicas más utilizadas están los árboles de decisión y las técnicas bayesianas [1-8].

Un árbol de decisión es un conjunto de condiciones organizadas de forma jerárquica para clasificar una serie de atributos y predecir el valor de la clase. Los árboles están formados por nodos y ramas donde cada nodo representa una condición sobre algún atributo y cada rama corresponde a un posible valor para ese atributo. Pueden manejar valores de tipo nominal y/o de tipo numérico [10, 12]. Los algoritmos de árboles de decisión más utilizados son ID3, C4.5 (J48) y Naïve Bayes Tree [1-8]. Cabe aclarar que el ID3 no trabaja con datos numéricos, únicamente con categóricos.

Por otra parte, los algoritmos Naïve Bayes son un grupo de clasificadores estadísticos que al ser aplicados a una instancia nueva, dan como resultado la probabilidades de que dicha instancia pertenezca a una clase determinada [11, 13]. Algunos de los trabajos realizados utilizan principalmente el algoritmo de Naïve Bayes y las redes Bayesianas [2, 3, 10, 15]. Los algoritmos basados en Bayes funcionan de manera correcta con datos del tipo nominal y/o numérico y son independientes.

Los árboles de decisión y los algoritmos Bayesianos han demostrado tener un alto índice de precisión cuando de predicción se trata, de hecho han sido incluidos dentro de los diez mejores algoritmos de minería de Datos [14]. Por ello en este trabajo se realiza un análisis comparativo entre algoritmos de árboles de decisión y Bayesianos, particularmente, ID3 (solo para valores nominales), J48 (C4.5), Naïve Bayes Tree, Naïve Bayes, y redes Bayesianas, los cuales se encuentran disponibles en el software WEKA de la universidad de Waikato, de Nueva Zelanda [21].

4 Experimentos y resultados obtenidos

Las pruebas se realizaron en dos grandes bloques: uno para los datos de tipo nominal y otro para los datos de tipo numérico. En ambos casos, se aplicaron los algoritmos elegidos para conducir 3 experimentos que varían en cuanto a los datos empleados en los mismos y que se explican a continuación. Todos los modelos fueron evaluados

utilizando la validación cruzada de 10 pliegues, la cual divide el conjunto de datos en diez partes y utiliza nueve partes para entrenamiento y una para prueba. El proceso es repetido diez veces [10-11].

En el primer experimento realizado se aplicaron los algoritmos elegidos a los datos de cada generación por separado para construir su modelo. Las tablas 4 y 5 muestran los resultados obtenidos por cada algoritmo, de la siguiente forma: porcentaje de precisión, instancias clasificadas (correctamente / incorrectamente).

Tabla 4. Resultados utilizando datos nominales

Algoritmo	**Porcentaje de precisión por generación usando datos nominales**			**Promedio**
	2008	**2009**	**2010**	
ID3	95.7746 (68/71)	85.4839 (53/63)	98.3051 (58/59)	93.19
J48	88.7324 (63/71)	88.7097 (55/63)	98.3051 (58/59)	91.92
Naïve Bayes Tree	92.9577 (66/71)	83.871 (52/63)	96.6102 (57/59)	91.15
NaïveBayes	92.9577 (66/71)	87.9068 (54/63)	96.6102 (57/59)	92.49
BayesNet	91.5493 (65/71)	87.9068 (54/63)	96.6102 (57/59)	92.02

Podemos observar que para los datos de tipo nominal, si consideramos las generaciones 2008 y 2010, el mejor algoritmo resulta ser ID3. Pero si consideramos 2009 y 2010, el mejor resulta ser el algoritmo J48. Al obtener el promedio de las 3 generaciones podemos notar que el mejor es el ID3 para valores de tipo nominal. Por otro lado, cuando se trata de datos numéricos el mejor algoritmo en las 3 generaciones es el Naïve Bayes Tree. Al comparar los resultados de los categóricos con los numéricos, resulta mejor el Naive Bayes Tree, lo cual es comprensible si consideramos que los datos son de naturaleza numérica y al ser transformados para trabajarlos como categóricos, se pierde la precisión.

Tabla 5. Resultados obtenidos utilizando datos numéricos

Algoritmo	**Porcentaje de precisión por generación usando datos numéricos**			**Promedio**
	2008	**2009**	**2010**	
ID3	NA	NA	NA	NA
J48	88.7324 (63/71)	90.4762 (57/63)	98.3051 (58/59)	92.50457
Naïve Bayes Tree	92.9577 (66/71)	92.0635 (58/63)	98.3051 (58/59)	94.4421
NaïveBayes	85.9155 (61/71)	74.6032 (47/63)	98.3051 (58/59)	86.2746
BayesNet	84.507 (60/71)	92.0635 (58/63)	98.3051 (58/59)	91.6252

Como una muestra de los modelos generados, en las figuras 2 y 3 se presentan los árboles de decisión para las generaciones 2008 y 2009 utilizando los algoritmos de ID3 y J48 respectivamente. En ellas podemos observar que la materia que provee mayor información para la separación de las clases es Arquitectura de Computadores.

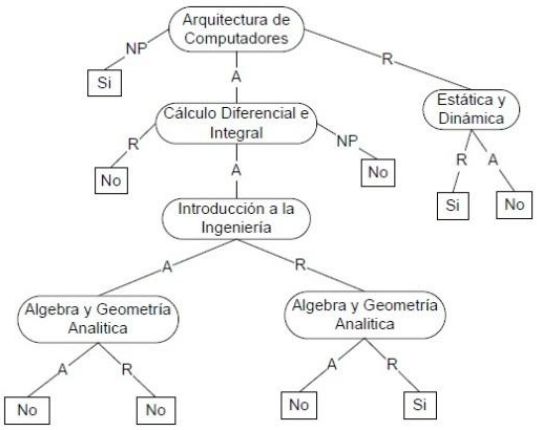

Fig. 2. Árbol para la generación 2008 usando ID3.

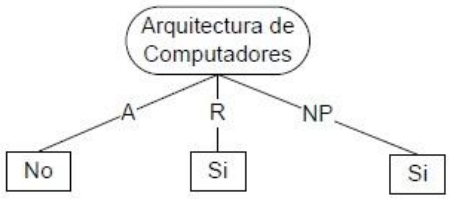

Fig. 3. Árbol para la generación 2009 usando J48(C4.5).

Como un segundo experimento se aplicaron los algoritmos elegidos a todo el conjunto de datos, es decir, generaciones 2008-2010 y los resultados referentes a la precisión obtenida se muestran en la tabla 6.

Tabla 6. Resultados obtenidos al combinar las tres generaciones, 2008-2010

Algoritmo	% de precisión	
	Variables de tipo nominal	Variables de tipo numérico
ID3	86.4583	NA
J48	90.625	88.7755
Naïve Bayes Tree	91.667	90.3061
NaïveBayes	89.5833	82.6530
BayesNet	89.0625	87.7551

Podemos observar que en este caso, el algoritmo con mayor precisión es el Naïve Bayes Tree tanto para variables nominales como numéricas. El árbol obtenido usando ID3 en este conjunto de datos se muestra en la figura 4, en él podemos observar que la unidad de aprendizaje Arquitectura de computadores sigue siendo la que se encuentra en el nodo raíz del árbol.

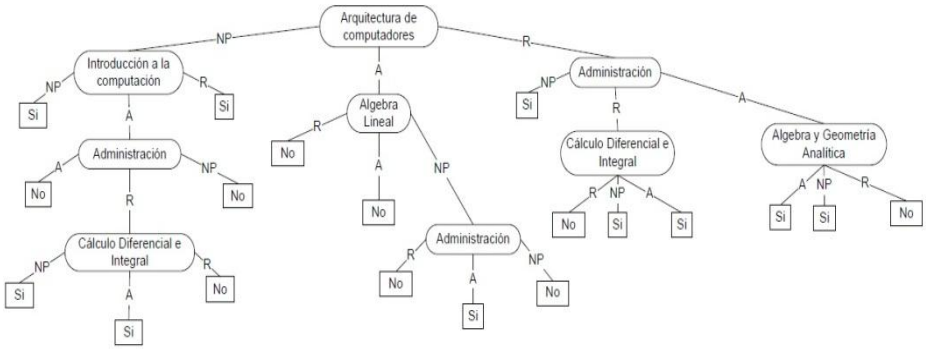

Fig. 4. Árbol para las generaciones 2008-2010 usando ID3.

En cuanto al algoritmo Naïve Bayes Tree para valores numéricos, el árbol generado es de un nivel y se muestra en la figura 5. Podemos notar que la unidad de aprendizaje en la raíz es la de Arquitectura de computadores, y las hojas son los clasificadores bayesianos.

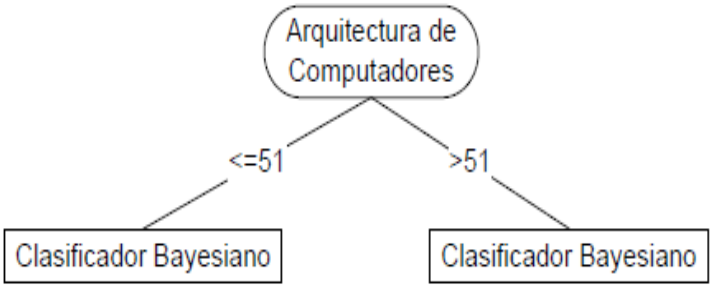

Fig. 5. Árbol para las generaciones 2008-2010 usando Naïve Bayes Tree

De acuerdo a los resultados obtenidos, fue detectado que la calificación nominal NP estaba provocando ruido en el sistema, por lo que se realizó un tercer experimento en el que se transformó el NP a reprobado R, pues un alumno con calificación NP tendrá que volver a cursar forzosamente la unidad de aprendizaje, como si estuviese reprobado. Los resultados obtenidos al realizar este cambio se muestran en la tabla 7.

Tabla 7. Resultados obtenidos al combinar las tres generaciones, 2008-2010, sin usar NP

Algoritmo	% de precisión en las variables de tipo nominal
ID3	88.5417
J48	88.0208
Naïve Bayes Tree	90.625
NaïveBayes	89.0625
BayesNet	89.0625

Los árboles generados por Naïve Bayes Tree y J48, se muestran en las figuras 6 y 7. En ellas podemos apreciar de manera más clara, qué grupos de materias llevan, en conjunto, al abandono de los estudios por parte del alumno.

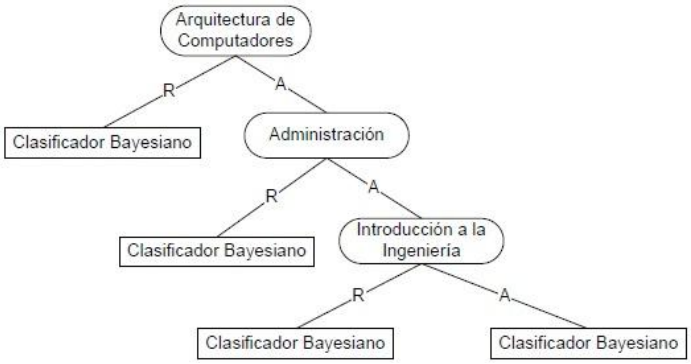

Fig. 6. Árbol generado por Naïve Bayes Tree sin usar NP

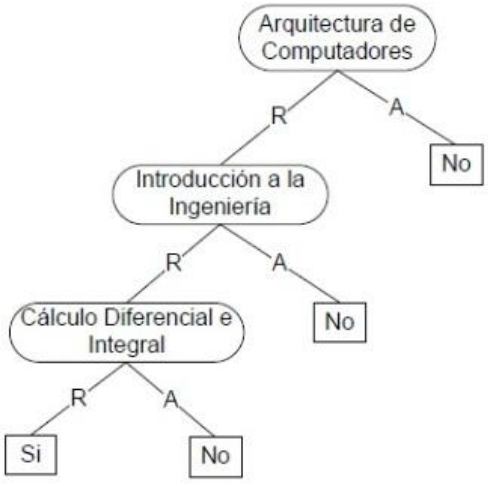

Fig. 7. Árbol generado por J48 sin usar NP

5 Conclusiones y trabajo futuro

En este trabajo fue presentado un análisis comparativo entre varias técnicas de minería de datos para determinar si un alumno es propenso a desertar de sus estudios en la carrera de Ingeniería en sistemas y Comunicaciones del Centro Universitario UAEM Valle de México. Los resultados obtenidos muestran que es posible obtener un modelo de predicción de la deserción escolar utilizando las calificaciones obtenidas por los alumnos en el primer año de sus estudios.

En los experimentos realizados con los datos de las generaciones, podemos concluir que los mejores algoritmos son Naíve Bayes Tree y J48. El algoritmo de Naïve Bayes Tree es, desde el punto de vista cuantitativo, el que tiene el menor error al momento de clasificar. Sin embargo, desde el punto de vista cualitativo, el árbol de inducción generado por el algoritmo J48 provee información que puede ser de utilidad para el tutor académico, pues le indica las unidades de aprendizaje en las que debe poner atención y planear estrategias que apoyen el desempeño académico del alumno.

Como trabajo futuro, se utilizarán los datos de más generaciones para hacer un estudio a detalle del comportamiento académico histórico que existe en la carrera de Ingeniería en Sistemas y Comunicaciones. También podrían incluirse en el análisis otros algoritmos de clasificación como CART, AdaBoost, SVM entre otros.

Referencias

1. Vera, C. M., Morales, C. R., & Soto, S. V.: Predicción del Fracaso Escolar mediante Técnicas de Minería de Datos. Revista Iberoamericana de Tecnologías del/da Aprendizaje/Aprendizagem, 109. (2012).
2. Nguyen Thai Nghe, Paul Janecek, and Peter Haddawy. A Comparative Analysis of Techniques for Predicting Academic Performance. Paper presented at the 37th ASEE/IEEE Frontiers in Education Conference. October 10 – 13, Milwaukee, WI. (2007).
3. García, E. P. I., & Mora, P. M.: Model Prediction of Academic Performance for First Year Students. In Artificial Intelligence (MICAI), 2011 10th Mexican International Conference on (pp. 169-174). IEEE. (2011).
4. Vasile Paul Bresfelean: Data Mining Applications in Higher Education and Academic Intelligence Management, Theory and Novel Applications of Machine Learning, Meng Joo Er and Yi Zhou (Ed.), ISBN: 978-953-7619-55-4, InTech, DOI: 10.5772/6684. (2009).
5. Alcover, R., Benlloch,J., Blesa P., Calduch, M. A., Celma, M., Ferri, C.: Análisis del rendimiento académico en los estudios de informática de la Universidad Politécnica de Valencia aplicando técnicas de minería de datos. XIII Jornadas de Enseñanza universitaria de la Informática, Teruel, España. (2007).
6. Orea, S. V., Vargas, A. S., & Alonso, M. G.: Minería de datos: predicción de la deserción escolar mediante el algoritmo de árboles de decisión y el algoritmo de los k vecinos más cercanos. Ene, 779(73), 33. (2005).
7. Spositto, O. M., Etcheverry, M. E., Ryckeboer, H. L., & Bossero, J. Aplicación de técnicas de minería de datos para la evaluación del rendimiento académico y la deserción estudiantil. Memorias de la 9ª Conferencia Iberoamericana en Sistemas, Cibernética e Informática CISCI 2010. Orlando, Florida, USA, (2010).

8. Pereira, R. T. Detección de Patrones de Bajo Rendimiento Académico y Deserción Estudiantil con Técnicas de Minería de Datos. Memorias de la 8ª Conferencia Iberoamericana en Sistemas, Cibernética e Informática CISCI 2009. Orlando, Florida, USA, (2009).
9. Moine, J. M., Haedo, A., & Gordillo, S.: Estudio comparativo de metodologías para minería de datos. In XIII Workshop de Investigadores en Ciencias de la Computación. (2011).
10. Sharma M., Mavani M.: Development of predictive model in education system: using naïve bayes classifier. International conference and workshop on emerging trends in technology-ICWET, (2011).
11. Orallo, J. H., Quintana, M. J. R., & Ramírez, C. F.: Introducción a la Minería de Datos. Pearson Prentice Hall. (2004).
12. Han, J., Kamber, M., & Pei, J.: Data mining: concepts and techniques. Morgan kaufmann. (2006).
13. Russell, S. J., Norvig, P., Canny, J. F., Malik, J. M., & Edwards, D. D.: Artificial intelligence: a modern approach (Vol. 74). Englewood Cliffs: Prentice hall, (1995)
14. Wu, X., & Kumar, V. (Eds.). (2010). The top ten algorithms in data mining. CRC Press.
15. Salazar, A., Gosalbez, J., Bosch, I., Miralles, R., & Vergara, L.: A case study of knowledge discovery on academic achievement, student desertion and student retention. In Information Technology: Research and Education, 2004. ITRE 2004. 2nd International Conference on (pp. 150-154). IEEE, (2004).
16. Morales S. J., Rodríguez I, García S.: Propuesta de un sistema de información para la Tutoría Académica en una institución de educación superior. III Congreso Internacional de Innovación Educativa. Xalapa, Veracruz. México, (2008).
17. Sistema Inteligente para la Tutoría Académica, https://www.sita.uaemex.mx/tutoria/
18. Dirección General de Educación Superior Universitaria, http://www.dgesu.ses.sep.gob.mx/Principal/subdirecciones/indicadores/desercion.aspx
19. Universidad Autónoma del Estado de México, http://www.uaemex.mx/planeacion/NumEstadis.html.
20. Publicaciones ANUIES, http://publicaciones.anuies.mx/
21. WEKA 3: Data Mining software in java, http://www.cs.waikato.ac.nz/ml/weka/

Web Page Generator: an Online Tool for Supporting Web Programming Courses

Carlos R. Jaimez-González, Alfredo R. Vargas-Rodríguez

Departamento de Tecnologías de la Información, Universidad Autónoma Metropolitana - Cuajimalpa, Av. Constituyentes No. 1054, Col. Lomas Altas, C.P. 11950, México D.F.
{cjaimez,207363956}@correo.cua.uam.mx

Abstract. This paper presents Web Page Generator, which is an online tool for supporting Web Programming courses. Users of Web Page Generator can create a web page graphically, by placing web elements on a work area; they can also modify the style of the web page through an edition bar, and add validations to input fields. Additionally, users can navigate the web page structure using a tree bar, and visualizing it in a preliminary view. The resulting web page is generated in three separated files: an HTML file for its structure, a CSS file with styles for its presentation, and a JavaScript file for its validations. Web Page Generator allows web developers producing web pages, but also supports teaching activities in courses related to web programming.

Keywords. Web page generator, web programming, automatic code generation, html, javascript, CSS, web page, WYSIWYG.

1 Introduction

The creation of web sites in recent years has been increasing, given the popularity of the Internet to allow advertising products and services with no restrictions of time, 24 hours a day, 365 days a year. This situation opens the need for tools that allow the development and automatic generation of HTML code, so web sites can be implemented rapidly and efficiently. Web developers have had to adapt to the existing development environments, which are sometimes complicated and difficult to understand; some of these need some training previous to their use [1], [2]; and some others are very expensive [1]. A similar problem can be found in some undergraduate degrees, in which there are courses where students are introduced to web site development and the use of graphical tools. This is the case of two undergraduate degrees at our faculty: Design, and Information Technologies and Systems, in which students take courses where they are required to create web pages, such as Web Design, Web Pages Development, Web Programming, etc.

This paper presents Web Page Generator, an online tool for creating web pages and generating HTML, CSS and JavaScript code automatically. This tool has been created not only for web developers, but also to support teaching activities in courses related to web programming. One of the key advantages of this online tool is the clear dis-

© E. A. Santos, J. C. Chimal, L. Cabrera, E. Castillo.
Advances in Computer Science and Engineering
Research in Computing Science 67, 2013 pp. 23–33
Paper Recived 31-08-2013 and Acepted 21-10-2013

tinction of HTML, CSS, and JavaScript code, which is generated in separated files. The work presented in this paper is based on the initial architecture described in [3].

The rest of the paper is organized as follows. Section 2 presents some existing tools that are relevant to this development; mainly related to code generators by conceptual models, and generators by edition. Section 3 describes the architecture of the online tool, its modules and their functionality. The web user interface of the tool and its components are presented in section 4. Some examples of web pages generated with Web Page Generator are presented in section 5. Finally, section 6 provides conclusions and future work.

2 Existing generation tools

There are some online tools that generate HTML, but their functionality is limited [4], [5]. Some others also generate HTML code, but also allow restructuring the data that is the source of the web page, the generation by conceptual models or customization, and modification from web pages already generated. Given the different objectives of these code generators, they are classified in two types: 1) generators by conceptual models or customization; and 2) generators by edition. The following sections present these types of generators, as well as the problems in these areas.

2.1 Tools based on conceptual models

The tools that work based on conceptual models generate a kind of platform that can be used by developers to produce web content through an easy-to-use and customizable interface. This is the case of the Web Interface Development Environment (WIDE) [6], which provides automatic generation of web content, starting from a conceptual model. To facilitate the construction of web content, this tool incorporates a layers system, which allows the visualization of control and its functionality; and also has a zoom system to increase the level of detail in the production of content.

Another tool based on the development by conceptual models is the Web Application Rapid Prototyping (WARP) [7]. This application offers a set of online software tools that help the designer in the navigation of a web application, using the UWA methodology [8]. GIWA is another tool based on conceptual models, which provides a generator of adaptive web applications [9]. Its main objective is to facilitate the design and automatic generation of web interfaces through several levels, which go from functionality to presentation.

2.2 Tools based on edition

The edition tools work on existing content and aim to have an easy web site administration and upgrade. The administration goes from the web site presentation to the modification of its source data. Nakano [10] developed a tool that edits a web site based on a bidirectional transformation, with an upgrade system called Vu-X. This way, users modify directly the web page, without the need of accessing the database;

and the result is shown automatically in the database using the bidirectional transformation language Bi-X [11]. Vu-X also implements an editing system similar to those called What You See Is What You Get (WYSIWYG). There is also the tool called Dido [12], which allows editing web pages; it contains an interactive AJAX interface, a data editor, and a MetaEditor that allows WYSIWYG editing. AJAX is the acronym of Asynchronous JavaScript and XML, which is a web development technique used to create interactive applications or Rich Internet Applications (RIA). Dido does not need installation because it works on browsers; this way author documents can share information and at the same time edit it according to their needs. It is limited to certain functionality, such as create, read, update, and delete. WebSheets [13] is another tool that allows the creation and modification of HTML pages with dynamic content; it modifies the database and the structure of the web pages with a WYSIWYG editor.

The tools described in this section are dedicated to the modification of HTML and XML code; but there are also other tools that are aimed to the creation of styles, such as the XSLbyDemo [14] tool, which generates XSL stylesheets from an HTML page, using a WYSIWYG editor. XML is a markup language created by the World Wide Web Consortium (W3C); it derives from SGML, and allows defining the grammar of specific languages (it should be noticed that HTML is also derived from SGML). The eXtensible Stylesheet Language (XSL) is an extensible language based on stylesheets. These languages are part of a family of languages based on XML, which allow describing the information contained in an XML document, and transform it or format it, in order to be presented in a digital media. One of the main features of XSLbyDemo is the generation of a stylesheet from a well-formed XHTML document. The produced XSL file can be associated to several documents derived from the same Document Type Definition (DTD), which describes the rules for the structure and syntax of XML or SGML documents. XSLbyDemo is based mainly in insertions, modifications, copies and elimination of rules that are defined in the file. The generation of that file is carried out through the Document Object Model (DOM) for accessing and manipulating the objects contained in it. DOM is an application programming interface that provides a standard set of objects to represent XML and HTML documents; it is a standard model to access and manipulate these objects.

3 Architecture

Web Page Generator allows the graphical edition of web pages, and generates automatically HTML, CSS and JavaScript code. It uses a WYSIWYG editor, and it is accessible through the web. When the user finishes editing the web page, the result is a set of files with the programming code of the technologies mentioned. In the following sections it will be described the modules that are part of this tool.

The online tool uses a client-server architecture, which is shown in Figure 1. The client side is composed of two blocks: the user interface, and the modules that support it; while the server side is composed of the code generators for HTML, CSS and JavaScript, and the module for generating files. The rest of this section provides a detailed explanation of the components of this architecture.

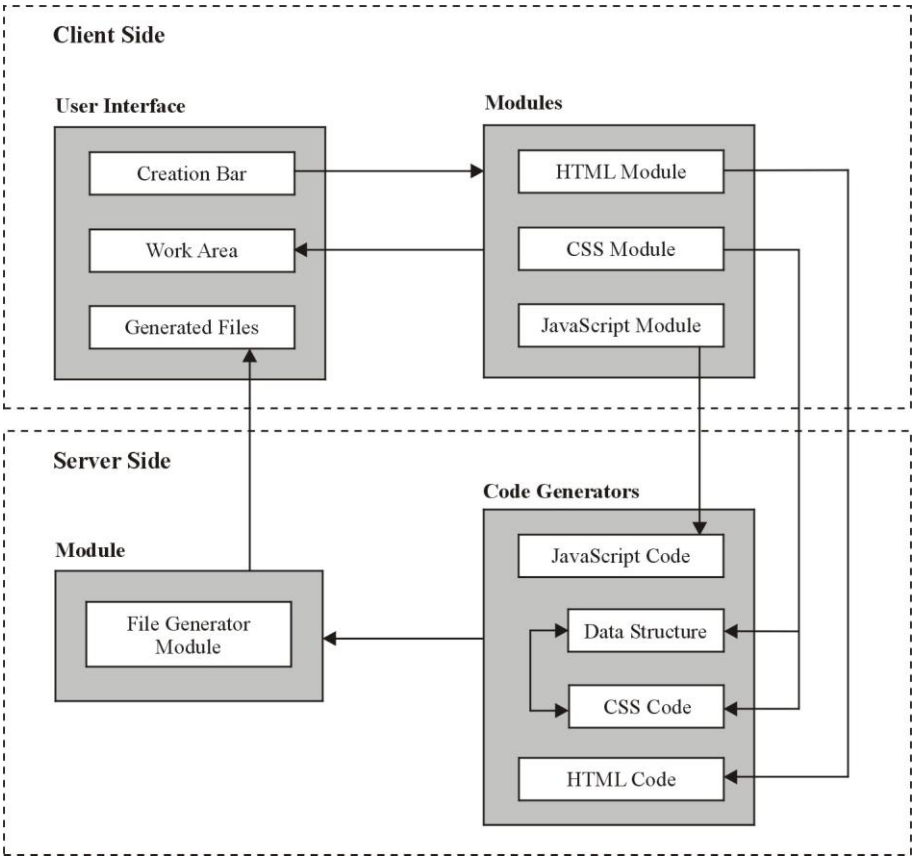

Fig. 1. Web Page Generator client-server architecture.

3.1 Client side

The client side of the tool has two main blocks, which are shown in Figure 1. The first block involves a set of modules for the generation of HTML, CSS and JavaScript code. The second block involves a set of components for the web interface, such as the creation bar, the work area, and the component for the generated documents. The first block is described in the following paragraphs.

HTML Module. This module works on the client side. The user of the tool can place HTML elements on the work area, through the creation bar. This module is also in charge of administering the attributes of the elements used.

CSS Module. This module works mainly on the client side, but it also has part of its functionality on the server side. It allows the creation of CSS styles, which are applied to the HTML elements placed on the work area. It also stores a data structure for the styles created, which are then used for the generation of the code. The tool is able to apply CSS styles at three different levels: 1) *Class level* allows creating a CSS class, defining attributes and values, and applying that class to any element; 2) *Ele-*

ment level allows applying a style to all the elements of the same type on the work area (for example, all div elements on the work area); 3) *Element id level* allows defining a style for a unique element, which is the element selected on the work area.

JavaScript Module. The functionality of this module is on the client side. It allows providing the validation for HTML input elements, where the validation of such elements can be seen instantly on the work area.

3.2 Server side

There are two blocks that are part of the server side, which are illustrated in Figure 1: the code generators and the file generator module. These blocks are described below.

Code Generators. There are three code generators: one for HTML, one for CSS, and one for JavaScript; which generate the necessary code to pass it to the file generator module. The CSS code generator uses a data structure to store in memory all the CSS styles that were created in the CSS module, described previously. The aim of the data structure is to contain, modify or delete all the CSS style information.

File Generator Module. The functionality of this module is divided in two steps. In the first step, it collects the information from the HTML, CSS and JavaScript code generators. In the second step, once the tool has loaded in memory all the code from the three code generators, it applies the format and constructs all the necessary files. It then takes the created files and zips them; finally, a link is returned to the web user interface, where the files generated can be downloaded.

4 Web user interface

The web user interface for the online tool is shown in Figure 2, where its components are identified by numbers: 1) creation bar, 2) work area, 3) edition bar, 4) tree bar, and 5) visualization bar. These components are described in this section.

Creation Bar (1). This bar shows all the HTML elements that can be placed on the work area. The user clicks on the icon of the HTML element desired in order to place it on the work area where the cursor is located. Table 1 illustrates some of the icons used on the creation bar, and the actions associated with them.

Work Area (2). The work area shows the construction of the web page, the HTML elements placed, the CSS styles associated with the elements, the validations for the text fields, and in general any element that is created. The work area has some editor features, so that the cursor can be placed anywhere on it, and write directly with no need of introducing any HTML element explicitly through the bar. Figure 3 shows the work area of the Web Page Generator, with some HTML content placed graphically on it by the user, such as tables with several rows and cells, images, formatted text, hyperlinks, div containers, paragraphs, headers, etc. Additionally, in section 5 there are some examples of completed web pages generated with this tool.

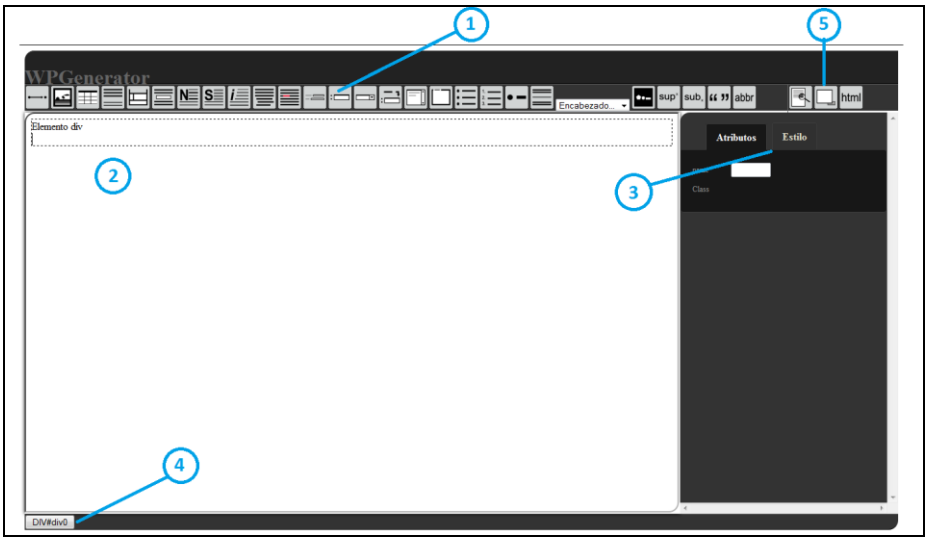

Fig. 2. Web Page Generator user interface.

Edition Bar (3). There are two important tasks that can be accomplished with the edition bar, through the two tabs that appear on it. The *Attributes* tab shows the attributes used on the selected HTML element; and the *Styles* tab shows all the CSS styles that can be applied to the HTML element selected, in different levels: *class level*, *element level*, or *element id level*.

Table 1. Some icons of the creation bar and their associated actions.

Icon	*Action*	*Icon*	*Action*
	It places an element *a* on the work area.		It shows options for placing an element *img* on the work area.
	It shows options to place an element *table* on the work area.		It places an element *p* on the work area.
	It places an element *div* on the work area.		It places an element *iframe* on the work area.
	It places an element *form* on the work area.		It places an element *select* on the work area.
	It places an element *textarea* on the work area.		It places an element *ol* on the work area.

Tree Bar (4). This bar shows information about the elements tree in the web page being generated. It shows how nested an HTML element is with respect to other HTML elements. It is also used as a selector of HTML elements. It should be noticed that the structure of HTML is based on nesting elements.

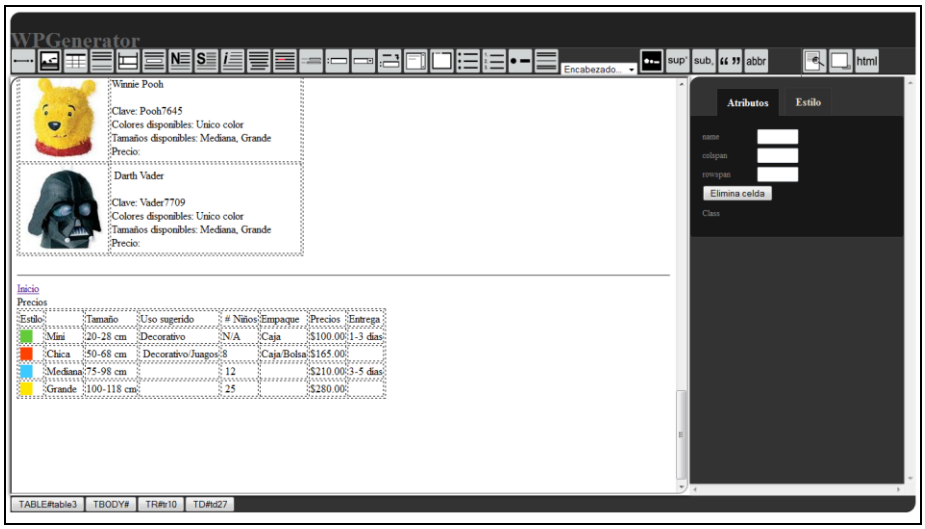

Fig. 3. Work area with some HTML content placed graphically.

Visualization Bar (5). This bar contains three buttons, which are the following (from left to right): *Preview*, *Hide Panel*, and *Generate Code*. The *Preview* button allows visualizing a preliminary view of the web page in full screen; the *Hide Panel* button hides or visualizes the *Edition Bar*; the *Generate Code* button allows generating the three files (with the HTML, CSS and JavaScript code), which are the result of the web page created on the work area. The *Generate Code* button also generates a zip file with the files mentioned, which can be downloaded from the web interface. Figure 4 shows a very small fragment of the HTML code generated automatically (Darth Vader image and text) for the web page illustrated in Figure 3. For display purposes and due to the lack of space, the code is shown without break lines.

```
<tr id="tr8">
  <td id="td16"> <img src="starWars.jpg" id="img15"
    title="starWars.jpg" /> </td>
  <td id="td17"> <span id="span40"
    style="font-weight: bold;">Darth Vader</span><br/><br/>
   <!-- rest of the code omitted -->
```

Fig. 4. Fragment of the HTML code generated automatically.

5 Examples of web pages generated

This section shows two examples of web pages that have been generated with Web Page Generator, which has been in constant use. Figure 5 shows a web page with nested HTML elements, which have CSS styles. The web page was generated using div elements, tables, rows and cells, text formats, headers, images and a form with JavaScript validation. It can be observed the use of CSS styles to modify the presentation of the web page, such as the background color at different levels, text color for different headers and text on the page, some other text attributes, table borders, cell borders, text alignment, etc. JavaScript code is only used for validation of the input HTML elements of the form, at the end of the web page.

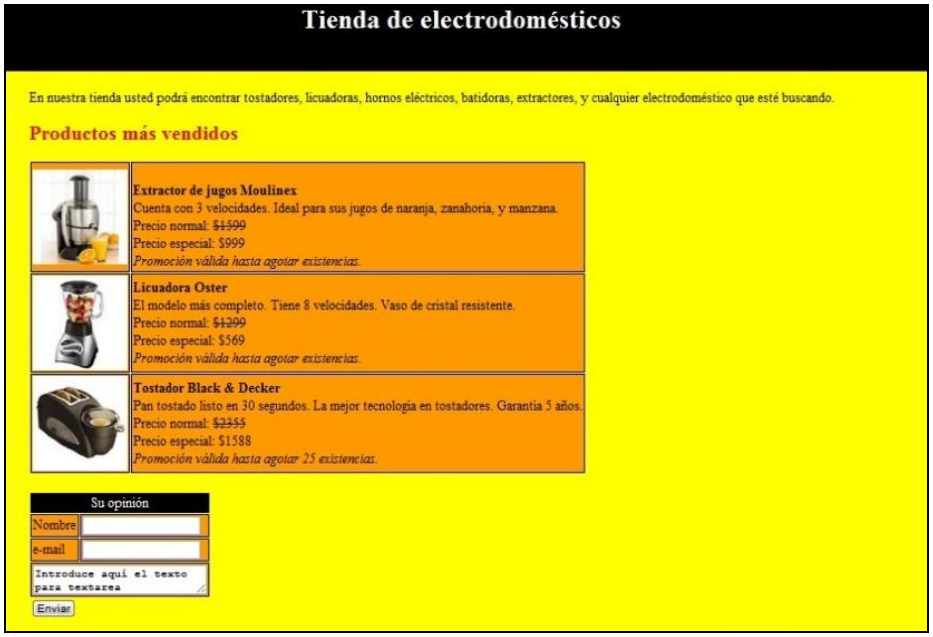

Fig. 5. Web page generated with Web Page Generator.

Figure 6 illustrates a web page with a more complex distribution of elements, background images, a menu, and text formats. It also uses div elements to separate the content of the web page; it has a banner on top, a top menu, a right menu, and the content aligned to the left. Some of the HTML elements used are the following: lists, tables, images, forms, inputs, paragraphs, headers, hyperlinks, divs, etc. The use of CSS styles to modify the presentation of the web page is also illustrated with color attributes, text attributes, table attributes, div attributes, paragraph attributes, and some other CSS attributes. Concerning the JavaScript programming language, the web page generated in this example, also includes a form with input elements and validations on them, such as the email format.

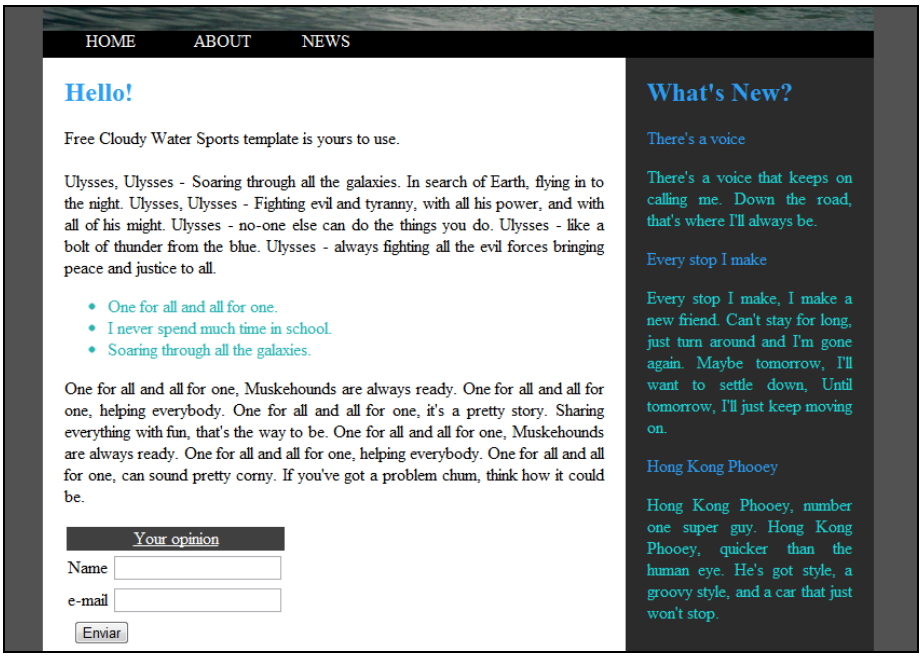

Fig. 6. Web page generated with a more complex distribution of elements.

6 Conclusions and future work

The aim of this work was to create an online tool that allows the construction of web pages graphically, and the automatic generation of HTML, CSS and JavaScript code. The Web Page Generator presented in this paper not only constructs web pages, but it also generates separated source files with clean code for the three languages mentioned; and it is also an open source tool. It should be noticed that none of the tools analyzed in the state of the art has all the features explored. Web Page Generator can generate web pages with most of the existing HTML elements, such as paragraphs, headers, lists, images, tables, forms, divs, image maps and areas, input elements, etc.

There has been some testing for the creation of web pages with the tool, and it has been successfully observed that the code generated for any of the web pages created, is understandable, clean, well structured, and editable; so that users with more experience in these three languages can modify, delete, or insert more content to the source files of the web page created. Currently, the online tool generates source files for HTML, CSS and JavaScript. However, in the future it is planned to create a module for reading existing source files. The main idea of this new module is to provide the possibility of opening source files from the web user interface, so that the tool can construct the page graphically, without the need of modifying the source manually.

Further work is needed to implement some other modules, such as a module for the administration of web pages, and a module for the construction of web pages with more than one HTML and CSS files. The first module aims to create user accounts;

where users can create their web pages and store them in the online tool, edit them and administer them later on. The construction of web pages with more than one file will allow users creating more than one HTML file and associate it with several CSS files, and have a complete web site composed by several HTML and CSS files.

Once the usability tests are finished, the web interface will be modified according to the results. It is also planned to use the tool to support some of the exercises for a Web Programming course of the Information Technology undergraduate program.

References

1. Peña de San Antonio, O.: Dreamweaver CS5, Madrid, Anaya.
2. CodeRun-Online IDE. Available at http://www.coderun.com/ide/. [Accessed in June 2013].
3. Jaimez-González, C., Vargas-Rodríguez, A.: An Online Tool for Creating Web Pages and Generating Code Automatically, In Proceedings of the International Conference on Applied Computing 2013 (AC 2013), ISBN: 978-989-8533-20-3, pp. 211-215, Fort Worth, Texas, USA, 23-25, (2013).
4. HTML Editor. Available at http://htmledit.squarefree.com/. [Accessed in June 2013].
5. CKEditor. Available at http://ckeditor.com/demo. [Last accessed in June 2013].
6. Okamoto, S., Dascalu, S., Egbert.: Web Interface Development Environment (WIDE): Software Tool for Automatic Generation of Web Application Interfaces, In Proceedings of the World Automation Congress (WAC 2006), pp.1-7, 24-26, July (2006).
7. Bochicchio, M., Fiore, N.: WARP: Web Application Rapid Prototyping, In Proceedings of the 2004 ACM symposium on Applied computing (SAC 2004). ACM, New York, NY, USA, 1670-1676. DOI=10.1145/967900.968232.
8. UWA Project. Available at http://www.uwaproject.org/. [Last accessed in June 2013].
9. Djemaa, R.B., I. Amous, Hamadou, A.B.: GIWA: A generator for adaptive Web applications, In Proceedings of the International Conference on Internet and Web Applications and Services/Advanced Telecommunications (AICT-ICIW 2006), pp. 211, (2006).
10. Nakano, K., Hu, Z., Takeichi, M.: Consistent Web site updating based on bidirectional transformation, In Proceedings of the 10th International Symposium on Web Site Evolution (WSE 2008), pp.45-54, 3-4 October 2008. doi: 10.1109/WSE.2008.4655395,(2008).
11. Liu, D., Hu, Z., Takeichi, M.: Bidirectional interpretation of XQuery, In Proceedings of the 2007 ACM SIGPLAN Symposium on Partial evaluation and semantics-based program manipulation (PEPM '07). ACM, New York, NY, USA, pp. 21-30, (2007).
12. Karger, D., Ostler, S., Lee, R.: The web page as a WYSIWYG end-user customizable database-backed information management application, In Proceedings of the 22nd annual ACM symposium on User interface software and technology (UIST '09). ACM, New York, NY, USA, 257-260, 2009. DOI=10.1145/1622176.1622223.
13. Wolber, D., Su, Y., Chiang, Y.: Designing dynamic web pages and persistence in the WYSIWYG interface. In Proceedings of the 7th international conference on Intelligent user interfaces (IUI 2002). ACM, New York, NY, USA, 228-229, (2002).
14. Ono, K., Koyanagi, T., Abe, M., Hori, M.: La generación de hoja de estilo XSLT por ejemplo con un editor WYSIWYG, Simposio de Aplicaciones e Internet (SAINT 2002), pp.150-159, de 2002. doi: 10.1109/SAINT.2002.99447, (2002).

Towards a Web Learning Environment for Supporting Object Oriented Programming Courses

Carlos R. Jaimez-González, Wulfrano A. Luna-Ramírez

Departamento de Tecnologías de la Información, Universidad Autónoma Metropolitana - Cuajimalpa, Av. Constituyentes No. 1054, Col. Lomas Altas, C.P. 11950, México D.F.
{cjaimez,wluna}@correo.cua.uam.mx

Abstract. Computer programs written in the Java programming language require the Java development kit in order to be compiled and run; this can be accomplished through a command line or using an integrated development environment on the computer where the program is being written. This paper presents a web learning environment, which is composed of an online code editor, initially for the Java programming language, but it can be extended to other object-oriented programming languages, such as C++. This web environment is designed with features that support students during the process of learning this programming paradigm, such as allowing them running the code edited, showing the output of the program, showing the list of exceptions occurred during compilation and pointing out the place of the exception. All these features are accessible through the web environment, which can be used by students through a web browser on any computer with Internet access.

Keywords. Java programming language, object-oriented programming, web learning environment, online compilation, interactive web environment.

1 Introduction

The Information Technologies and Systems undergraduate program at our faculty has an Object-Oriented Programming course, additionally to other courses that require the use of object-oriented programming languages. It could be of great support for students to have a web learning environment that helps them in the process of learning object-oriented programming, such as its main principles and concepts (classes, objects, methods, attributes, inheritance, polymorphism, etc.), and make transparent the compilation and execution of programs.

A web learning environment for supporting object-oriented programming courses is being developed, which uses the Java programming language, but it can be extended to other object-oriented languages, such as C++. This web environment will support the process of teaching and learning for object-oriented programming courses. The reason for using Java is simply because most of the lecturers use Java as the programming language for their courses. There are some projects available on the web, which are tools for supporting programming from a web platform, but some of them are very simple [8], expensive [6][7], or they do not provide the possibility of work-

© E. A. Santos, J. C. Chimal, L. Cabrera, E. Castillo.
Advances in Computer Science and Engineering
Research in Computing Science 67, 2013 pp. 33–41
Paper Recived 31-08-2013 and Acepted 21-10-2013

ing with Java [5]. Some others provide the possibility of working with several files at the same time [7][8], or compiling online and running offline [4].

Computer programs written in the Java programming language require the Java Development Kit (JDK) in order to be compiled and run; this can be accomplished through a command line or using an Integrated Development Environment (IDE) on the computer where the program is being written. Figure 1 shows the process of edition, compilation, and execution of Java programs. The complete process starts with the creation of .java files with the source code, the use of the editor for writing the program (source files), the delivery of the files for compilation, the actual compilation, the generation of the .class files (in case there are no syntax errors), the execution of the program through the Java Virtual Machine (JVM), and the visualization of the program output.

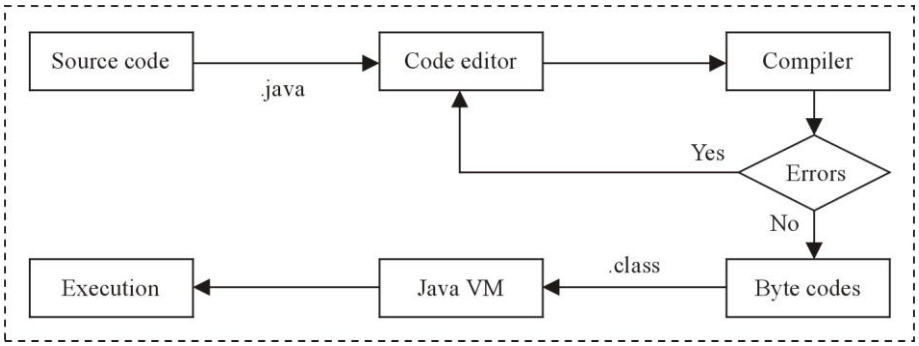

Fig. 1. Process of edition, compilation and execution of Java programs.

The web environment is composed of an online code editor for object-oriented programming languages, such as Java or C++. The environment has features to help students during the learning process of this programming paradigm; such as allowing them executing the edited code; showing them the output of the program; showing them the list of errors during compilation, and where they are inside the code. Students do not need to leave the web learning environment to use all these features, because they are built in the environment. A remote compiler will also be provided by the environment, so students do not need to install any. This way, they can learn and practice object-oriented programming while studying a tutorial, without the need of navigating between different applications (source files, web browser, books, etc.).

This web learning environment is thought to be stand-alone, which allows the student accessing it and working with it through a web browser, from any computer with Internet access. Additionally, this learning environment is planned to be incorporated to the online interactive tutorials platform, which is being developed [16].

The rest of the paper is organized as follows. Section 2 presents a brief summary of some existing tools that are relevant to this project; mainly tools for edition, compilation and execution of code. Section 3 describes the architecture of the web learning environment; the software and supporting tools used; the edition, compilation, and

execution of programs; and the help section for the segments of code with errors. Finally, section 5 provides conclusions and future work.

2 Related tools and applications

This section reviews some existing tools that are related to the web learning environment being developed. Among the tools found, there is a tool that covers some of the features desired in the web learning environment; however, it is expensive, and it is thought as an online IDE and not as a tool for learning a programming paradigm. There are also some tools that are actually plug-ins, which can be used to implement some of the features planned for the web learning environment. Table 1 shows some of the existing tools, along with a brief description of their purpose.

Table 1. Tools for edition, compilation, and execution.

Name	*Description*
Compilr	Online IDE.
Codepad	Compiler/interpreter.
DJGPP Public Access	Cross-compiler service for creating small programs in DOS.
Ideone	Online compiler and debugger.
JXXX Compiler Service	Remote compilation service for Java files.
OnlineCompiler	Online compiler.
CodeMirror	JavaScript component that provides a code editor for Web.
CodePress	Online code editor, written in JavaScript.
EditArea	Code editor, written in JavaScript.

Compilr [7] is a web application that allows creating projects in different object-oriented programming languages. It provides a file browser interface, it is multi-language and allows the edition of more than one file at the same time; it has a code editor and syntax highlighting; it provides a remote compiler, and executes the code with input parameters taken from the user; it visualizes the output, and allows the execution of Java *Applets* [15]; it is similar to *Eclipse* [13] and *Netbeans* [14].

Codepad [5] is a compiler/interpreter of code that can be used by 10 different programming languages. It has no support for the Java programming language, but for others, such as Python, Ruby and C++. *It* provides a multi-language code editor, remote compilation, and it allows visualizing the output of the program after execution; its functionality is more oriented to code debugging, because it highlights the code lines where it finds an error.

DJGPP Public Access Cross-Compiler [8] is a service designed for users that need to create small programs in DOS and do not have access to a computer with a compiler. It only has support for programs in the C programming language. It is a very basic application, because it only has support for one language, and its interface is limited with only a small text area with two options: *Warnings* and *Optimize*.

Ideone [10] is an online compiler and debugger, which allows compiling and executing code in 40 programming languages. It has a code editor, syntax highlighting,

multi-language, remote compiler, and it allows input from the user for the execution; it also visualizes the output of the program. It can only executes programs with one source file; it does not allow the execution of Java *Applets*.

JXXX Compiler Service [11] is a service for remote compilation of source files written in the Java programming language. This tool allows the execution of *Applets* without having installed the JDK. This tool is basically a form with remote compilation, loading of libraries, selection of different JDK, and the possibility of compiling several files at the same time. This service also includes the option to load an HTML file for visualizing *Applets*. It does not have a text editor to write code.

OnlineCompiler [12] is a web site to paste and compile code. It does not show any output from the programs, because its main functionality is to detect syntax errors of the 5 different languages it supports (C/C++, Fortran, Java, Pascal and Basic). It has a code editor, it is multi-language, and it can compile source files remotely. The web interface of this tool allows writing or pasting code on a text area, in order to compile it. The result of the compilation is a web page with a link to the source file, and another link for the executable or compiled file.

CodePress [6] is a source code editor, written in *JavaScript*, which colors the text as it is being written on the web browser. Some of its main advantages are the following: syntax highlighting, auto-complete, possibility of having multiple windows of code inside the same web page, and the support for several programming languages.

EditArea [9] is a free code editor, written in *JavaScript*, which is designed for editing source code inside of a *<textarea>* element; it has several functionalities that are useful, such as syntax highlighting, tabs support, well-formatted text, search and find functions, auto-indent, and the possibility of having multiple instances.

CodeMirror [4] is a *JavaScript* component that provides a code editor with syntax highlighting, indentation, search and replace. It is a code editor that can be embedded in a web page, and can be adjusted to the desired window size, which affects the way it visualizes the code.

3 The web learning environment

This section presents the architecture of the web learning environment, the software and supporting tools used for its development (edition, compilation, and execution of programs), and the help sections that are provided for the code with errors.

3.1 System architecture

The web learning environment is based on a client-server architecture. The server is in charge of the compilation and execution of programs; it also registers the output of the program and any errors or exceptions occurred. The client side shows the web interface, which is composed of a source code editor, where the user can edit the code and send it to the server side to be compiled and executed, as it is shown in Figure 2.

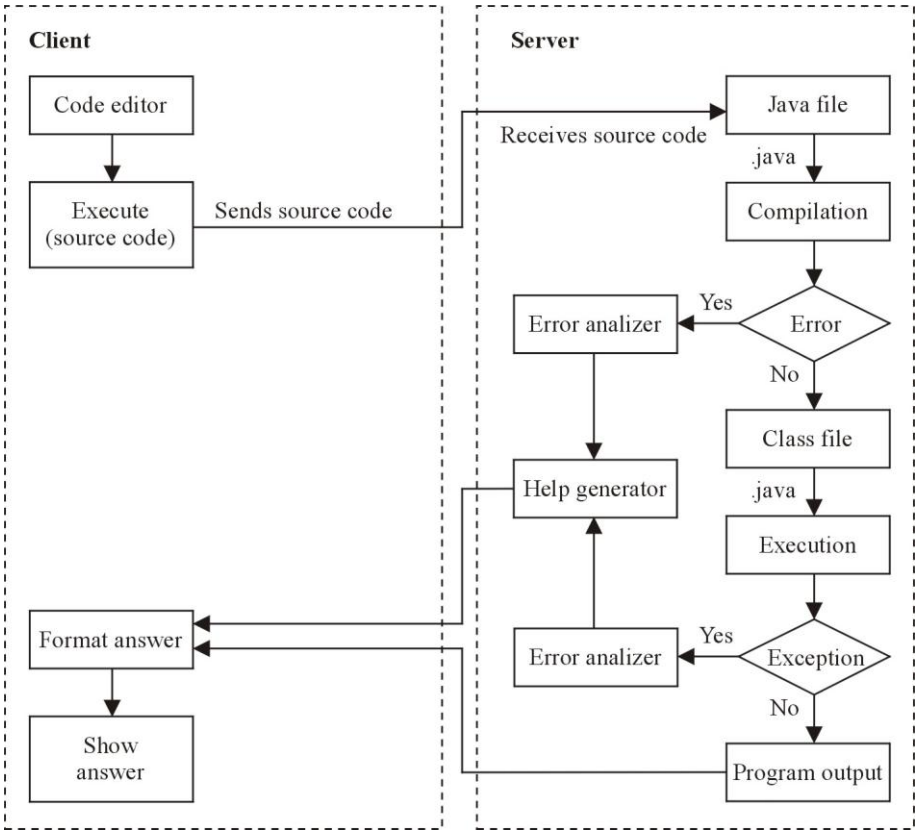

Fig. 2. Client and server sides: edition, compilation and execution of Java programs.

3.2 Software and supporting tools

The web environment uses Apache Tomcat as a web server and container of Java Server Pages; it is also used for the dynamic generation of content, and database connectivity. Java is the programming language for the business classes; it also has the *JavaCompiler* class, which is used for the compilation of programs on the server side. For the web user interface it is used HTML, CSS, and JavaScript: HTML for the structure of the content, CSS for the presentation of the content, and JavaScript for the interaction with the user and for the asynchronous method calls to the server.

3.3 Edition

After having reviewed several code editors with syntax highlighting [4][6][9], *CodeMirror* was chosen, because it is the most complete editor from the ones evaluated. Although the web learning environment is only using syntax highlighting and

auto-indentation, in the future it can use more features of *CodeMirror*, such as auto-complete, pre-visualization of HTML, auto-complete of XML tags, etc.

Figure 3 shows the initial version of the web interface, where it can be observed three panels. The left panel shows some examples of the syllabus established for the environment; the top panel shows the code editor, and the bottom panel shows the console for compilation and execution of programs. The top panel has an example of a Java class, which is also shown in Figure 4.

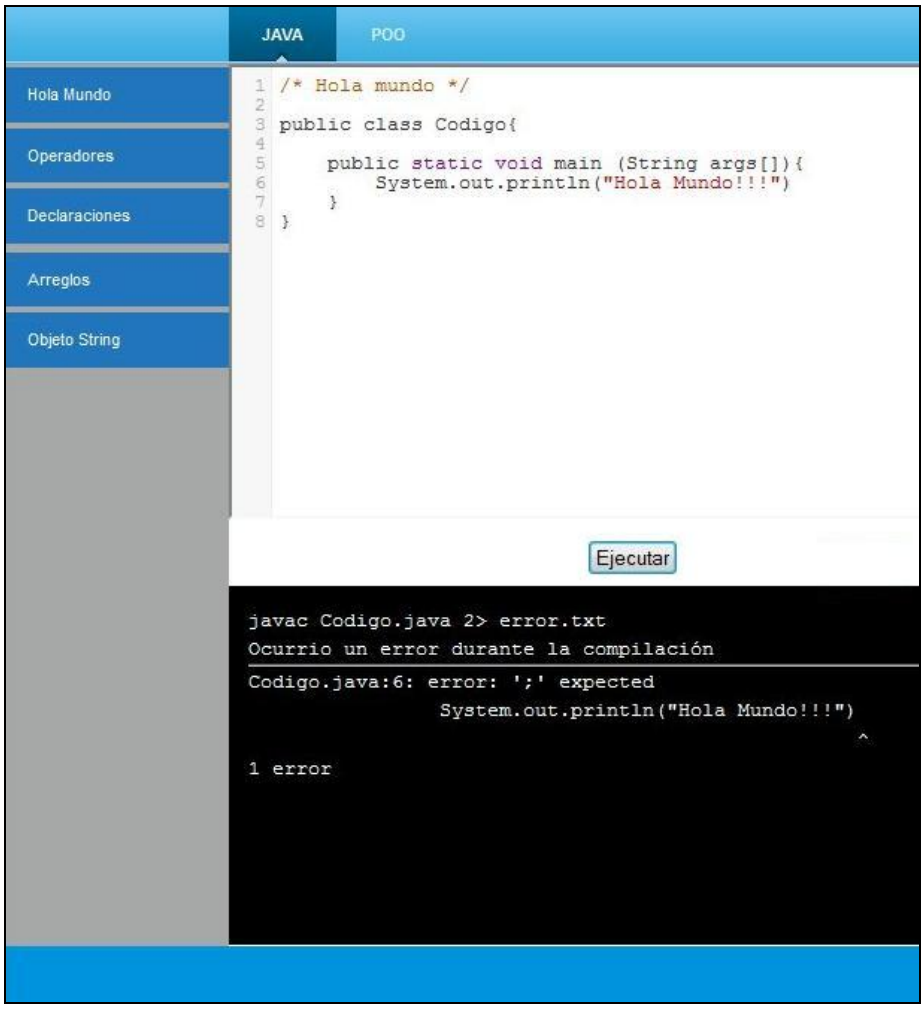

Fig. 3. Interface of the web learning environment, with examples and code editor.

Figure 4 shows an example with a syntax error. Due to this error, it can be observed in Figure 3 the error message at the bottom panel.

```
public class Codigo{
    public static void main (String args[]){
        System.out.println("Hola Mundo!!!")
    }
}
```

Fig. 4. Java class example with a compilation error.

3.4 Compilation and execution

There is a Java interface called *JavaCompiler*, which allows invoking programs; it provides methods for compiling the source code generated in the code editor, and also for capturing the errors generated during compilation and execution. Inside the web learning environment, this interface is implemented on the server side to provide compilation and execution services.

3.5 Help

This is one of the most difficult tasks. The web environment will offer information about the errors occurred during compilation, or exceptions occurred during execution. The environment will have a menu, from which there will be well-commented examples with brief explanations, which will serve as support for students for familiarizing and understanding the object-oriented programming paradigm. This is accomplished through the Java programming language, using simple examples of the topics covered for the web environment, such as those found in [1], [2], or [3].

The editor area will provide the help material. The main features of this editor are the following: 1) edition of code with syntax highlighting; 2) online compilation and execution of source code with only one click; 3) visualization in the web interface of compilation or execution errors, with an option to see an example related with the error; 4) mapping of errors inside the source code (highlighting the line where the error occurred), 5) viewer of applets.

4 Conclusions and future work

This paper presented a web learning environment, which is composed of an online code editor, initially for the Java programming language, but it can be extended to other object-oriented programming languages, such as C++. This web environment is designed with features that support students during the process of learning this programming paradigm, such as allowing them running the code edited, showing the output of the program, showing the list of exceptions occurred during compilation and pointing out the place of the exception. All these features are accessible through the web environment, which can be used by students through a web browser on any computer with Internet access. The web learning environment is under development, alt-

hough there is an initial working version. Additionally, it is planned that this environment could be incorporated to an online tutorials platform.

Further work is needed to finish the web environment with the complete functionality to compile and execute programs; as well as the functionality to implement the help for students, which will show the exact place of the error, along with examples to reinforce the knowledge acquired; and the possibility to include a reference to the Java API corresponding to the topics covered. It is needed to carry out tests and evaluations to determine the effectivity of the web learning environment in the teaching-learning process in the object-oriented programming courses.

References

1. Eckel, B. Thinking in Java (4th Edition), Prentice Hall (2006).
2. Flanagan, D. Java in a Nutshell (5th Edition), O'Reilly Media (2005).
3. Arnold, K., Gosling, J., Holmes, D. The Java programming language (4th Edition), Addison Wesley Professional.
4. CodeMirror. Available at: http://codemirror.net/. Last access in July 2013.
5. Codepad. Available at: http://codepad.org/. Last access in July 2013.
6. CodePress. Available at: http://codepress.sourceforge.net/. Last access in July 2013.
7. Compilr. Available at: http://www.compilr.com/. Last access in July 2013.
8. DJGPP Public Access Cross-Compiler. Available at: http://www.delorie.com/djgpp/compile/. Last access in July 2013.
9. EditArea. Available at: http://www.cdolivet.com/editarea/. Last access in July 2013.
10. IdeOne. Available at: http://ideone.com/. Last access in July 2013.
11. Java Compiler. Available at: http://www.innovation.ch/java/java_compile.html. Last access in July 2013.
12. Online compiler. Available at: http://www.onlinecompiler.net/. Last access in July 2013.
13. Eclipse. Available at: http://www.eclipse.org/org/. Last access in July 2013.
14. NetBeans. Available at: http://netbeans.org/. Last access in July 2013.
15. Oracle Corporation Applets. Available at: http://java.sun.com/applets/. Last access in July 2013.
16. Jaimez-González, C., Sánchez-Sánchez, C., Zepeda-Hernández, S. Creating and Administering Interactive Online Tutorials and Performance Evaluation Tests Through a Novel Web Platform. International Journal for Cross-Disciplinary Subjects in Education (IJCDSE), Volume 2, Issue 3, ISSN: 2042 6364 (Online), pp. 447-455, 2011.

An Epistemological approach for Learning Computer Programming Languages

Emilio Buendía Cervantes[1], Jesús Manuel Olivares Ceja[2]

[1] Acciones para el Aprendizaje Autónomo, S. C.
CP 03300 D. F., México, Ciudad de México

[2]Centro de Investigación en Computación del Instituto Politécnico Nacional (CIC-IPN)
Av. Juan de Dios Bátiz esq. Othon de Mendizabal S/N
CP 07738, Ciudad de México

expressdelavida@yahoo.com.mx, jesuso@acm.org

Abstract. This article presents the results of applying an epistemological model for students learning computer programming languages. The proposal is based on a characterization of the typical elements that form an information system.

Three learning principles, an epistemological model are used to facilitate students' knowledge acquisition. Information availability, activity performance and feedback are applied for each epistemological category to detect student advances and provide guidance and supplementary materials.

Motivation toward innovative ideas proposal and development is provided whenever possible during knowledge acquisition process.

Learning evaluation is based on the mastering of the epistemological categories and final evaluation is assigned considering the best category reached during learning process.

Keywords: epistemological model; programming languages learning; learning principles

1 Introduction

This paper presents an epistemological model and learning principles as an alternative to promote knowledge acquisition in e-learning [1] [2] and F2F (Face to Face) teaching-learning process mainly focused on learning computer programming languages, as an attempt to contribute in the formation of professionals required by enterprises, the academy and the science. It is known that programmers with adequate preparation and experience each year are increasingly needed for software development since software crisis started in 1968.

© E. A. Santos, J. C. Chimal, L. Cabrera, E. Castillo.
Advances in Computer Science and Engineering
Research in Computing Science 67, 2013 pp. 41–51
Paper Recived 21-09-2013 and Acepted 21-10-2013

What to teach and how [3] has been considered by free thinkers like Plato, Rousseau, Froebel, Dewey and others dating back several centuries. The ideas discussed by those people follow two extremes: on one hand, children and young people must learn what government dictates, or on the other hand, they should be given freedom to learn knowledge and skills. Currently both initiatives are used for teaching and learning and it is hard to notice any separation.

Technology and computer development during the late twentieth century promoted interest to include them in classrooms as tools to support the teaching-learning process. Many terms to describe this trend have emerged such as learning online, virtual learning, Computer Assisted Learning (CAL), e-Learning, m-Learning, among others. In many cases the teacher can be replaced by computer programs like online tutorials or online content that use computer questionnaires for students to check their progress.

Computer science advances are notable, starting with the representation of numbers using bits, continuing with coding letters using groups of bits, sequences of characters, and until recent information representation in augmented reality systems and high speed networks for information exchange. However, technology advances are not enough to guarantee that people could learn how to build computer programs. Besides technology cannot reach people with no electricity service, and software advances are out of reach of those who lacks of computers.

In literature there are many papers and online reports on the use of learning platforms and tools [4] [5] [6] [7] [8]. Learning styles [9] could be grouped on presence, distance, and blended learning; and have been applied with different success levels. Evaluation considering several variables measures student progress and the learning process (tools, schedule, and contents) to improve online courses. Interest on these new learning styles is concentrated on teaching different subjects.

Nowadays, the most common strategy to promote knowledge is "reward and punishment". For example, many children attend school to avoid punishment from parents, and at school they pretend attending the class and learning to avoid punishment or lose points for not paying attention. However, the reality is revealed during exams; the students did not learn and failed the exams. As a consequence of the "reward and punishment" strategy many students decide to abandon schools at different levels.

Technology and developments such as computers, tablets, smartphones, the Internet and Web do not guarantee that the learning processes occur or students get motivated for learning, nor eliminate dropping out of school. Despite technology and the introduction of multimedia presentations students are abandoning the learning process.

As a consequence of teaching problems and lack of interest of the students, some researchers [10] [11] question whether reviewing learning theories should be considered. Some theories of learning already proposed are:

A. Behavioral theory [12] (attributed to B. F. Skinner)

This theory is based on reinforcing the action of a person that corresponds to what is expected to be learned. For measuring learning it is observed if there is a change in behavior. To promote learning both the stimuli and the environment need to be organized adequately.

B. Cognitive Theory (represented by J. Bruner)

In this theory knowledge acquisition involves an internal coding and structuring by the student. Learning is a process of rearranging or transforming the data so that a student acquires and understands. Learning is expected to occur by discovery (serendipity).

C. Soci –historical–cultural theory (attributed to L. S. Vygotsky)

This theory considers that the human being is a social being and learning occurs when multiple people interact.

D. Theory of observation and imitation (attributed to A. Bandura)

This theory shows that there are internal mechanisms of information representation that allow learning by observation and imitation.

E. Eclectic theory (attributed to R. Gagne)

The learning process is organized based on needs and priorities; therefore this theory is aimed for students achieving specific goals.

F. Theory of constructivism (attributed to J. Piaget)

Learning takes place through two simultaneous and opposite movements: assimilation and accommodation. In assimilation individuals explore the environment and make decisions that transform and integrate parts that are found in the environment. In accommodation, the individual trans-

forms their inner structure to reflect the nature of the objects found in the environment.

G. Theory of complexity (attributed to E. Morin)

Consider learning as based on a combined epistemology: social, biological, mind, spiritual, logic, linguistic, cultural, social and historical; as opposed to traditional epistemology that is only cognitive. This means that systems under study are "complex systems" that should be considered under different viewpoints.

H. Conexionism theory (attributed to G. Siemens and S. Downes)

This theory was created to take into account the influence of technology (mainly computer and networks) on the learning process.

The inclusion of computers in the teaching-learning process is an alternative tool that provides contributions to the transmission of knowledge and also helps detect the progress of students learning. Furthermore, learning theories have greatly contributed to the development of mankind. However, it requires some guide in the learning process that in this work is provided by an epistemological model.

2 Epistemological model for learning computer programming languages

Epistemology is a discipline dedicated to study knowledge and its genesis. Based on experiences looking for models to enable students to acquire knowledge, particularly in computer programming languages, an epistemological model was proposed in [13] and adapted [14] for this paper as shown in figure 1 considering that computer programs could be considered formed by three main elements [15] [16]:

a) Data, those representing values, variables and real entities representations.
b) Process, those that transform data.
c) Structure that determines the order of process application on data.

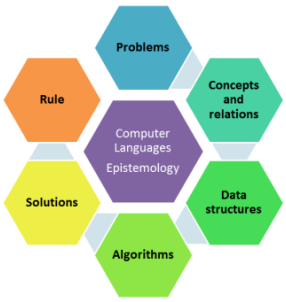

Figure 1. Epistemology for learning computer languages

A. Scenario

The scenario consist in configuring with materials and tools needed to promote learning and exercise activities and practices related with the topic of interest that in this case is computer languages learning and application. This is the main labor of the teacher who makes arrangements and prepares materials, projections and the agenda for the teaching–learning process guided with the epistemological model.

B. Problem establishment and hypothesis

Each problem is proposed, discussed and has a hypothesis to solve it. This activity is mainly carried out by the student with the teacher supervising them and asking to use their imagination in a certain situation related with the problem. Sub-problems may arise during the process. In this step, it was found that many times some student proposed solutions instead of problems; therefore, the feedback was devoted to help students on detecting what a problem is and what is not. The tools that were used to register problems and hypothesis were text processors.

C. Concepts and relations among them

In this epistemological category, each student is given questions with concepts related with the problem under consideration. They are asked to look for answers in different media including books, magazines, Web pages, or their own experience. The answers must be placed in documents showing the question, the author (student name), the reference, the answer and an example.

Students answer questions using a text editor and send the result to the teacher via email. Feedback on each answer is provided by the teacher and the student is asked to produce a conceptual map that reflects the understanding on the concept relationship. In this activity any soft-

ware tool can apply (e. g. EDraw Mindmap®). The result is also sent to the teacher via email and returned with feedback and teacher's conceptual map for the student to review it. After the student reviews, a group discussion is carried out to obtain conclusions.

Once the students have knowledge [17] [18] [19] about concepts and relationships among them, the next step is on applying the knowledge implementing data structures and algorithms to solve small problems first then more difficult ones.

D. Data structures

In this category, a problem is proposed for the student to apply the concepts learned to data structures. Here it is expected that the student implements the solutions using a computer programming language. Data and the structures are formed using variables relating them in different ways. For example sorting a list of integers, and asked how to solve the problem (hypothesis), compare their proposal with known methods and then to identify which data and structures appear in the proposals. Teachers provide feedback to precise and complete the proposals. For this and the following categories it is necessary that the student manages an Integrated Development Environment (IDE), like Java programming language or C language.

E. Process

Computer processes transforms data in different ways: operators in expressions, control structures in program flow and functions in both of them.

Computer languages nowadays are provided with rich libraries of functions devoted to provide specific solutions. Regardless of that, students are motivated to build their own code to show their abilities to produce computer programs. The teacher reviews and analyzes each algorithm and invite students to compare their solution against other existing implementations to check which one has a better performance and then a discussion is opened.

F. Solutions

Solution is the category intended for the students to show their programs running with test data prepared by the teacher. For postgraduate students measuring performance is a very important topic.

G. Applications

Application is a category related with the use by a third party of the program produced.

H. Rule

Rule category reflects the experience obtained by each student during the development process; it is expressed in the form of a principle, postulate or in the best case a rule.

This model was applied to students from several universities and states of the Mexican Republic, providing for each of its categories the appropriate feedback as soon as possible.

3 Evaluating Learning

Evaluation is an important concern in the teaching–learning process. In this proposal, evaluation is related with mastering each of the categories of the epistemological model. Students are qualified related to the best epistemological category that each student reaches.

In a group of 19 students randomly selected to produce computer programs guided with the epistemological model proposed, the results shown in table III were obtained. Each student is represented with a confidential number.

Table III show the results of applying [13] the Epistemological Category Oriented Evaluation (ECOE). In that 4 out 19 students reached the rule category, resulted excellent oral presenters. Self-motivation is found in students that reached top categories.

Application level students are close to finding rules and therefore the labor of the teacher is to invite them to reflect and write on the learning process to find patterns that may be established as a principle or rule.

In other students, it was observed that they only learned concepts and rejected applying their knowledge on computer program implementation. They did not want to attend practices due to lack of interest. It is considered that should be incentivized to learn by providing more simple exercises and eventually provide more complex ones until they are able to face problems and develop a solution with data structures and algorithms.

Between the two mentioned distinguishable groups there are some students that are considered having reached the data structure or process

categories, and therefore, the teacher labor for them is to provide more practice that prepares them to eventually face real-life problems is an important concern in the teaching–learning process. In this proposal, evaluation is related with mastering each of the categories of the epistemological model. Students are qualified related to the best epistemological category that each student reaches.

TABLE III. EPISTEMOLOGICAL CATEGORY ORIENTED EVALUATION (ECOE)

Student	**Aspect evaluated**		
	Epistemological level	***Oral presentation***	***Feedback provided***
1	Relations	good	Personal attention
2	Rule	Excellent	Already self-motivated
3	Rule	Excellent	Do more practice
4	Rule	Excellent	Apply skills
5	Application	No	Share skills
6	Concepts	Very good	Try to learn
7	Concepts	Regular	Get interested
8	Concepts	No	Get interested
9	Rule	Excellent	Self-motivated
10	Concepts	Bad	Get interested
11	Process	Regular	Must try to learn
12	Application	Very good	Learn more
13	Application	Very good	Learn more
14	Application	Very good	Self-motivated
15	Process	Good	Must try to learn
16	Concepts	Good	Get interested
17	Application	Very good	Need Learn more
18	Relations	Good	Need Learn more
19	Relations	Good	Need Learn more

TABLE IV. COMPARISON AMONG PROPOSALS FOR LEARNING COMPUTER PROGRAMMING LANGUAGES

Proposal	**Criteria**				
	Explicit epistemology	***Information availability***	***Activities***	***Feedback on activities***	***Explicit thought formation***
[4]	No	Yes	Yes	Yes	No
[5]	No	Yes	Yes	Yes	No
[6]	No	Yes	Yes	Yes	No
[7]	No	Yes	Yes	Yes	No
[8]	No	Yes	Yes	Yes	Yes
This proposal	Yes	Yes	Yes	Yes	Yes

4 Comparison with other approaches

Different authors and organizations have proposed tools for learning computer programming languages [4] [5] [6] [7] [8]. Table IV shows a comparison among those works and the proposal of this paper. It is possible to notice that in most cases information is provided to the student, examples and evaluation, but some of them lack of an explicit epistemological model to guide knowledge learning, for example, distinction among problem statement and solution is not emphasized; therefore students usually are guided to develop code without an application and as consequence students sometimes learn that code production do not deserve a benefit.

5 Conclusions and future work

In this paper an epistemological model and an evaluation approach based on categories are proposed to guide the teaching–learning process.

The application of the proposed model guides students in learning computer languages to produce computer programs by categories: concepts, relations among them, distinguish data and process, and implement algorithms that solve a problem. Preferably, the students should provide the program to solve a real-life problem and establish learned knowledge as a rule. The proposal was applied with students (male and female) at the graduate and postgraduate level from several universities in Mexico.

It was observed that the students who understood the model became self-motivated while other refuse to develop practices and only obtained limited concept learning. That indicates that the model should be learned first. More tests with students should be carried out to determine if the proposed model is convenient for computer language learning.

6 References

1. L. García, "Educación a distancia; ayer y hoy", retrived from http://www.quadernsdigitals.net/, published 1996
2. L. García, "De dónde venimos y hacia dónde vamos en Educación a Distancia" (Spanish), retrived 27.08.2013 from http://www.youtube.com
3. B. Cohen, Introducción al pensamiento educativo (Spanish), Ed. Publicaciones Cultural, S.A., México, D. F., 1977
4. Z. Harley, E. R. Harley, "A wizard for e-learning computer programming", International Congress on e-Learning and e-Technologies in Education (ICEEE), pp 95-98, 2012

5. S. Almajali, "Computer-Based Tool for Assessing Advanced Computer Programming Skills", International Congress on e-Learning and e-Technologies in Education (ICEEE), pp 114-118, 2012
6. A. Williams, "The Development of a Computer-Aided Learning Tool for Supporting the Teaching of Assembly Language Programming", Proceedings of the 29th Annual Hawaii International Conference on System Sciences, pp 323-331, 1996
7. A. Dzib-Tun, et. al., Una herramienta didáctica interactiva para la enseñanza-aprendizaje de los autómatas finitos deterministas en Memoria COMTEL 2013, ISBN 978-612-4050-69-5, Lima Perú, 2013
8. E. Vidal Duarte, Python como primer lenguaje de programación: un enfoque orientado a juegos en Memoria COMTEL 2013, ISBN 978-612-4050-69-5, Lima Perú, 2013
9. J. Stal, G. Paliwoda-Pekosz, "Teaching computer science blended-learning modules: A case study", International Congress on e-Learning and e-Technologies in Education (ICEEE), pp 119-123, 2012
10. R. Andrews, "Does e-learning require a new theory of learning? Some initial thoughts", Journal for Educational Research Online, Vol. 3, No. 1, pp 104-121, 2011
11. Hoyos M. C., et al., Epistemología y objeto pedagógico ¿es la pedagogía una ciencia?, editorial UNAM, Instituto de Investigaciones sobre la Universidad y la Educación, editorial Plaza y Valdes, ISBN 978-607-402-234-6, 2010
12. Skinner B. F., The Behavior of Organisms: An Experimental Analysis, Cambridge, Massachusetts: B. F. Skinner Foundation. ISBN 1-58390-007-1, ISBN 0-87411-487-X, 1938
13. E, Buendia, S. Leger, Epistemología para el aprendizaje autónomo (Spanish) (in press), Ed. Saber-hacer-comprender, México, 2013
14. Bochenski I. M., Los Métodos Actuales del Pensamiento (Spanish), octava edición, Ediciones Rialp, S. A., Madrid, España, ISBN 84-321-0106-0, 1973
15. F. Galindo Soria, Sistemas Evolutivos (Spanish) in *Boletín de Política Informática*, México 1986
16. F. Galindo Soria, Sistemas Evolutivos: nuevo paradigma de la informática (Spanish), in *memorias del congreso TEC-COMP 91*, México 1991
17. J. M. Olivares, A. Guzmán, "Aprendizaje aprovechando las ontologías del usuario y una fuente de conocimiento" (Spanish), Proceedings of the "28 Simposium internacional de computación en la educación" (Spanish), México, 2010
18. Vargas-Medina E., Figueroa N. J., Redes semánticas naturales y construcción de ontologías, en Metodología para la educación a distancia, CIC-IPN, México, ISBN 978-970-36-0431-9, 2007
19. Diez-Rodríguez H., Olmedo-Aguirre J.O., Gerencia del conocimiento en entornos virtuales de aprendizaje constructivista mediante ontologías, en Metodología para la educación a distancia, CIC-IPN, México, ISBN 978-970-36-0431-9, 2007

Análisis de la Influencia de las Inteligencias Múltiples en el Desempeño Académico Aplicando Técnicas de Minería De Datos

Maricela Quintana López, Jorge Eduardo Hernández Patlán

Centro Universitario UAEM Valle de México

mquintanal@uaemex.mx, lb.lalo_2558@hotmail.com

Resumen. Se presenta el trabajo realizado en el Centro Universitario UAEM Valle de México para generar un modelo del desempeño académico de un alumno de la carrera de Ingeniería en Sistemas y Comunicaciones basándose en la teoría de las Inteligencias Múltiples, utilizando técnicas de Minería de Datos. El objetivo principal es determinar si es posible predecir el desempeño académico de un alumno en unidades de aprendizaje del núcleo de Ciencias Básicas y Matemáticas, basándose en sus inteligencias múltiples, y comprobar si la inteligencia que más influye es la lógica matemática. Para lograrlo, se utilizaron los algoritmos de clasificación C4.5 y Naïve Bayes, primero aplicados a las instancias de todas las unidades del núcleo y posteriormente a cada unidad en particular. Los resultados muestran que sí es posible determinar el desempeño de un alumno y permiten determinar cuáles inteligencias son las más influyentes.

Palabras clave: Minería de datos, Árboles de Decisión, Naïve Bayes, Clasificación.

1 Introducción

En el área de la educación, existen investigaciones que centran su interés en determinar cuáles son los factores que influyen en el desempeño académico de un alumno [1, 4, 9, 11, 14, 15, 16]. Esto se debe a que si se sabe cuál es el factor más influyente, entonces es posible crear estrategias para minimizar los efectos negativos de dicho factor. Los factores que se han encontrado que influyen son pedagógicos, psicológicos, sociológicos, fisiológicos e institucionales.

Por otro lado, la inteligencia propia del sujeto, es determinante para su desempeño escolar. Al respeto, en 1900 Alfred Binet creó una forma cuantificable de medir la inteligencia, su test de Coeficiente Intelectual (CI). Sin embargo, este test está orientado únicamente a medir la inteligencia lingüística y la lógica, por lo cual otros investigadores surgieron con teorías que postulan que hay más inteligencias. Tal es el caso de Daniel Coleman con la Inteligencia Emocional [10] y Howard Gardner con la Teoría de las Inteligencias Múltiples (IM)[6].

© E. A. Santos, J. C. Chimal, L. Cabrera, E. Castillo.
Advances in Computer Science and Engineering
Research in Computing Science 67, 2013 pp. 51–61
Paper Recived 23-09-2013 and Acepted 21-10-2013

En el centro universitario UAEM Valle de México, estamos interesados en determinar si es posible predecir el desempeño académico de un alumno en unidades de aprendizaje del área de las ciencias básicas y matemáticas, basándose en sus inteligencias múltiples, y a su vez comprobar si la inteligencia que más influye es la lógico matemática.

El documento está organizado de la siguiente manera: en la sección 2 se describe brevemente la teoría de las Inteligencias Múltiples de Gardner. En la sección 3, presentamos de manera sucinta las técnicas de minería de datos a utilizar. Posteriormente en la sección 4 se muestra los procesos realizados para la preparación de los datos, y en la sección 5 se muestran los experimentos realizados y los resultados obtenidos. Finalmente, en la sección 6 se dan las conclusiones y el trabajo futuro, respectivamente.

2 Inteligencias múltiples

La teoría de las Inteligencias Múltiples de Howard Gardner menciona que cada persona tiene diferentes capacidades y habilidades para resolver problemas o elaborar productos de gran valor en un determinado contexto comunitario o cultural, y define esas capacidades como inteligencias. Las definiciones de las inteligencias se muestran a continuación:

- **Lógica Matemática**: se refiere a la habilidad para efectuar cálculos matemáticos y resolver problemas.
- **Lingüística-Verbal**: esta habilidad trata con la facilidad de palabra, y comprender el orden y el significado de las palabras.
- **Musical Rítmica**: facilidad para tocar un instrumento, cantar y escuchar.
- **Corporal Cinestésico**: se refiere a la habilidad de tener coordinación corporal y buen equilibrio.
- **Visual Espacial**: la facilidad de crear mapas e imágenes mentales.
- **Intrapersonal**: trata acerca de plantearse metas, y reflexionar acerca de sus habilidades personales.
- **Interpersonal**: se refiere a la habilidad de trabajar bien en equipo, ser empáticos, y puede identificar y superar problemas.

De acuerdo al estudio realizado por Gardner, cada perfil profesional requiere del desarrollo de una determinada inteligencia. En la tabla 1, se muestran las siete inteligencias, la clave para referirse a cada una, y el perfil profesional recomendado [6].

Por otro lado, existen investigaciones en las que se utilizan las inteligencias múltiples, tal es el caso de la Universidad Complutense de Madrid que requería saber cuáles eran las capacidades, habilidades y destrezas de los estudiantes de las licenciaturas de Periodismo, Comunicación audiovisual, Publicidad y Relaciones Públicas. Se aplicaron los test a los alumnos de diferentes carreras y se encontró que los estudiantes de Periodismo mostraron altos niveles de inteligencia Lingüística-Verbal, los de Comunicación Audiovisual altos niveles de inteligencia Visual-Espacial, Musical y los de

Publicidad y Relaciones Públicas un mejor resultado en la inteligencia Interpersonal [5].

Tabla 1. Perfiles profesionales para cada una de las 7 inteligencias múltiples y clave.

Inteligencia múltiple	Clave	Perfil profesional
Lógica-Matemática	ILM	Economistas, ingenieros, científicos.
Lingüística-Verbal	ILV	Líderes políticos o religiosos, poetas y escritores.
Musical-Rítmica	IMR	Músicos, compositores y críticos musicales.
Corporal-Cinestésico	ICK	Escultores, cirujanos, actores, bailarines, deportistas y atletas.
Visual-Espacial	IVE	Artistas, fotógrafos, arquitectos, diseñadores y publicistas.
Intrapersonal	INTRA	Psicólogos y sociólogos.
Interpersonal	INTER	Administradores, docentes, psicólogos y terapeutas.

Otro de los estudios consistió en identificar la relación que tienen las inteligencias múltiples con los estilos de aprendizaje de los estudiantes, para ello se aplicó el test de las inteligencias múltiples (con una escala del 1 a 5) y el inventario de estilos de aprendizaje (divergentes=D, convergentes=C, asimilador=AS y acomodadores=CA) obteniendo 231 reglas que servirán para predecir el estilo de aprendizaje nuevos estudiantes [13].

En el presente trabajo, nuestro interés se centra en saber si es posible determinar el desempeño de un alumno en las unidades de aprendizaje del área de las ciencias básicas y matemáticas, y comprobar que para esta área debe haber mayor predominio de la inteligencia lógica-matemática. A continuación se presentan las técnicas de minería de datos a utilizar para dicho propósito.

3 Técnicas de minería de datos

Existen varios trabajos de clasificación del desempeño escolar que utilizan algoritmos de minería de datos, algunos utilizan árboles de decisión y otros métodos bayesianos [2] [14] [15][16]. En nuestro caso, los algoritmos a utilizar C4.5 y Naïve Bayes pertenecen a lista de los 10 mejores [12].

Debido a que uno de nuestros intereses se centra en determinar si la inteligencia lógica matemática es la que más influye en el desempeño académico de los alumnos de ingeniería en sistemas y comunicaciones en el núcleo de las ciencias básicas y matemáticas, decidimos utilizar un árbol de decisión. Lo anterior, debido a que los árboles de decisión, utilizan para su construcción una estrategia de "divide y vencerás" es decir, los árboles se construyen de arriba hacia abajo partiendo de un nodo raíz [7]. Dicho nodo raíz representa al atributo que da la mayor ganancia, de ahí que

al emplearlo, nos permite determinar cuál de todas las inteligencias es la más influyente.

Por otro lado, la naturaleza numérica de los datos nos obliga a utilizar algoritmos que puedan procesarlos, tal es el caso del algoritmo c4.5 desarrollado por J. Ross Quinlan en 1993 como una mejora del ID3 [8].

Por otro lado, al tomar en cuenta la naturaleza de las inteligencias, sería válido considerarlas como independientes y de ahí que resulte interesante aplicar una técnica basada en la probabilidad condicional de Bayes, tal es el caso del algoritmo Naïve Bayes que considera que todos los atributos influyen de la misma manera.

La metodología empleada para realizar el presente trabajo es el modelo *KDD (*Knowledge Discovery in Databases) que consiste esencialmente en el proceso de preparación de datos, el proceso de minería de datos y la validación de resultados [7] [8] [16] [18]. Para el proceso de minería de datos utilizamos el software WEKA de la universidad de Waikato, Nueva Zelanda, el cual es una herramienta de minería de datos de distribución libre para la obtención de los modelos de clasificación [3] [17].

4 Datos y su preparación

Para poder realizar el presente trabajo, fue necesario aplicar el test de Inteligencias Múltiples de Howard Gardner a los alumnos del Centro Universitario UAEM Valle de México, específicamente a los alumnos de la carrera de Ingeniería en Sistemas y Comunicaciones. El test de IM está conformado por 70 preguntas que se responden con una escala del uno al cinco. Hay 10 preguntas para cada una de las siete inteligencias.

Además de estas preguntas, cada test va acompañado de un formulario donde se solicitan los datos de identificación del estudiante, tanto personales (nombre, edad y sexo), así como académicos (matrícula, grupo, semestre y estatus académico). La información anterior se relacionó con las calificaciones obtenidas en el periodo anterior cursado.

Dentro los atributos a utilizar además de las inteligencias múltiples, están las unidades de aprendizaje que comprenden el Área de las Ciencias Básicas y Matemáticas así como el semestre en que se imparte.

En cuanto a la limpieza de los datos, se eliminaron aquellos registros de los alumnos que no completaron el test de las IM. También los de aquellos que completaron el test pero no cursaron una unidad de aprendizaje se descartaron al momento de realizar la minería de datos para esa unidad de aprendizaje en particular.

En la tabla 3 se muestra el registro de un alumno que no completó el test de IM pero si curso sus materias correspondientes al tercer semestre; por otro lado, en la tabla 4 el alumno si completo su test de IM pero no curso la materia de métodos numéricos.

Cabe mencionar que las calificaciones de cada unidad de aprendizaje están en valores numéricos y se transformaron a valores nominales de acuerdo a la escala de la tabla 5.

Tabla 2. Asignaturas que comprenden el núcleo las Ciencias Básicas y Matemáticas

Semestre	Asignatura	N° de alumnos
1	Álgebra y Geometría Analítica	58
1	Estática y Dinámica	58
2	Química	58
2	Álgebra lineal	56
2	Cálculo diferencial e integral	58
3	Matemáticas discretas	44
3	Ecuaciones diferenciales	43
3	Métodos numéricos	42
4	Lógica matemática	43
4	Cálculo vectorial	39
4	Electromagnetismo	43
4	Probabilidad y estadística	43

Tabla 3. Datos de inteligencias múltiples incompletos

I. Intrapersonal											I. Interpersonal											I. Lingüístico-Verbal										
4	5	4	3	2	3	2	3	2	2	30	3	2	2	3	2						12											0

I. Lógico-Matemático											I. Musical-Rítmico											I. Corporal-Cinestésico										
										0											0											0

I. Visual-Espacial											Métodos numéricos	Matemáticas discretas	Ecuaciones diferenciales
										0	7	7.8	6.3

Tabla 4. Alumno que no curso una unidad de aprendizaje

I. Intrapersonal											I. Interpersonal											I. Lingüístico-Verbal										
4	4	4	5	5	4	5	5	5	4	45	5	4	2	4	3	5	4	4	5	4	40	4	5	5	4	3	5	4	3	4	4	41

I. Lógico-Matemático											I. Musical-Rítmico											I. Corporal-Cinestésico										
4	5	4	5	4	5	3	2	4	2	38	5	5	5	5	5	4	4	3	3	5	44	5	4	4	4	5	4	5	5	4	5	45

I. Visual-Espacial											Métodos numéricos	Matemáticas discretas	Ecuaciones diferenciales
5	4	5	4	4	4	3	4	5	2	40		8.5	6.4

Tabla 5. Transformación de valores numéricos a nominales.

Referencia numérica	Nivel de desempeño
8 a 10	A
Menor a 8	B

5 Experimentos y resultados

El primer experimento se realizó con 585 instancias que representan a los alumnos que tomaron una o más unidades de aprendizaje del núcleo de las ciencias básicas y matemáticas. De estos, 210 pertenecen a la clase A y 375 a la clase B. Se aplicaron los algoritmos C4.5 (J48 en el software Weka) y Naïve Bayes. En ambos casos se utilizó la validación cruzada con 10 particiones, la cual consiste en utilizar el 90% de los datos para entrenar y el 10% restante para validar; repitiendo este proceso 10 veces [16].

Como podemos apreciar en la tabla 6, los resultados obtenidos por ambos algoritmos en cuanto a la eficiencia del clasificador, no difieren por mucho. Sin embargo, el árbol de decisión resulta mejor.

Tabla 6. Comparación de algoritmos

Área	**Árbol de Decisión (C4.5)**		**Naïve Bayes**	
	Correctas	Incorrectas	Correctas	Incorrectas
Ciencias básicas y matemáticas	66.1538 %	33.8462%	61.8803%	38.1197%

En la figura 1, se muestra el árbol obtenido al aplicar el algoritmo C4.5 a los datos, se puede apreciar que el nodo raíz ILM, hace referencia a la inteligencia lógica matemática, lo que nos indica que este atributo fue el que proporcionó la mejor ganancia al momento de construir el árbol, y concuerda con los resultados que se esperaban.

Otra situación que podemos observar es que la inteligencia lógica matemática por sí sola no es suficiente para determinar la clase de desempeño que tendrá un alumno, podemos observar esto en las ramas más cortas del árbol donde al menos son dos las inteligencias que se utilizan.

Por poner un ejemplo para la clase A, veamos la rama más corta que se encuentra del lado derecho del árbol, esta rama nos indica que si la inteligencia lógica matemática es mayor a 46 y la intrapersonal es menor o igual a 42, el desempeño del alumno será A, es decir que tendrá un promedio entre 8 y 10 en unidades del núcleo.

Para el caso de la clase B, veamos la rama del camino más largo que termina en el nodo B(101/18). En este caso particular, la lectura sería que si la inteligencia lógica matemática es menor o igual a 46 y la inteligencia cinestésica es mayor a 35, y la visual espacial es mayor a 36 entonces debemos revisar nuevamente la inteligencia lógica matemática, si es menor o igual a 39 entonces el desempeño del alumno en materias del núcleo de las ciencias básicas y matemáticas será menor a 8.

También es posible observar que las inteligencias musical rítmica (IMR) y lingüística verbal (ILV) no aparecen en ninguna parte del árbol. Lo que significa que no son relevantes para las unidades de aprendizaje del núcleo básico.

Si bien este primer experimento nos permite ver, a grosso modo, cuál será el desempeño de un alumno en las unidades de aprendizaje, no nos permite determinar qué ocurrirá en una unidad de aprendizaje particular, por lo que decidimos realizar un segundo experimento en el cuál se realiza la minería de datos a cada unidad. Los algo-

ritmos empleados en este segundo experimento siguen siendo C4.5 y Naïve Bayes. Los resultados obtenidos se muestran en la tabla 7, en ella se puede observar que el algoritmo C4.5 tiene mejor desempeño que el de Bayes, con excepción de la unidad de electromagnetismo.

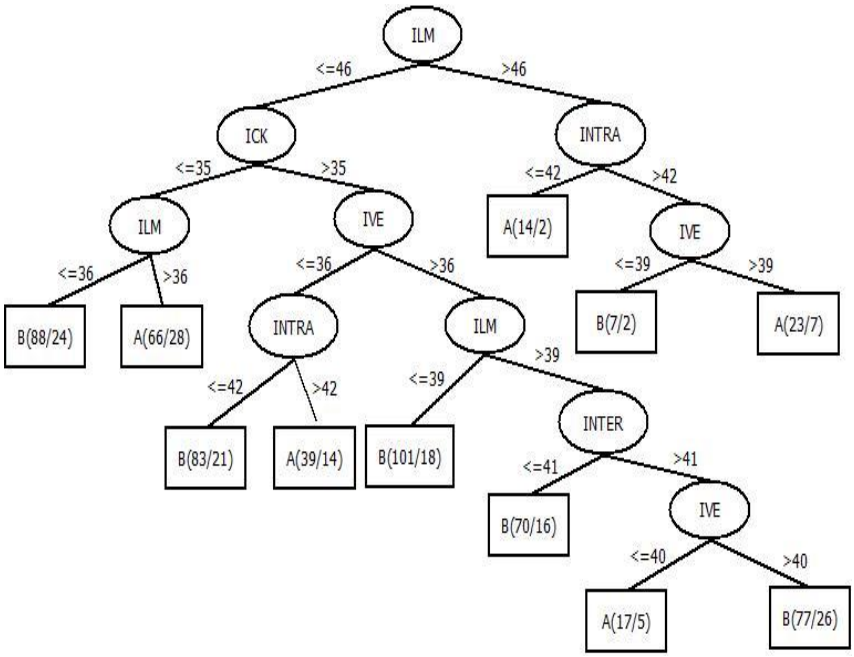

Fig. 1. Árbol generado por el algoritmo C4.5 para el núcleo de Ciencias básicas y Matemáticas.

Tabla 7. Resultados de los algoritmos C4.5 y Naïve Bayes.

Unidad de Aprendizaje	Árbol de Decisión (C4.5)		Naïve Bayes	
	Correctas	Incorrectas	Correctas	Incorrectas
Matemáticas Discretas	68.18%	31.82%	61.36%	38.64%
Electromagnetismo	58.14%	41.86%	62.79%	37.21%
Estática y Dinámica	68.97%	31.03%	56.90%	43.10%
Probabilidad y estadística	74.42%	25.58%	51.16%	48.84%
Química	53.45%	46.55%	51.72%	48.28%
Álgebra lineal	51.79%	48.21%	50.00%	50.00%
Álgebra y geometría analítica	100.00%	0.00%	100.00%	0.00%
Lógica matemática	62.79%	37.21%	53.49%	46.51%
Métodos numéricos	78.57%	21.43%	57.14%	42.86%
Cálculo vectorial	66.67%	33.33%	64.10%	35.90%
Ecuaciones diferenciales	55.81%	44.19%	46.51%	53.49%
Cálculo diferencial e integral	56.90%	43.10%	46.55%	53.45%

Podemos observar en la tabla 7, que la unidad de aprendizaje de Álgebra y geometría analítica tiene un 100%, esto se debe a que ningún alumno obtuvo 8 o más.

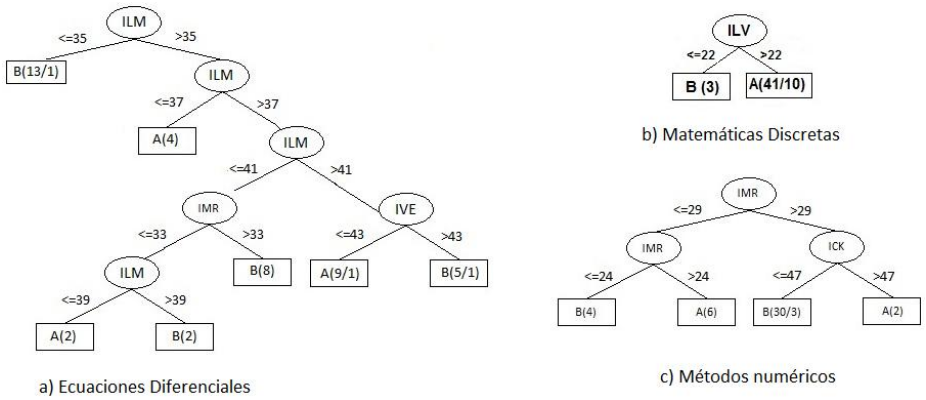

Fig. 2. Árboles para las unidades de aprendizaje del tercer semestre.

Por otro lado, vale la pena recordar que algunas de las unidades de aprendizaje se imparten en el mismo semestre, por lo que los mismos valores de inteligencias múltiples se utilizan para clasificar resultados de unidades de aprendizaje diferentes. Por ejemplo, en la figura 2 se muestra que para ecuaciones diferenciales las inteligencias relevantes son lógica matemática, inteligencia visual espacial, y la musical rítmica mientras que para matemáticas discretas, la única inteligencia a considerar es la lingüística verbal. En el caso de métodos numéricos las que más afectan son la musical rítmica y la cinestésica.

6 Conclusiones y trabajo futuro

Una de las principales conclusiones, es que sí es posible obtener un modelo que permita clasificar el desempeño académico de un alumno basándose en las inteligencias múltiples, y que una de las inteligencias más influyente es la inteligencia lógica matemática. Sin embargo, el desempeño no es el mejor, consideramos que en el momento que tengamos más datos en nuestra base, podremos tener mejores desempeños e incluso ampliar los intervalos de calificación.

Consideramos de suma importancia aplicar las encuestas cada semestre para llevar un seguimiento histórico de la evolución de las inteligencias desde que el alumno ingresa hasta el término de su carrera. Esto permitirá generar clasificadores no solo para el área de las ciencias básicas y matemáticas sino también en las áreas de la ingeniería aplicada, ciencias de la ingeniería, y ciencias sociales y humanidades.

Como trabajo futuro queda el desarrollo de una herramienta que utilice los modelos generados y permita realizar la clasificación de un estudiante en dos niveles, primero a nivel macro determinando su desempeño en general en el núcleo de materias en

particular y luego a nivel micro, generando el detalle del desempeño en una materia dada.

Referencias

1. Alcover, R., Benlloch, J., Blesa, P., Calduch, M. A., Celma, M., Ferri, C., & Zúnica, L. R.: Análisis del rendimiento académico en los estudios de informática de la Universidad Politécnica de Valencia aplicando técnicas de minería de datos. XIII Jornadas de Enseñanza universitaria de la Informática. Teruel, España. Disponible en: http://bioinfo. uib. es/~ joemiro/aenui/procJenui/Jen2007/alanal. Pdf. (2007).
2. Berry, M., & Gordon, L.: Data mining Techniques. Canada: Wiley Computer Publishing. (2004).
3. Dapozo, G. N., Porcel, E., López, M. V., Bogado, V. S., & Bargiela, R.: Aplicación de minería de datos con una herramienta de software libre en la evaluación del rendimiento académico de los alumnos de la carrera de Sistemas de la FACENA-UNNE. En VIII Workshop de Investigadores en Ciencias de la Computación. (2006).
4. Garbanzo, V., Guiselle, M.: Factores asociados al rendimiento académico en estudiantes universitarios, una reflexión desde la calidad de la educación superior pública. Educación, . 43-63. (2007).
5. GARCÍA NIETO, M. T.: La dimensión comunicativa de las inteligencias múltiples. CIC. Cuadernos de Información y Comunicación, 14( ) 141-157. Recuperado de http://www.redalyc.org/articulo.oa?id=93512977010. (2009).
6. Gardner, H.: Inteligencias múltiples: teoria en la practica. México: Paidós. (2008).
7. Han, J., Kamber, M., & Pei, J.: Data Mining Concepts and Techniques. USA: Morgan Kaufmann. (2011).
8. Hernández, J., Ramírez, Mª., & Ferri, C.: Introducción a la Minería de Datos. España: Pearson Educación. (2004).
9. Izar Landeta, J.M., Ynzunza Cortés, C.B. & López Gama, H.: Factores que afectan el desempeño académico de los estudiantes de nivel superior en Rio verde, San Luis Potosí, México. Revista de Investigación Educativa. vol. 12. Recuperado de http://www.uv.mx/cpue/num12/opinion/completos/izar-desempeno%20academico.html. (2011).
10. Martínez, C. E., Vicente, E. S., & Moreno, C. M.: Revisión histórica del concepto de inteligencia: una aproximación a la inteligencia emocional. Revista latinoamericana de Psicología, 30(1), 11-30 [6]. (1998).
11. Salagre, D. J., & Serrano, S. O.: Determinacion de los factores que afectan al rendimiento académico en la educación superior. XII Jornadas de la Asociación de Economía de la Educación. (2003).
12. Xindong, W., & Vipin, K.: The top ten algorithms in data mining. USA: CRC Press. (2009).
13. Narlı, S., Özgen, K., & Alkan, H.: In the context of multiple intelligences theory, intelligent data analysis of learning styles was based on rough set theory. Learning and Individual Differences, 21(5), 613-618. (2011).

14. Carvajal Olaya, P., Mosquera M., J. C. & Artamonova, I.: Modelos de predicción del rendimiento académico en matemáticas I en la Universidad Tecnológica de Pereira. Scientia Et Technica, XV(43) 258-263. Recuperado de http://www.redalyc.org/articulo.oa?id=84917310045. (2009).
15. Porcel, E., Dapozo, G. N., & López, M. V.: Modelos predictivos y técnicas de minería de datos para la identificación de factores asociados al rendimiento académico de alumnos universitarios. In XI Workshop de Investigadores en Ciencias de la Computación. (2009).
16. Moreno Sabido, M., & Martínez Maldonado, R., Modelo Clasificador para Predecir el Desempeño Escolar Terminal de un Estudiante.
17. Spositto, O. M., Etcheverry, M. E., Ryckeboer, H. L., & Bossero, J. Aplicación de técnicas de minería de datos para la evaluación del rendimiento académico y la deserción estudiantil.
18. Valcárcel Asencios, V.: Data Mining y el descubrimiento del conocimiento. Industrial Data, 7(2) 83-86. Recuperado de http://www.redalyc.org/articulo.oa?id=81670213. (2004).

Robotics & Mechatronics

Data Fusion of the Quaternion and Non Linear Attitude Observer Applied to the Determination and Stabilization of a Mobile Robot

B. B. Salmeron-Quiroz[1], J.F. Guerrero-Castellanos[2], G. Villegas-Medina[1], J.R. Aguilar-Sanchez[1], R. Villalobos-Martinez[1], and L. Castillo-Bermúdez[3]

[1] Instituto Politécnico Nacional (I.P.N.), SEPI ESIME Azcapotzalco, Av. de la Granjas 682, 02250, México, D.F., México.
bsalmeron@ipn.mx
[2] Facultad de Ciencias de la Electrónica, Benemérita Universidad Autónoma de Puebla - BUAP, C. U., 72450, Puebla, México.
[3] Universidad Politécnica de Puebla, Tercer Carril del Ejido Serrano s/n San Mateo Cuanalá. Juan C. Bonilla, Puebla, México
.

Abstract. Generally, the attitude estimation and the measurement of the angular velocity are a requirement for the attitude control. As a result, the computational cost and the complexity of the control loop are relatively high. In the present paper, a technique for attitude stabilization is proposed. The rigid body orientation is modeled with quaternion, which eliminates attitude estimation singularities. The real-time implementation is done unifying a quaternion error formulation of Wahba's and a nonlinear observer. It includes the gyro bias model. A quaternion measurement model is introduced. It avoids the linearization step that induces undesirable effects. The global convergence of the proposed technique is proved. Simulations with some robustness tests are performed.

Keywords: Quaternion, Attitude, Stabilization, Nonlinear Observer, Robot Mobile, MEM's

1 Introduction

Underactuated mechanical systems are systems that have fewer control inputs than configuration variables. Underactuated systems appear in a broad range of applications including Robotics, Aerospace Systems, Marine Systems, Flexible Systems, Mobile Systems, and Locomotive Systems. The "underactuation" property of under actuated systems is due to the following four reasons [1]: *i) dynamics of the system* (e.g. aircraft, spacecraft, helicopters, underwater vehicles, locomotive systems without wheels), *ii) by design for reduction of the cost or some practical purposes* (e.g. satellites with two thrusters and flexible-link robots), *iii) actuator failure* (e.g. in a surface vessel or aircraft), *iv) imposed artificially to create complex low-order nonlinear systems* for the purpose of gaining insight in control of high-order underactuated systems (e.g. the Acrobot, the Pendubot, the Beam-and-Ball system, the Cart-Pole system, the Rotating Pendulum, the TORA system).

© E. A. Santos, J. C. Chimal, L. Cabrera, E. Castillo.
Advances in Computer Science and Engineering
Research in Computing Science 67, 2013 pp. 63–73
Paper Recived 05-08-2013 and Acepted 21-10-2013

A fundamental requirement for an autonomous vehicle is its ability to localize itself with respect to its environment. Navigation on a flat and horizontal ground only requires estimations of position and heading. However, in many cases, the environment is not so well structured, and the angular orientation of the vehicle may change along its path. In this case, a real time estimation of the attitude may be necessary.

The attitude estimation of an autonomous vehicle is a subject that has attracted a strong interest the last years. In addition to traditional attitude estimation in aerospace and automobile communities, the reduced cost of MEMS inertial sensors has spurred new applications in robotics [1], virtual reality [3] and biomechanics [2]. Furthermore, the increasingly interest in Unmanned Aerial Vehicles (UAVs) [4] has motivated the development of low cost, lightweight and low-power consumption Attitude and Heading Reference Systems (AHRS) and backup attitude indicators. An AHRS is composed of inertial and magnetic sensors, namely, three rate gyros, three accelerometer and three magnetometers, orthogonally mounted such that the sensor frame axes coincide with the body frame in question. In fact, an AHRS is an attitude estimator since the signal sensors are coupled with a proper mathematical background. This attitude estimation problem is described as following: Rate gyros provide continuous attitude information with good short-term stability when their measurements are integrated.

The first one deals with a constraint least-square minimization problem proposed firstly by Wahba [6],(see [7] pages 9-11) and [7].

The second approach is within the framework of the Extended Kalman Filter [8] (EKF) or Additive Extended Kalman Filter (AEKF) [9].

The third approach issues from nonlinear theory, and non linear observers are applied to the attitude determination problem [10], [12], [13]. In this approach, the convergence of the error to zero is proved in a Lyapunov sense.

In this paper, an attitude estimator using quaternion representation is studied. Here a novel method for solving Wahba's problem is used. This method allows to find an quaternion from the measures provided by an Attitude and Heading Reference Systems (AHRS), the error between current and desired orientations is directly determined thanks to the measurements of the reference vectors delivered by the body's sensors.

The present paper is organized as follows. In section 2 a quaternion-based formulation of the orientation of rigid body is given. The problem statement is formulated in section 3. The control law and attitude's estimation is presented in section 6. Simulation results are given in section 7. The paper ends with some concluding remarks given in section 8.

2 Mathematical Background

The attitude of a rigid body can be represented by a unit quaternion, consisting of a unit vector e, known as the Euler axis, and a rotation angle β about this axis. The quaternion q is then defined as follows:

$$q = \begin{pmatrix} \cos\frac{\beta}{2} \\ e\sin\frac{\beta}{2} \end{pmatrix} = \begin{pmatrix} q_0 \\ q \end{pmatrix} \in H \tag{1}$$

where

$$H = \{q \mid q_0^2 + q^T q = 1, \\ q = [q_0 q^T]^T, q_0 \in R,\ q \in R^3\} \tag{2}$$

$q = [q_1 \ \ q_2 \ \ q_3]^T$ and q_0 are known as the vector and scalar parts of the quaternion respectively. In attitude control applications, the unit quaternion represents the rotation from an inertial coordinate system $N(x_n, y_n, z_n)$ located at some point in the space (for instance, the earth NED frame (North, East, Down)), to the body coordinate system $B(x_b, y_b, z_b)$ located on the center of mass of a rigid body.

If r is a vector expressed in N, then its coordinates in B are expressed by:

$$b = \bar{q} \otimes r \otimes q \tag{3}$$

where $b = [0 \ \ b^T]^T$ and $r = [0 \ \ r^T]^T$ are the quaternions associated to vectors b and r respectively. $\otimes$ denotes the quaternion multiplication and $\bar{q}$ is the conjugate quaternion of q, defined as:

$$\bar{q} = [\, q_0 \ -q^T \,]^T \tag{4}$$

The rotation matrix $C(q)$ corresponding to the attitude quaternion q, is computed as:

$$C(q) = (q_0^2 - q^T q) I_3 + 2(qq^T - q_0 [q^\times]) \tag{5}$$

where I_3 is the identity matrix and $[\xi^\times]$ is a skew symmetric tensor associated with the axial vector ξ:

$$[\xi^\times] = \begin{pmatrix} \xi_1 \\ \xi_2 \\ \xi_3 \end{pmatrix}^\times = \begin{pmatrix} 0 & -\xi_3 & \xi_2 \\ \xi_3 & 0 & -\xi_1 \\ -\xi_2 & \xi_1 & 0 \end{pmatrix} \tag{6}$$

Thus, the coordinate of vector r expressed in the B frame is given by:

$$b = C(q) r \tag{7}$$

The attitude error is used to quantify the mismatch between two attitudes.

$$q_e = q \otimes q_d^{-1} \tag{8}$$

$\otimes$ denotes the quaternion multiplication and q_d^{-1} is the complementary rotation of the quaternion q_d, which is the quaternion conjugate (see ([5]) for more details).
The attitude dynamics of a rigid body is described by

$$J\dot{\omega} = -\omega \times J\omega + \Gamma \tag{9}$$

where $J \in R^{3\times 3}$ is the symmetric positive definite constant inertial matrix of the rigid body expressed in the B frame and $\Gamma \in R^3$ is the vector of control torques. Note that the torque also depend on the environmental disturbance (aerodynamic, gravity gradient, etc.).

3 Problem Statement

In the case of the attitude estimation, one seeks to estimate the attitude and accelerations of a rigid body. From now on, it is assumed that the system is equipped with a tri-axis accelerometer, three magnetometer and three rate gyros mounted orthogonally. In this section we describe the body's kinematic of the model [15], our typical capture configuration relies primarily on the Robot of figure 1 equipped with two 6 inch diameter wheels driven by 1 DC gear head motors. The mechanical model (seen in figure 1, is based on single pinion architecture suitable for light vehicles and consists of following elements: a steering rack, a steering column coupled to the steering rack through a pinion gear, and the assist motor. Tie-rods connect the steering rack to the tires.

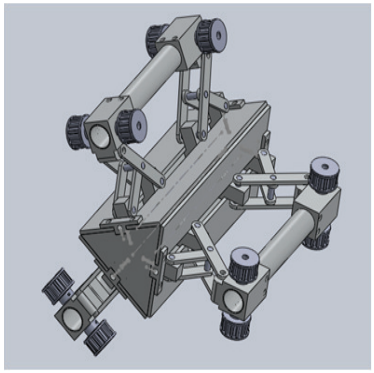

Fig. 1. Mobile Robot

The equation describing the relation between the quaternion and the body's kinematic is given in introducing the angular variation $\omega = [\omega_x \ \omega_y \ \omega_z]^T$ from this, it follows.

$$\dot{q} = \frac{1}{2}\Omega(\omega)q(t) = \frac{1}{2}\Xi(q)\omega(t) \tag{10}$$

Where $\Omega(\omega)$ y $\Xi(q)$ are defined as:

$$\Omega(\omega) \equiv \begin{bmatrix} -[\omega\times] & \vdots & \omega \\ \cdots & \vdots & \cdots \\ -\omega^T & \vdots & 0 \end{bmatrix} \tag{11}$$

$$\Xi(q) \equiv \begin{bmatrix} q_0 I_{3\times 3} + [q\times] \\ \cdots\cdots\cdots\cdots \\ -q^T \end{bmatrix} \tag{12}$$

The matrix $[\omega\times]$ and $[q\times]$ are obtained by the cross product issue of $a \times b = [a\times]b$ con $[a\times] \in R^{3\times 3}$:

$$[a\times] = \begin{bmatrix} 0 & -a_3 & a_2 \\ a_3 & 0 & -a_1 \\ -a_2 & a_1 & 0 \end{bmatrix} \tag{13}$$

The quaternion must be:

$$q^T q = q^T q + q_0^2 = 1 \tag{14}$$

In the other hand, the matrix $\Xi(q)$ has the relation:

$$\begin{array}{l} \Xi^T(q)\Xi(q) = q^T q I_{3\times 3} \\ \Xi(q)\Xi^T(q) = q^T q I_{4\times 4} - q^T q \\ \Xi^T(q)(q) = 0_{3\times 1} \end{array} \tag{15}$$

Generally $\Xi^T(q)\lambda = -\Xi^T(\lambda)q$, for any $\lambda \in H$.

$$\begin{array}{c} C(q) = (q_0^2 - q^T q)I_{3\times 3} + 2qq^T \\ -2q_0[q\times] \end{array} \tag{16}$$

that is denoted like the orientation matrix 3-D of dimension 3×3.

The angular velocity ω is obtained by finite differences from equation (10) at the instants k and $k-1$ (k estimation instant).

$$\omega = 2\Xi^T(q)\dot{q} \tag{17}$$

$$\omega = 2\Xi^T(q) * \left(\frac{q(k) - q(k-1)}{Ts}\right) \tag{18}$$

4 Modeling sensors

In application of inertial and magnetic sensors, the inertial coordinate frame N is chosen to be the *NED* coordinate frame. In this work the origin of N is located at San Luis Potosí, México ($GPS : 22°36'12''N\ 100°25'\ 47''W$). The ”reference vectors” are the gravitational and magnetic vectors, which are well known. The ”vectors observations”, i.e. the gravitational and magnetic vectors expressed in the body frame B, are obtained from an tri-axis accelerometer and a tri-axis magnetometer sensors. The angular velocity is obtained from three rate gyros orthogonally mounted.

4.1 Rate Gyros

The angular velocity $\omega = [\omega_1\ \omega_2\ \omega_3]^T$ is measured by the rate gyros, which are supposed to be orthogonally mounted. The output signal of a rate gyro is influenced by various factors, such as bias drift and noise. In the absence of rotation, the output signal can be modeled as the sum of a white Gaussian noise and of a slowly varying function, an integration process is required in order to obtain the current attitude quaternion.

The kinematics equation is given by:

$$\begin{aligned}\begin{pmatrix}\dot{q}_0\\ \dot{q}\end{pmatrix} &= \frac{1}{2}\begin{pmatrix}-q^T\\ I_3 q_0 + [q^\times]\end{pmatrix}\omega\\ &= \frac{1}{2}\Xi(q)\omega\end{aligned} \tag{19}$$

Even the smallest variation of the rate gyro measurement will produce a wrong estimation of the attitude . The bias is denoted by ν, belonging to space R^3. The rate gyro measurements are modeled by [14]:

$$\omega_G = \omega + \nu + \eta_G \tag{20}$$

$$\dot{\nu} = -T^{-1}\nu + \eta_\nu \tag{21}$$

where η_G and $\eta_\nu \in R^3$ are supposed by Gaussian white noises and $T = \tau I_3$ is a diagonal matrix of time constants. In this case, the constant τ which has been set to $\tau = 100\ s$. The bias vector ν will be estimated online, using the observer presented in the following section.

4.2 Accelerometers

Since the $3-axis$ accelerometer is fixed to the body, the measurements are expressed in the body frame B. Thus, the accelerometer output can be written as:

$$b_A = C(q)(a-g) + \eta_A \tag{22}$$

where $g = [0\ \ 0\ \ g]^T$ and $a \in R^3$ are the gravity vector and the inertial accelerations of the body respectively. Both are expressed in frame N. $g = 9.81\ m/sec^2$ denotes the gravitational constant and $\eta_A \in R^3$ is the vector of noises that are supposed to be white Gaussian.

4.3 Magnetometers

The magnetic field vector h_M is expressed in the N frame it is supposed to be $h_M = [h_{M_x}\ \ 0\ \ h_{M_z}]^T$. Since the measurements take place in the body frame B, they are given by:

$$b_M = C(q)h_M + \eta_M \tag{23}$$

where $\eta_M \in R^3$, denotes the perturbing magnetic field. This perturbation vector is supposed to be modeled by Gaussian white noises.

5 Attitude's Estimation and Prediction

The attitude estimator uses quaternion representation. Two approaches are jointly used, namely a estimation with a constraint least-square minimization technique and a prediction of the estate at the instant k. The prediction is performed in order to produce a pseudo-estimate of the accelerations and the attitude quaternion. This prediction is

driven by a estate which is obtained from the quaternion propagated through the kinematic equation and the one obtained via the constraint minimization problem.

In this paper a optimization criteria that take in account the evolution of the attitude state via determination of $x = [q_0, q_1, q_2, q_3, a_x, a_y, a_z]^T$ in the function $f(x)$ is proposed. The minimum error is chosen, but it takes in account the prediction of the state $\hat{x}$ and the coefficients of weight for the estate μ and the measures estimated ($MesEstimated = MS$) at the instant k.

$$\begin{aligned} f(x) = \tfrac{1}{2}[\mu(\textstyle\sum_{j=1}^{n}(MesEstimated - v_{mes}(j))^2) \\ +(1-\mu) \parallel (\hat{x}-x) \parallel_2^2] \end{aligned} \tag{24}$$

$$with \qquad q^T q - 1 = 0$$

The process of Estimation and Prediction needs the determination of their gradient g_q, g_a and their Hessian H_q, H_a.

$$H_q = \left[\frac{\partial^2 f}{\partial q^2} \cdot \frac{\partial q}{\partial x}\right]^T \tag{25}$$

$$\frac{\partial g_q}{\partial a} = \begin{bmatrix} 2\displaystyle\sum_{j=1}^{3}\left(2\left(q^T MS_j q - v_{mes}(j)\right)\frac{\partial MS_j}{\partial MS_1}q + q^T\frac{\partial MS_j}{\partial MS_1}qMS_j q\right) \\ 2\displaystyle\sum_{j=1}^{3}\left(2\left(q^T MS_j q - v_{mes}(j)\right)\frac{\partial MS_j}{\partial MS_2}q + q^T\frac{\partial MS_j}{\partial MS_2}qMS_j q\right) \end{bmatrix}. \tag{26}$$

Similarly, is the obtention for the gradient of the state for the case of acceleration.

Finally, the total Gradient is obtained by the fusion between the calcule show for the quaternion case an the gradient omitted for the acceleration case.

$$F(x) = \begin{bmatrix} H_q & \frac{\partial g_q}{\partial a} \\ \frac{\partial g_a}{\partial x} & H_a \end{bmatrix} \tag{27}$$

For the prediction's process of $\hat{x}$, several technique have been validated, for purpose of simplicity, the prediction via spline is chosen. Cubic spline is a spline constructed of piecewise third-order polynomials which pass through a set of n control points. The second derivative of each polynomial is commonly set to zero at the endpoints, since this provides a boundary condition that completes the system of $n-2$ equations. This produces a so-called "natural" cubic spline and leads to a simple tridiagonal system which can be solved easily to give the coefficients of the polynomials. However, this choice is not the only one possible, and other boundary conditions can be used instead.

Suppose we are given $n+1$ data points $(\hat{x}_k, MS_k)$ such that.

$a = x_0 < \ldots < x_n$, Then the coefficients of the vector μ exists cubic polynomials with coefficients $\mu_{j,i} \qquad 0 \le i \le 3$ such that the following hold.

1. $\mu(\hat{x}) = \mu_j(\hat{x}) = \sum_{j=0}^{3}(\hat{x}-x_j)^i \forall \hat{x} \in [\hat{x}-x_{j+1}]\, 0 \le k \le n-1$
2. $\mu(x_j) = y_k \qquad 0 \le k \le n-1$
3. $\mu_j(x_{j+1}) = \mu_{j+1}(x_{j+1}) \qquad 0 \le k \le n-2$

4. $\mu'_j(x_{j+1}) = \mu'_{j+1}(x_{j+1}) \qquad 0 \le k \le n-2$
5. $\mu''_j(x_{j+1}) = \mu''_{j+1}(x_{j+1}) \qquad 0 \le k \le n-2$

So we see that the cubic spline not only interpolates the data $(\hat{x}_k, MS_k)$ but matches the first and second derivatives at the knots. Notice, from the above definition, one is free to specify constraints on the endpoints. The end point constraint $\mu''(a) = 0 \quad \mu''(b) = 0$ is chosen.

The estimation of the torque is part of another work that is in process and only we present his basic model. Since the driver torque is not measured, we introduce another estimator for $\Gamma_{Mot} = \Gamma$,

Essentially, the estimated value of the driver torque is

$$\Gamma_{iest} = G^{(-1)}(\Gamma_{LZ}(z) - H(z).\Gamma_{Mot(z)}) \tag{28}$$

Where Γ_{LZ} is the torque in the steering column part and Γ_{Mot} is the assist motor torque. In order that $G^{(-1)}$ can be physically realizable (numerator degree of the transfer function is always less or equal than denominator degree), it is necessary to introduce a correction transfer function $G_c(z)$ to maintain the properness. With this correction, the inverse transfer function becomes

$$\Gamma_{iest} = G^{(-1)} * G_c(z) * (\Gamma_{LZ}(z) - H(z).\Gamma_{Mot(z)}) \tag{29}$$

6 Nonlinear attitude observer

The attitude nonlinear observer that includes the bias and the error update is given by:

$$\dot{\hat{q}} = \frac{1}{2}\Xi(\hat{q})\left[\omega_G - \hat{\nu} + K_1\varepsilon\right] \tag{30}$$

$$\dot{\hat{\nu}} = -T^{-1}\hat{\nu} - K_2\,\varepsilon \tag{31}$$

where T has been defined in (21) and $K_i, i = 1,2$ are positive constant parameters. $\hat{q}$ is the prediction of the attitude at time t. It this obtained via the integration of the kinematics equation (30) using the measured angular velocity ω_G, the bias estimate $\hat{\nu}$ and $\varepsilon = q_e$ which is the vector part of the quaternion error q_e. Remember that q_e measures the discrepancy between $\hat{q}$ and the pseudo-measured attitude q_{ps} (32). In this paper, q_{ps} is obtained thanks to an appropriate treatment of the accelerometer and magnetometer measurements.

Combining (19),(21), (30) and (31) the error model is expressed as:

$$\dot{q}_e = \frac{1}{2}\begin{pmatrix} 0 & \gamma^T \\ -\gamma\,[2\omega^{\times}] + [\gamma^{\times}] \end{pmatrix}\begin{pmatrix} q_{e_0} \\ q_e \end{pmatrix} \tag{32}$$

$$\dot{\tilde{\nu}} = -T^{-1}\tilde{\nu} + K_2\,\varepsilon \tag{33}$$

where $\gamma = \tilde{\nu} + K_1\varepsilon$, and $\tilde{\nu} = \nu - \hat{\nu}$. The system (33)-(32) admits two equilibrium points $(q_{e_0} = 1\ q_e = 0\ \tilde{\nu} = 0)$ and $(q_{e_0} = -1\ q_e = 0\ \tilde{\nu} = 0)$. This is due to fact that quaternions q and $-q$ represent the same attitude. From (1), one obtains:

$$q_{e_0} = 1 \quad \Rightarrow \beta = 0$$
$$q_{e_0} = -1 \ \Rightarrow \beta = 2\pi\ (generally\ 2n\pi)$$

7 Validation

In this section, some simulation results are presented in order to show the performance of the proposed control laws. A rigid body with low moment of inertia is taken as the experimental system. In fact, the low moment of inertia makes the system vulnerable to high angular accelerations which proves the importance to apply the control.

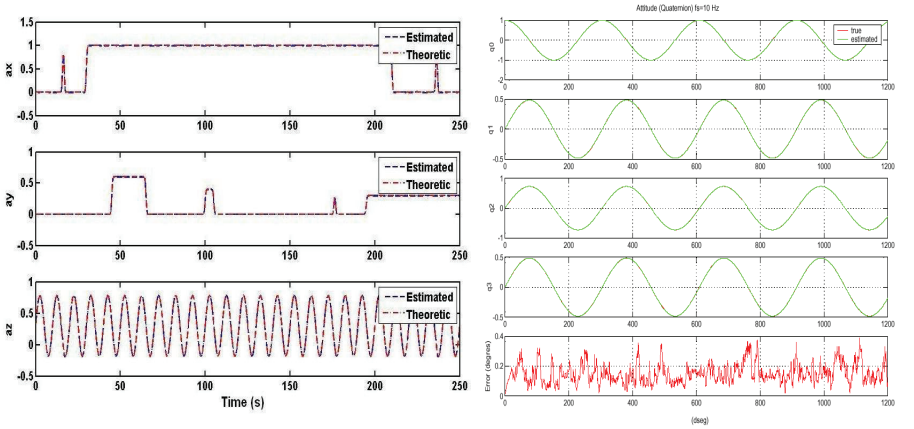

Estimation and Prediction of the Acceleration Estimation and Prediction of the Quaternion

Fig. 2. Validation de Movements

The proposed technique is compared to the existing methods (namely, the Multiplicative Extended Kalman Filter (MEKF) and the Additive Kalman Filter (AEKF)). Initial conditions are set to extreme error values in order to assess the effectiveness of attitude estimation. These results are depicted in figures 2.

8 Conclusion and future works

In this paper, a control law for the global stabilization of a rigid body was proposed. The presented methodology is especially simple. It is based on quaternion error and a nonlinear observer the attitude is parameterized by the unit quaternion. Furthermore, the proposed approach can be extended to the stabilization of a pico-satellite or a micro-satellite. Remain to perform several validations in the robot mobil and to those provided by a vision-based human motion capture system that will be used as a reference attitude estimation system and embebed in robots to assist people and improve human performance in daily and task-related activities, focusing in particular on populations with special needs, including those convalescing from trauma, rehabilitating from cognitive and/or physical injury, aging in place or in managed care, and suffering from developmental or other social, cognitive, or physical disabilities. Another application

desired for the presented approach is the stabilization of micro-satellite and UAV, simulations using the dimension and the actuator characteristics of a pico-satellite and a micro-satellite and to compare the proposed approach with other control schemes.

Acknowledgment

The authors would like to thank to the Instituto Politécnico Nacional (IPN) - SEPI ESIME Unidad Azcapotzalco and the SIP for the projects 20130784, and 20130853 , the CONACyT the B.U.A.P-F.C.E. and the U.P.Pue.

References

1. S.I. Roumeliotis, G.S. Sukhatme, and G.A. Bekey. Smoother based 3D attitude estimation for mobile robot localization. In IEEE International Conference on Robotics and Automation, ICRA'99, 1999.
2. H. Fourati, N. Manamanni, L. Afilal, and H. Handrich. A nonlinear filtering approach for the attitude and dynamic body acceleration estimation based on inertial and magnetic sensors: Bio-logging application. IEEE Sensor Journal, 11(1):233 to 243, 2011.
3. J. D. Hol, T. B. Sch¨on, F. Gustafsson, and P. J. Slycke. Sensor fusion for augmented reality. In The 9th International Conference on Information Fusion, 2006.
4. T. Hamel, R. Mahony, and A. Tayebi. Introduction to the special issue on aerial robotics. Control Engineering Practice, 18(17), 2010.
5. Shuster, M.D., A survey of attitude representations, Journal of the astronautical sciences, 1993, pages 439-517.
6. Whaba, G., A Least Squares Estimate of Spacecraft Attitude, SIAM Review, 1965, pages 409.
7. Choukroun, D., Novel methods for attitude determination using vector observations, Israel Institute of Technology, Haifa, Israel,2003.
8. Lefferts, E.J. and Markley, F.L. and Shuster, M.D., Kalman Filtaring for Spacecraft Attitude Estimation,Journal of Guidance, Control, and Dynamics,1982,pages 417-429.
9. Markley, F.L., Attitude Error Representations for Kalman Filtering,Journal of Guidance, Control, and Dynamics, 2003, pages 311-317.
10. Salcudean, S., A globally convergent velocity obsever for rigid body motion,IEEE Transactions on Automatic Control, 1991 pages 1493-1497.
11. B. B. Salmerón-Quiroz,Mendez-Barrios,J. F. Guerrero-Castellanos,S. A. Rodriguez-Paredes,G. Villegas-Medina,Towards Human Capture Movement: Estimation of Anatomical Movements of the Shoulder, Hindawi Publishing Corporation Discrete Dynamics in Nature and Society, Volume 2013.
12. Vik, B. and Fossen, T.I., An Nonlinear Observer for GPS and INS Integration, 40th IEEE Conference on Decision and Control, 2001.
13. Thienel, J. and Sanner, R.M., A coupled nonlinear spacecraft attitude controller and observer with an unknown constant gyro bias and gyro noise, IEEE Transactions on Automatic Control, 2003, pages 2011-2014,
14. Brown, R.G. and Hwang, P.Y.C , Introduction to Random Signal and Applied Kalman Filtering, Wiley, New, 1997.
15. J. L. Crassidis F. and L. Markley.(2004).A Minimum Model Error Approach for Attitude Estimation. Catholic University of America. Washington, USA, 2004.
16. microstrain http://www.microstrain.com/3dm-gx1.aspx August 2005.

Arquitectura Digital Difusa Embebida en un FPGA para Control de un Péndulo Invertido sobre un Carro

Andrés Flores[+] , Elsa Rubio, Víctor Ponce, Luis Luna[*]

Centro de Investigación en Computación, Laboratorio de Robótica y Mecatrónica, Instituto Politécnico Nacional, México
[+] ing.andresfc.2415@gmail.com

Resumen. Se presenta una arquitectura que permite embeber un sistema de control no lineal difuso sobre un FPGA de Xilinx XC3S500E. Este tiene el objetivo de controlar al péndulo invertido sobre un carro. El modelo difuso y los conjuntos de membresía difusos propuestos tienen como objetivo estabilizar al sistema en la posición vertical. Se describe en Verilog y VHDL el modelo. Este modelo es comparado con la respuesta generada por los sistemas difusos simulados en Matlab y la simulación del comportamiento generada en Isim de Xilinx, obteniendo resultados exitosos. La frecuencia máxima del controlador es 24.17 MHz la cual es tomada del resumen de ISE.

Palabras clave: Control difuso embebido, FPGA, lenguajes de descripción de hardware, péndulo invertido sobre carro.

1 Introducción

Un sistema embebido envuelve cómputo, pero este no es su principal objetivo. Por otro lado la lógica difusa tiene un amplio rango de aplicaciones y entonces el hilo común que une todas esas aplicaciones es que un experto (operador humano) puede, al menos en un principio, ejecutar la tarea requerida. Sin embargo, cuando el modelo matemático es demasiado complicado para tener un uso práctico, un modelo lingüístico llega a ser ventajoso [1]. El sistema del péndulo invertido es del tipo lazo abierto inestable pues se necesita un tipo de control para mantener al péndulo en la posición vertical [2]. Existen numerosas aplicaciones embebidas de lógica difusa para control de sistemas mecánicos [3, 4, 5]. La presente investigación se basa en la implementación de un sistema de Control Difuso para resolver el problema conocido del péndulo invertido sobre un carro. Los bloques fundamentales del sistema Difuso embebido se describen en los principales Lenguajes de Descripción de Hardware (HDL): Verilog yVHDL. Se utiliza la técnica de Modulación por Ancho de Pulso descrito dentro del

[+] Alumno becario CONACyT y PIFI, estudiante de Maestría en Ciencias en Ingeniería de Cómputo del Centro de Investigación en Computación-IPN, México.
* Alumno estudiante de Ingeniería en Control y Automatización de *ESIME-IPN*, México.

© E. A. Santos, J. C. Chimal, L. Cabrera, E. Castillo.
Advances in Computer Science and Engineering
Research in Computing Science 67, 2013 pp. 73–83
Paper Recived 16-08-2013 and Acepted 21-10-2013

sistema embebido en HDL para otorgar la ley de control adecuada a la etapa de potencia electrónica, misma que hace trabajar a un motor de corriente directa que funciona como actuador principal para estabilizar la posición del péndulo invertido. Se utiliza un FPGA de la familia de Xilinx Spartan XC3S500E y la tarjeta de desarrollo Spartan 3E [16].

2 Estructura del sistema

El objetivo principal de este desarrollo tecnológico es embeber en HDL un sistema difuso que sea capaz de estabilizar al péndulo invertido que se encuentra montado sobre un carro, esa es la idea de forma general. En esta sección se explica cada una de las etapas que conforman al sistema, y la Figura 1 muestra el diagrama de bloques general empleado.

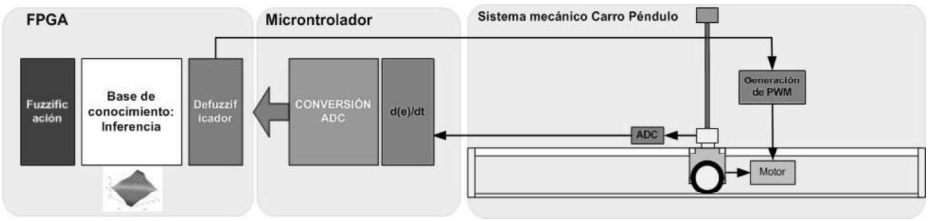

Fig. 1. Diagrama de bloques del sistema diseñado para el control del péndulo invertido.

La primera etapa permite la medición de nuestra variable de posición angular del péndulo. Se acopla mecánicamente al péndulo un potenciómetro y para asegurar que la medición fuese lo más exacta posible se decide utilizar un potenciómetro de precisión industrial de la empresa BI-Technologies. Este sensor tiene una sensibilidad adecuada debido a que es construido de plástico conductivo. La segunda etapa permite la conversión AD del dato proveniente del potenciómetro y es convertido a su resolución de 8 bits. Se utiliza el microcontrolador PIC16F887 [16] para realizar operación de conversión analógica digital. La etapa 3 llamada de Control es donde se encuentra embebido el Sistema Difuso en sus tres etapas: fuzzificación, inferencia y defuzzificación y una etapa extra para realizar la derivada de la señal de error.

Finalmente, la señal defuzzificada es interpretada y convertida a su correspondiente señal PWM con salida de 0 a 5 volts, la cual se direcciona a una frecuencia mayor a 20 KHz hacia una tarjeta de potencia MD03 de la empresa Robot Electronics [15] para controlar al péndulo invertido.

2.1 Definición de la conversión y de la derivada

En la literatura se encuentra la forma de hacer discreto el controlador PID. En la presente investigación se toma en cuenta el enfoque de [14] para describir la función que realiza la derivada del error en forma discreta. Siendo específicos, de la ecuación

(1) correspondiente al controlador PID discreto, se toma la parte derivativa y se describe según la Figura 2, donde k_d es la constante derivativa y $e(n)$ es el error medido.

$$u(n) = k_p e(n) + k_i \sum_{j=0}^{n} e(j) + \boldsymbol{k_d}(\boldsymbol{e(n) - e(n-1)}) \quad (1)$$

```
always @(clk)            //D=Kd*[ e(n) - e(n-1) ]
    begin
    en=entrada;          // e(n)
    en_1=en;             // e(n-1)
    sal=Kd*(en-en_1);
end
```

Fig. 2. Código generado en Verilog que describe la derivada del error.

2.2 Descripción del módulo PWM en VHDL

El módulo PWM se encarga de tomar los 8 bits de salida correspondientes al cálculo del valor de la etapa de defuzzificación, por medio del uso de la técnica del promedio de los centros se genera el pulso PWM a una frecuencia de 20 KHz que es enviado al módulo MD03 que controla el motor de CD, mismo que posiciona al carro para estabilizar al péndulo. Para lograr conseguir el pulso PWM mediante lenguajes de descripción de hardware, se ha tomado la técnica reportada en [6], donde se utiliza un contador y un comparador para generar el pulso con el ancho deseado a la frecuencia deseada. Por lo general, todo sistema que procesa información binaria para controlar un proceso analógico requiere una etapa de entrada analógica digital y una etapa de salida digital analógica (convertidores ADC y DAC). Para reducir costos en los diseños que no requieren alta resolución en la etapa de salida, es posible sustituir el DAC por un algoritmo de Modulación por Ancho de Pulsos (PWM). Una unidad PWM permite asignar cierta duración de tiempo en alto o en bajo a un dato digital de n bits, misma que se considera la salida de la etapa de defuzzificación. Lo anterior se logra conectando un contador y un circuito comparador, tal y como se aprecia en la Figura 3. La Figura 4 muestra un extracto de código en VHDL para conseguir generar el PWM según la descripción dada anteriormente.

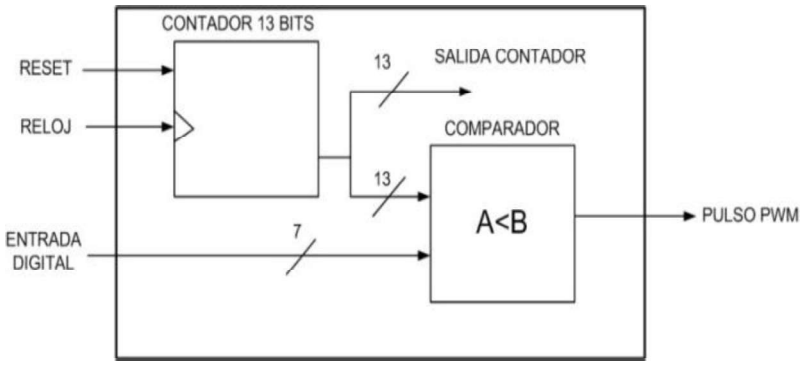

Fig. 3. Diagrama general del módulo que genera el pulso PWM en VHDL.

```
cuenta_inicial: process (reloj, reset, sal,
base, aux)
begin
if reset='0' then
      base <= "0000000000000";
   elsif reloj='1' and reloj'event then
         if base /=1 then
               base <= base + 1;
          sal <= '0';
         else
               base <= "0000000000000";
          sal <= '1';
         end if;
    end if;
frec_25KHz <= sal;
end process cuenta_inicial;
```

Fig. 4. Extracto de código que describe al módulo PWM.

2.3 Carro péndulo invertido

Recientemente, muchos sistemas robóticos diseñados con péndulo invertido sobre ruedas (WIP[2]) tales como el Segway PT y el Segway para Robonautas (Robot astronautas de la NASA), han tenido gran popularidad en la comunidad de la disciplina de la Robótica [7].

El péndulo invertido sobre un carro, es un sistema clásico de control bien conocido y estudiado durante años; debido a que sirve como sistema de prueba para el desarrollo de nuevos algoritmos de control, principalmente de control de sistemas no lineales.

El objetivo principal de este sistema es mantener estabilizado el péndulo, el cual se encuentra montado sobre un carro que tiene la capacidad de moverse libremente sobre el eje horizontal (véase Figura 5). Se han reportado varios enfoques de control clásico para el control del carro péndulo invertido, e incluso se han propuesto técnicas de control manejando el enfoque Lagrangiano, con el objetivo de manejar adecuadamente una función de energía, basada en una función de Liapunov para estabilizar dicho sistema no lineal [8]. Se conocen por igual técnicas de Control Neuronal [9] y técnicas de Control Difuso [10, 11, 12].

En la teoría de control se requiere exactitud de los parámetros de la variable controlada. Además, no aplica el modelo lineal cuando el péndulo tiene inclinaciones muy amplias. Por otro lado, el control basado en redes neuronales requiere de sucesivas iteraciones con el objetivo de obtener el conocimiento necesario para su aprendizaje. Sin embargo, en el Control Difuso, podemos usar reglas basadas en la experiencia para aproximar el control de una forma más precisa.

---

[2] Por su siglas Wheeled Inverted Pendulum (WIP).

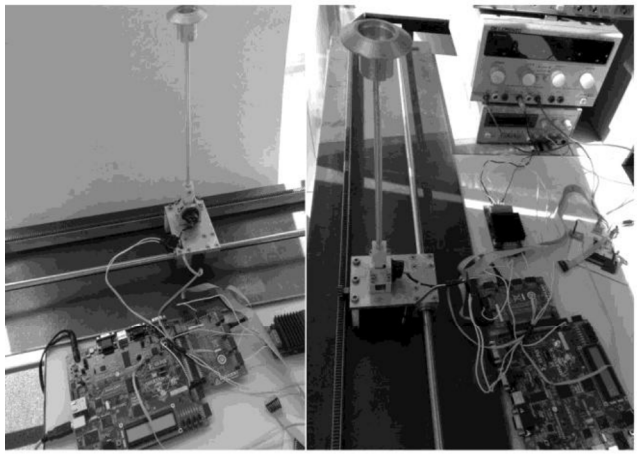

Fig. 5. Péndulo invertido construido para el laboratorio del CIC.

3 Arquitectura del Controlador Difuso en HDL

Las tres principales partes que conforman éste sistema de control descrito en HDL se muestra en la Figura 6.

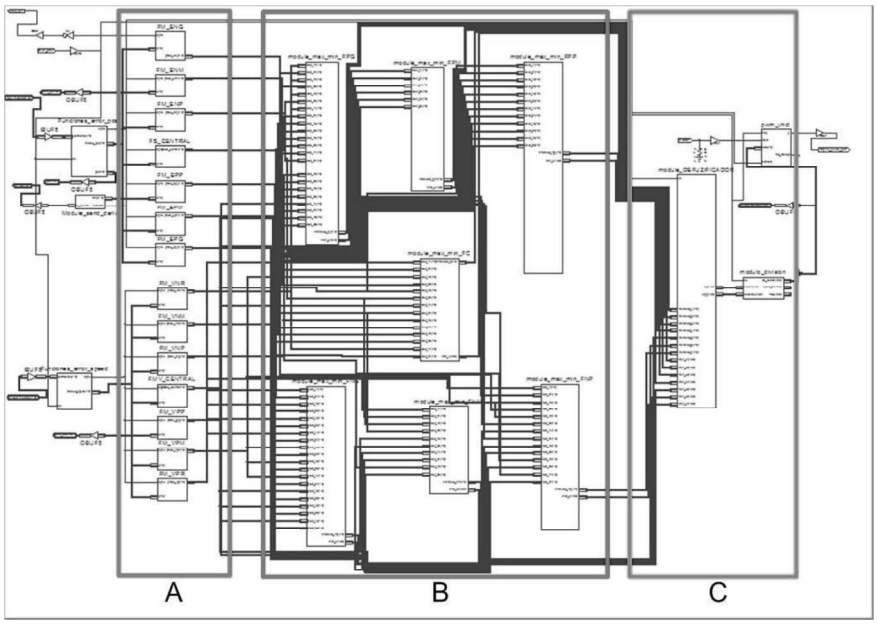

Fig. 6. Arquitectura difusa completa embebida en FPGA. A) Módulos de Fuzzificación, B), Módulos de inferencia difusa ó base de conocimiento, C) Módulo defuzificador.

La etapa de fuzzificación se realiza a través de cálculos sucesivos para obtener el grado de membresía de la señal de entrada con respecto a las funciones de membresía (FM), que en este caso fueron de la forma triangular y trapezoidal. En la entrada del sistema se tiene almacenada en memoria el punto de referencia para obtener una posición y derivada deseada para mantener al péndulo en la posición vertical. Lo anterior ayuda a obtener un error en la posición y un error en la derivada del error. El FPGA únicamente realiza la operación de diferencia entre la posición deseada y la posición medida, valor que es enviado hacia el microcontrolador que calcula su derivada y envía su valor hacia el FPGA. De esta forma se tienen las dos variables que van a ser fuzzificadas en HDL por el primer módulo. La Figura 7 muestra el diagrama del método descrito para el cálculo del valor de membresía de la señal fuzzificada en su correspondiente universo de discurso.

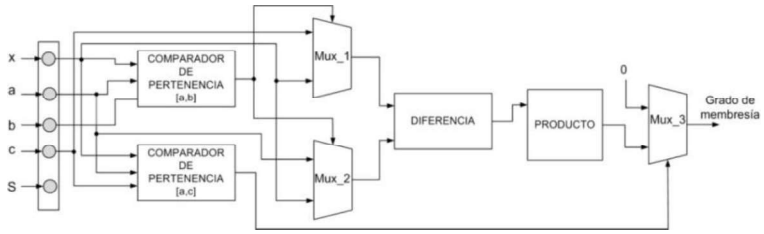

Fig. 7. Diagrama de bloques para permitir calcular el grado de membresía en funciones de membresía triangular y trapezoidal.

El cálculo del grado de membresía se limita a conocer si el dato de entrada se encuentra en alguna de las FM. Si es una función triangular, se detecta en que parte de la función cae el dato para conocer si se encuentra dentro de la pendiente negativa o positiva y realizar la operación necesaria para obtener su correspondiente valor dentro del intervalo difuso [0-255] que es la resolución del controlador de 8 bits. La Figura 8 muestra las funciones de membresía para las variables del fuzificador del error y de derivada del error, así como el universo de discurso de salida diseñado con funciones de salida Singleton, cuyo valor es enviado al módulo generador PWM.

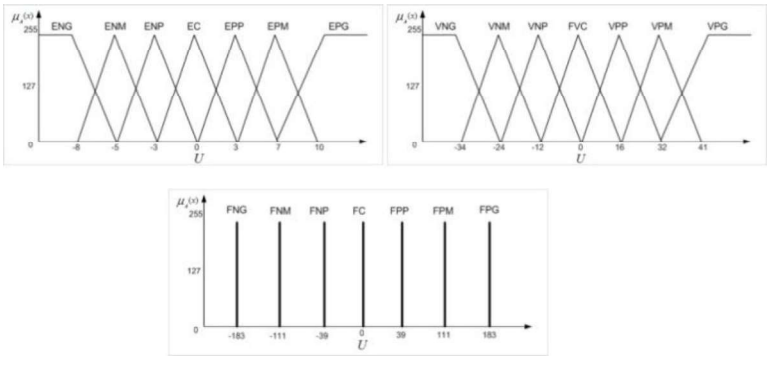

Fig. 8. Funciones de membresía para evaluar a las variables error, derivada y funciones de membrecía de Singleton de salida.

El módulo de inferencia toma los grados de membresía calculados, evalúa que reglas difusas se activan y aplica la operación difusa MIN-MAX.

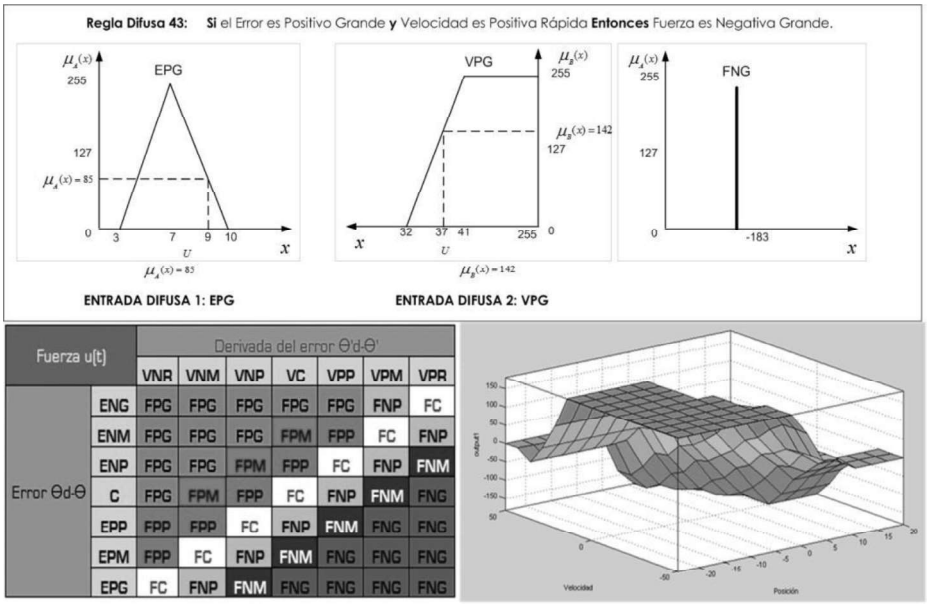

Fig. 9. Ejemplo de cálculo de grado de membresía y tabla de reglas difusas que permiten evaluar el valor del error y su derivada.

El objetivo de la etapa Defuzzificación es obtener la función de membresía final que es la agregación ó la suma de todas las combinaciones de conjuntos difusos enlazados según la base conocimiento y que se activan en un momento dado según la combinación de las dos entradas etiquetadas como error y derivada del error. Se produce una función o una superficie total, ver Figura9, Este función representa la suma de todas las implicaciones y el método de defuzzificación permite obtener el valor adecuado que representa a la función total. La implementación del Método Promedio de los Centros que se utiliza en el presente desarrollo de investigación en tecnología embebida, toma como base la investigación realizada en [13], donde se propone una arquitectura paralela para el cálculo de la salida defuzzificada a partir de la operación correspondiente para encontrar el Centro de Gravedad de la función agregada. La ecuación general para el cálculo del promedio de los centros se muestra en la ecuación (2).

$$z^* = \frac{\sum_{l=1}^{M} z*w_l}{\sum_{l=1}^{M} w_l} \qquad (2)$$

El valor de la variable de salida Z* está determinado por el promedio de los centros de los M conjuntos difusos de salida con los pesos *w,* siendo igual a la altura de los conjuntos difusos correspondientes. En cada uno de los módulos de inferencia difusa correspondiente a cada uno de los consecuentes de salida (FNG, FNM, FNP, FC, FPP,

FPM, FPG), se realizan las dos operaciones difusas MAX-MIN, cuyo resultado es tomado por el módulo defuzzifcador.

4 Resultados

Para poder validar que la salida del control difuso es la adecuada para estabilizar al péndulo es necesario corroborar los resultados generados en las tres situaciones descritas a continuación:

1. Los resultados de las simulaciones del control difuso generado en el Toobox de Matlab.
2. Los resultados de las simulaciones del control difuso embebido en el software ISIM del fabricante del FPGA XILINX.
3. Los resultados del control real en el motor de CD por el pulso PWM generado por el FPGA.

Los dos primeros resultados permiten comparar que tan cercanos están los sistemas difusos descritos; dicha comparación permite entrever que tan preciso es el método de inferencia y de defuzzificación entre ambas simulaciones. En ésta simulación se toma en cuenta que se hace cero la variable derivada y se mantiene variante la posición en su intervalo de movimiento. La Figura 10 muestra la comparación entre las situaciones en simulación y el aporte real de la salida del sistema difuso para control del péndulo, según se observa en la gráfica, el comportamiento del sistema será devolver la posición del péndulo al cero digital.

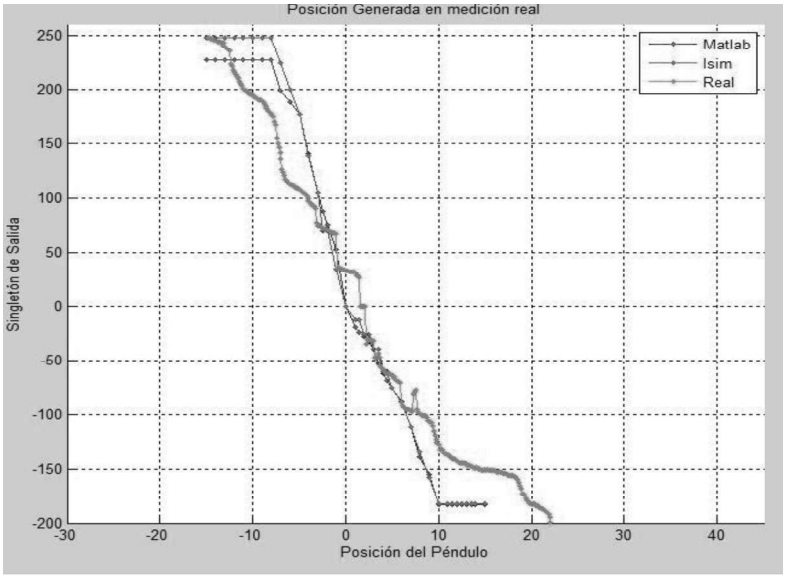

Fig. 10. Comparación del comportamiento del sistema difuso embebido en FPGA, el generado en Matlab y la señal PWM generada en el sistema real.

Finalmente se presentan los recursos utilizados en el FPGA de Xilinx XC3S500E para lograr embeber el sistema difuso de control que estabiliza el péndulo invertido. Como se observa, únicamente se utilizó el cien por ciento de los elementos lógicos con que cuenta el FPGA, usados como módulos de multiplicación y de los demás módulos se tienen suficientes recursos para hacer mejoras e incluso hacer más robusto al sistema difuso, por medio de otros operadores de inferencia o compartir el sistema de control con un algoritmo PID.

Table 1. Recursos lógicos utilizados en la descripción del sistema de control difuso en el FPGA XC3S500E de Xilinx.

Dispositivo seleccionado: 3s500efg320-5	
Slices:	2045 de 4656 43%
Slice Flip Flops:	1002 de 9312 10%
4 input LUTs:	3428 de 9312 36%
Logic:	3394
Shift registers:	34
IOs:	60
Bonded IOBs:	60 de 232 25%
MULT18X18SIOs:	20 de 20 100%
GCLKs:	1 de 24 4%

5 Conclusiones

El uso de FPGA como sistema de procesamiento es viable para el uso de sistemas de control que requieren tiempo real. El sistema difuso embebido fue del tipo Mamdani y el uso de HDL para su descripción facilitó su implementación al usar sólo una parte de todos los elementos lógicos del FPGA de Xilinx. La estabilización del péndulo invertido en una vecindad, se consiguió utilizando el sistema anterior, como es posible ver en la Figura 10, se obtienen resultados adecuados en el control. Como trabajos futuros se piensa embeber el sistemas difuso en un Soft-Processor, para su comparación con un modelo Takagi-Sugeno-Kang y un modelo neurodifuso implementados en la misma plataforma.

Agradecimientos

Se agradece el apoyo brindado al IPN, a través del programa PIFI y COFAA; a la SIP-IPN a través de los proyectos: SIP 20131505, SIP20131182, SIP20131514 y al CONACyT 155014.

Referencias

1. M. Togai and H. Watanabe, A VLSI implementation of fuzzy inference engine: Toward an expert system on a chip. International Journal of Information Sciences, vol. 38, pp. 147-163, (1986).
2. John H. Lilly. Fuzzy control and identification. Wiley, pp. 231, (2010).
3. Chen Yong, Huang Sheng-hua, Wan Shan-ming and WU Fang, A novel fuzzy logic direct torque controller for a permanent magnet synchronous motor with a field programmable gate array. Journal of Chongqing University, vol. 7, no.3, pp. 228-233, (2008).
4. Oscar Montiel, Yazmin Maldonado, Roberto Sepúlveda, and Oscar Castillo, Simple Tuned Fuzzy Controller Embedded into an FPGA, Conference of the North American Fuzzy Information Processing Society - NAFIPS, pp.1-6, (2008).
5. Jacobo Alvarez, Alfonso Lago and Andres Nogueiras, FPGA Implementation of a Fuzzy Controller for Automobile DC-DC Converters, IEEE International Conference on Field Programmable Technology, pp. 237-240, (2006).
6. Lozada, H. Juan Carlos, Apuntes del curso impartido sobre Diseño de Procesadores Dedicados. Centro de Innovación y Desarrollo Tecnológico en Cómputo, Instituto Politécnico Nacional, México, (2013)
7. Zhijun Li, Chenguang Yang, Liping Fan. Advanced Control of Wheeled Inverted Pendulum Systems. Springer-Verlag London 2013, pp. 218.
8. C. Aguilar-Ibáñez, O. Octavio Gutiérrez F., and H. Sossa A. Controlled Lagrangian approach to the stabilization of the inverted pendulum system. Revista Mexicana de Física.Vol.54, No. 4, pp. 329-335, (2008).
9. Tomasz Praczyk. Using assembler encoding to solve inverted pendulum problem. Computing and Informatics, vol. 28, pp. 895–912, (2009).
10. S. Kizir, Z. Bingul and C. Oysu. Fuzzy control of a real time inverted pendulum system. Journal of Intelligent & Fuzzy System. Vol. 5177, pp. 674–681, (2008).
11. Seiji Yasunobu and Munehito Mori. Swing up Fuzzy Controller for Inverted Pendulum Based on a Human Control Strategy. In Proceedings of the Sixth IEEE International Conference on Fuzzy Systems, pp. 1621-1625, (1997).
12. Tzuu-Hseng S Li, Ming-Yuan Shieh. Switching-type fuzzy sliding mode control of a cart-pole system. Mechatronics Vol. 10, pp. 91-109, (2000).
13. Bit Techonologies. hoja de especificaciones. Internet: http://www.bitechnologies.com/pdfs/6180.pdf. (2006).
14. R. Isermann, Digital Control Systems, Springer-Verlag, (1989).
Maurice Gaymer Road, Devantech Ltd (Robot-Electronics). Hoja de especificaciones. Internet: http://www.robot-electronics.co.uk/htm/md03tech.htm. [Noviembre 2013].
15. MPLAB, hoja de especificaciones. Internet: http://ww1.microchip.com/downloads/en/DeviceDoc/41291D.pdf. [Noviembre 2013].

Functional Equivalence between Fuzzy PID and Traditional 2DOF PID Controllers

P. Jorge Escamilla-Ambrosio, Raúl Acosta-Bermejo

Instituto Politécnico Nacional, Centro de Investigación en Computación, Mexico City, Mexico
{pescamilla,racosta}@cic.ipn.mx

Abstract. This paper demonstrates that under certain conditions a class of fuzzy PID controllers are functionally equivalent to a class of traditional two-degree-of-freedom (2DOF) PID controllers. Furthermore, although nonlinearities can be integrated to a traditional 2DOF PID controller, its fuzzy counterpart is intrinsically nonlinear. These nonlinearities, reside in the fuzzy rule base. Although fine tuning can be achieved in both traditional and fuzzy PID controllers, the latest one is superior due to that non-linear control surface that is obtained by modifying the parameters that define the fuzzy rules set. The findings are demonstrated by simulating two benchmark processes taken from the literature.

Keywords. PID control, Fuzzy control, 2DOF PID control, nonlinear control.

1. Introduction

Due to their simple structure, traditional proportional-integral-derivative (PID) controllers continue to be the most adopted controllers in practical cases [1-4]. Furthermore, they are relatively easy to tune and their basic structure is well understood by engineers and industrial practitioners [5-7].

Over time, fuzzy logic control (FLC) has been widely used in industrial processes [8, 9]. These applications exploit the heuristic nature of FLC for both linear and nonlinear systems. In particular, due to the success of traditional PID control, several structures of PID-type FLC (PID-FLC) have been proposed and studied (including PI and PD) [10-14]. As a result, several approaches have investigated the relationship between traditional PID control and PID-FLC [12, 14-16].

The degree of freedom of a controller is determined by the number of closed-loop transfer functions that can be adjusted independently [17]. Due that 2DOF PID control offers natural advantages over one-degree-of-freedom PID control, various 2DOF PID controllers have been proposed in the literature [17-19]. Similarly, there have been proposed 2DOF FLC [20, 21]. However there are not related to their traditional 2DOF PID counterpart. In this work there is demonstrated that under certain conditions a class of PID-FLC is functionally equivalent to a class of traditional 2DOF PID control. In addition, the main advantage of the PID-FLC over its traditional counterpart is that a nonlinear control surface can be achieved through the manipulation of the parameters that define the fuzzy rule set.

© E. A. Santos, J. C. Chimal, L. Cabrera, E. Castillo.
Advances in Computer Science and Engineering
Research in Computing Science 67, 2013 pp. 83–93
Paper Recived 17-08-2013 and Acepted 21-10-2013

The paper is organized as follows. In Section 2 the functional equivalence between 2DOF PID and fuzzy PID controllers is presented. In Section 3 simulation of two benchmark processes taken from the literature is developed in order to demonstrate the findings. Conclusions are drawn in Section 4.

2. Functional equivalence between 2DOF PID and fuzzy PID controllers

2.1 Traditional PID control

The traditional PID controller has the following standard form in the time domain:

$$u(t) = K_p\left[e(t) + \frac{1}{T_i}\int_0^t e(\tau)d\tau + T_d\frac{de(t)}{dt}\right] \tag{1}$$

where: $u(t)$ is the control action, $e(t)$ is the system error, K_p is the proportional gain, T_i is the integral time constant and T_d is the derivative time constant. Also (1) can be written as:

$$u(t) = K_p e(t) + K_i\int_0^t e(\tau)d\tau - K_d\frac{de(t)}{dt} \tag{2}$$

where $K_i = K_p/T_i$ and $K_d = K_pT_d$. In this case the tuning problem consists in selecting the values of these three parameters.

2.2 DOF PID control

Although several equivalent forms of 2DOF PID controllers have been proposed [20, 21], in this work the one proposed by Panagopoulose, et al. [22] is utilized, as is illustrated in Fig. 1. From this figure, the process transfer function G(s) is controlled with a PID controller with two degrees of freedom. The transfer function $G_c(s)$ describes the feedback from process output y to control signal u, and $G_{ff}(s)$ describes the feed forward from set point y_{sp} to u. The external signals that act on the controller loop are the set point y_{sp} and the load disturbance l. Note that for simplicity, measurement noise is not being considered. In this case, the corresponding 2DOF PID controller has the following form in the time domain:

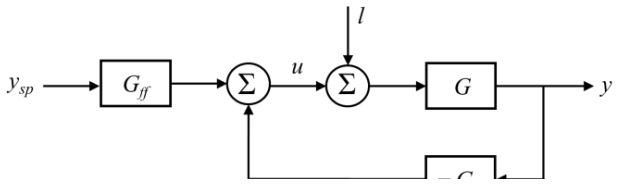

Fig. 1. Block diagram of the 2DOF PID controller.

$$u(t) = K_p\left(by_{sp}(t) - y(t)\right) + K_i\int_0^t\left(y_{sp}(\tau) - y(\tau)\right)d\tau - K_d\left(c\frac{dy_{sp}(t)}{dt} - \frac{dy(t)}{dt}\right) \tag{3}$$

where K_p, K_i , K_d, b and c are the controller tuning parameters.

2.3 Fuzzy PID control

As in traditional control, in fuzzy control there are the analogous structures of the PI type fuzzy logic controller (PI-FLC), PD type fuzzy logic controller (PD-FLC) and the PID type fuzzy logic controller. For the case of the PID-FLC several structures have been proposed. In this work, the one referred to as Modified Hybrid PID-Fuzzy Logic Controller (MHPID-FLC) is adopted. In this structure a combination of a PI-FLC and a PD-FLC is used to implement a PID-FLC with a common two-dimensional rule base, as is shown in Fig. 2(a). Therefore, once appropriate scaling factors G_E, $G_{\Delta E}$, $G_{\Delta U}$ and G_U are selected, a PID control strategy is implemented by combining a PI incremental algorithm and a PD positional algorithm using a two-term fuzzy control rule base.

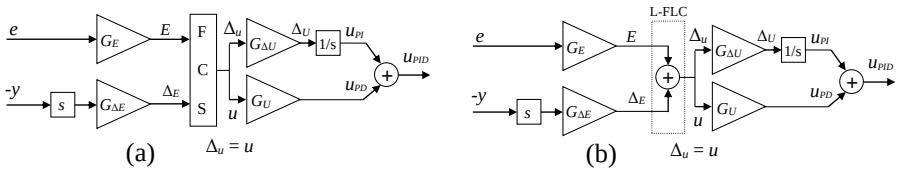

Fig. 2. (a) Schematic representation of the MHPID-FLC; (b) Simplified structure.

2.4 Functional equivalence

This section demonstrate that under certain conditions the 2DOF PID control and the MHPID-FLC are functionally equivalent. Let's define the next set of conditions:

1. The Fuzzy Control System (FCS) inside the MHPID-FLC structure is a first-order Sugeno fuzzy model [23], with fuzzy rules of the form:

   If E is A and Δ_E is B then $u = pE + q\Delta_E + r$

   where A and B are fuzzy sets in the antecedent, while p, q, and r are all constants.
2. The FCS rule base consists of four rules:

   R1: If E is N and Δ_E is N then u = $p_1E + q_1\Delta_E + r_1$
   R2: If E is N and Δ_E is P then u = $p_2E + q_2\Delta_E + r_2$
   R3: If E is P and Δ_E is N then u = $p_3E + q_3\Delta_E + r_3$
   R4: If E is P and Δ_E is P then u = $p_4E + q_4\Delta_E + r_4$

   where the coefficient constants $p_i = q_i = 1$, and $r_i = 0$; for $i = 1, 2, 3, 4$. The linguistic labels for the fuzzy sets are defined as P = Positive and N = Negative.
3. The universe of discourse for both FCS inputs is normalized on the range [-1, 1].
4. The membership functions of the input variables, E and Δ_E, to the FCS are triangular complementary fuzzy sets [24], and they are defined as shown in Fig. 3(a).

5. The product-sum compositional rule of inference [25] is used in the stage of rule evaluation.
6. The weighted average method is used in the defuzzification process.

If all the above conditions are satisfied, then the 2DOF PID controller and the MHPID-FLC are functionally equivalent. Note that under assumptions 1-6 the FCS inside the MHPID-FLC structure is the simplest that can be considered, and its output is simply given by the sum of its inputs. This FCS is known as the normalized and linear Fuzzy Logic Controller (L-FLC); its control surface is shown in Fig. 3(b). This simplifies the structure of the MHPID-FLC as is shown in Fig. 2(b).

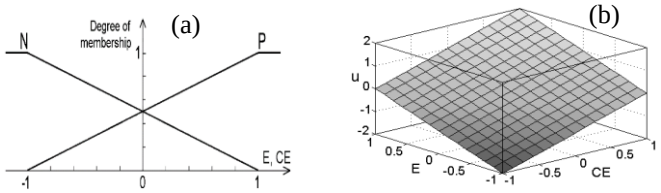

Fig. 3. (a) Membership functions of the L-FLC, (b) Control surface of the L-FLC

Therefore, from Fig. 2(b), the output of the MHPID-FLC is given as (for simplicity the time dependence is not denoted):

$$u_{PID} = u_{PI} + u_{PD} \tag{4}$$

$$u_{PID} = G_{\Delta U}\int\left[G_E e - G_{\Delta E}\frac{dy}{dt}\right] + G_U\left[G_E e - G_{\Delta E}\frac{dy}{dt}\right] \tag{5}$$

From here, performing operations an grouping terms, it is easy to arrive to:

$$u_{PID} = G_U G_E y_{sp} - \left(G_{\Delta U}G_{\Delta E} + G_U G_E\right)y + G_{\Delta U}G_E\int e - G_U G_{\Delta E}\frac{dy}{dt} \tag{6}$$

Therefore, if (3) and (6) are compared, then it is noted that the MHPID-FLC operates like a traditional 2DOF PID controller with the equivalent set-point weights, proportional, integral and derivative gains given by:

$$c = 0 \tag{7}$$

$$K_p b = G_U G_E \tag{8}$$

$$K_p = G_{\Delta U}G_{\Delta E} + G_U G_E \tag{9}$$

$$K_i = \frac{K_p}{T_i} = G_{\Delta U}G_E \tag{10}$$

$$K_d = K_p T_d = G_U G_{\Delta E} \tag{11}$$

Note that the weighting factor c is considered as zero, as it does not appear in the MHPID-FLC structure. However, the weighted derivative term $K_d c dy_{sp}(t)/dt$ can be added to the MHPID-FLC structure as a separated term, as is shown in Fig. 4. In this figure the term K_d has been replaced by $G_U G_{\Delta E}$ as given by (11). Therefore, by doing that, the controller shown in Fig. 4 is functionally equivalent to the 2DOF PID controller defined by (3) if the defined conditions are fulfilled.

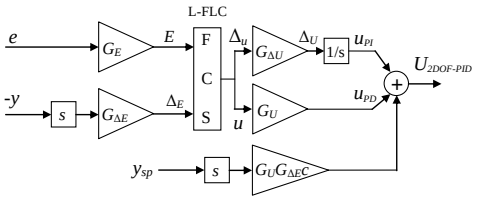

Fig. 4. MHPID-FLC structure with added weighted set-point derivative term.

2.5 Tuning procedure

Given the structure and the functional equivalence described in the previous section, now the problem is how to perform the tuning of the scaling factors G_E, $G_{\Delta E}$, $G_{\Delta U}$, G_U and the weighting factors b and c. If the values of K_p, K_i, and K_d or alternatively the values of K_p, T_i, and T_d are available, then the values G_E, $G_{\Delta E}$, $G_{\Delta U}$ and G_U in the MHPID-FLC structure (see figure 2) can be calculated as follows. First, let's define:

$$G_E = 1 \tag{12}$$

From (12) in (10):

$$G_{\Delta U} = K_i \tag{13}$$

Performing substitutions in (9) and (11) and making operations, it is easy to arrive to the next second order equation:

$$0 = K_p^2 b^2 - K_p^2 b + K_i K_d \tag{14}$$

The solution of this equation is given by:

$$b = \frac{1}{2} \pm \frac{\sqrt{(-K_p^2)^2 - 4K_p^2 K_i K_d}}{2K_p^2} \tag{15}$$

If the Ziegler-Nichols (Z-N) frequency response method is used to find the traditional PID gain parameters, they are given by the set of equations:

$$K_P = 0.6K_u;\ K_i = \frac{2K_p}{T_u};\ K_d = \frac{K_p T_u}{8} \tag{16}$$

From this set of equations it is straightforward to demonstrate that:

$$4K_iK_d = K_p^2 \tag{17}$$

Substituting (17) in (15) results in:

$$b = \frac{1}{2} \tag{18}$$

From here the remaining scaling factors are obtained as:

$$G_U = \frac{1}{2}K_p \tag{19}$$

$$G_{\Delta E} = \frac{2K_d}{K_p} \tag{20}$$

It is surprising to find that the value of the set point weighting factor *b* is uniquely determined as 0.5 when the Z-N tuning method is used and it is intrinsically included in the MHPID-FLC structure, although it is not explicitly included. This simplifies the calculation of the remaining scaling factors. With regard to the weighting factor *c* of the set point derivative term, it is left as an additional free adjusting factor, which can be manipulated for fine tuning, if needed. Note that the Z-N tuning parameters, K_u and T_u, can be obtained with the relay auto-tuning method [26].

3 Simulation results

In this section the results from the simulation of two bench mark processes taken from the literature are presented. The simulations for each process have been developed in the Matlab/Simulink simulation environment, together with the Fuzzy Logic Toolbox. The Z-N tuning parameters where obtained with the relay auto-tuning method, from there the scaling factors where obtained, as explained in the previous section.

Transfer function of a stable process [27]:

$$G_1(s) = \frac{e^{-0.4s}}{(s+1)^2} \tag{21}$$

Results: The comparison of the set point and load disturbance rejection responses are shown in Fig. 5 (a). Note that the response of the traditional 2DOF PID controller with *b*=0.5 and *c*=0, is exactly the same as the obtained with the MHPID-FLC, which demonstrate that they are functionally equivalent. In both cases, further fine tuning can be achieved by adjusting the weighting factor *c*. However, in the case of the MHPID-FLC additional tuning can be performed by adjusting the parameters that define the fuzzy rules or by modifying the scaling factors, or by modifying all these parameters altogether. As an example of further fine tuning, Fig. 5(a) also shows the comparison of the results obtained when the fuzzy rules have been modified by set-

ting the coefficients p_1=p_4=2.5, q_1=q_4=3, r_1=r_4=0, p_2=p_3=0.4, q_2=q_3=0.4, r_2=r_3=0, this controller is referred to as MHPID-FLC-MRS. In the same figure, the results obtained when modifying the scaling factors as G_E=1, $G_{\Delta E}$=0.735, G_U=1.8 and $G_{\Delta U}$=1.8, also are shown, controller referred to as MHPID-FLC-MSF. In addition, the results of performing additional tuning by adjusting the weighting factor *c*, for the three controllers, are shown in Fig. 5(b), compared with the original 2DOF PID controller. For better comparison, the obtained integral of the absolute error (IAE) for all the simulated cases are shown in Table 1, the integral is reset after the step response settling time to measure the IAE for the load rejection responses.

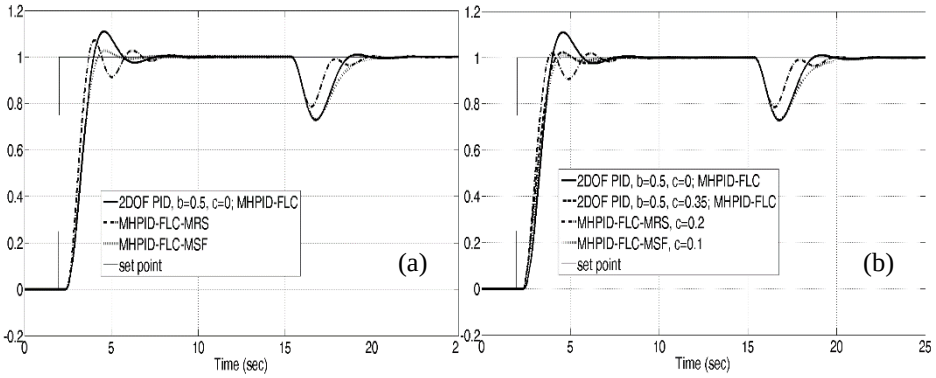

Fig. 5. (a) Step response and load rejection plots for process 1; (b) further tuning through the weighting factor *c* for process 1.

Table 1. IAE measurements for process $G_1(s)$

	IAE	
	Set point	Load rejection
2DOF PID, *b*=0.5, *c*=0; MHPID-FLC	1.4173	0.4739
MHPID-FLC-MRS	1.2533	0.3157
MHPID-FLC-MSF	1.3165	0.5554
2DOF PID, *b*=0.5, *c*=0.35; MHPID-FLC	1.2146	0.4739
MHPID-FLC-MRS, *c*=0.2	1.1816	0.3157
MHPID-FLC-MSF, *c*=0.1	1.2826	0.5554

Transfer function of an unstable process [27]:

$$G_1(s) = \frac{e^{-0.5s}}{s(s+1)} \tag{22}$$

The comparison of the set point and load disturbance rejection responses are shown in Fig. 6(a). Similarly than for the previous process, the response of the traditional 2DOF PID controller with *b*=0.5 and *c*=0, is exactly the same as the obtained with the MHPID-FLC, proving that they are functionally equivalent. Fig. 6(a) also shows the comparison of the results obtained when the fuzzy rules have been modified by set-

ting the coefficients p_1=p_4=1, q_1=q_4=1, r_1=r_4=0, p_2=p_3=3.4, q_2=q_3=3.8, r_2=r_3=0, this controller is referred to as MHPID-FLC-MRS. In the same figure, the results obtained when modifying the scaling factors as G_E=1, $G_{\Delta E}$=1.25, G_U=1.5 and $G_{\Delta U}$=0.9, controller referred to as MHPID-FLC-MSF, also are shown. The results of performing additional tuning by adjusting the weighting factor c, for the three controllers, are shown in Fig. 6(b), compared with the original 2DOF PID controller. The measured IAE for all the simulated controllers are shown in Table 2.

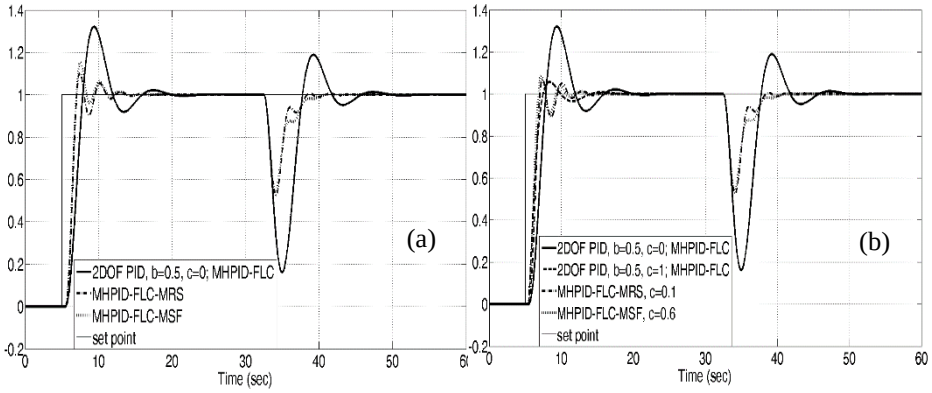

Fig. 6. (a) Step response and load rejection plots for process 2; (b) further tuning through the weighting factor c for process 2.

Table 2. IAE measurements for process $G_2(s)$

	IAE	
	Set point	Load rejection
2DOF PID, b=0.5, c=0; MHPID-FLC	2.9431	3.0544
MHPID-FLC-MRS	1.6324	1.0289
MHPID-FLC-MSF	1.6105	1.1128
2DOF PID, b=0.5, c=0.35; MHPID-FLC	1.4678	3.0544
MHPID-FLC-MRS, c=0.2	1.5853	1.0289
MHPID-FLC-MSF, c=0.1	1.3612	1.1128

4 Conclusions

In this work a functional equivalence between 2DOF PID control and MHPID-FLC has been demonstrated. From the simulations performed, the next tuning sequence is recommended for the MHPID-FLC:

1. Find the traditional proportional, integral and derivative gains using the autotuning relay experiment and Z-N formulae.
2. From the traditional proportional, integral and derivative gains calculate the scaling factors G_E, $G_{\Delta E}$, G_U and $G_{\Delta U}$, recall that intrinsically the weighting factor b=0.5.

3. Perform fine tuning by adjusting the parameters of the fuzzy rules p_i, q_i, and r_i; for $i = 1, 2, 3, 4$. Or by manipulating the scaling factors G_E, $G_{\Delta E}$, G_U and $G_{\Delta U}$.
4. If needed, further fine tuning can be achieved by manipulating the scaling factor c.

Note, that by modifying the parameters of the fuzzy rules, the control surface of the FCS inside the MHPID-FLC becomes nonlinear. As an example, Fig. 7 shows the control surface obtained when $p_1=p_4=1$, $q_1=q_4=1$, $r_1=r_4=0$, $p_2=p_3=3.4$, $q_2=q_3=3.8$, $r_2=r_3=0$, used for tuning the MHPID-FLC of plant $G_2(s)$. From the tuning procedure it was observed that the only way of improving the load rejection performance was precisely by introducing the nonlinear control surface in the MHPID-FLC. Further adjustment of the weighting factor c only produced a reduction in the step response overshot, but did not produced any change in the load rejection response. Although good results were obtained, more study of the proposed MHPID-FLC and the tuning procedure is needed to fully characterize it. This work is in progress.

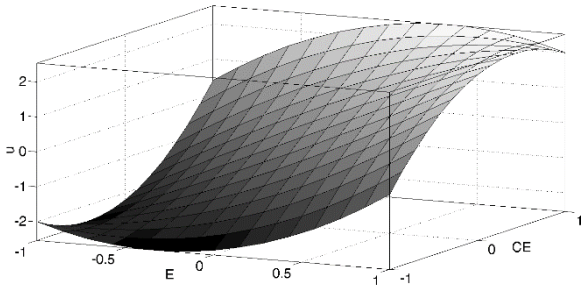

Fig. 7. Nonlinear control surface.

References

1. Yu, W., Rosen, J.: Neural PID control of robot manipulators with application to an upper limb exoskeleton. IEEE Trans. Cybernetics. 14, 673-684 (2013).
2. Ali, E.S., Abd-Elazim, S.M.: BFOA based design of PID controller for two area load frequency control with nonlinearities. Electrical Power and Energy Systems. 51, 224-231 (2013).
3. Godbolt, B., Vitzilaios, N.I., Lynch, A.F.: Experimental validation of a helicopter autopilot design using model-based PID control. J. Intell. Robot Syst. 70, 385-399 (2013).
4. Wai, R.J., Lee, J.D., Chuang, K.L.: Real-time PID control strategy for maglev transportation system via particle swarm optimization. IEEE Trans. Industrial Electronics. 58, 629-646 (2011).
5. Seki, H., Shigemasa, T.: Retuning oscillatory PID control loops based on plant operation data. Journal of Process Control. 20, 217-227 (2010).
6. Yu, Z., Wang, J., Huang, B., Bi, Z.: Performance assessment of PID control loops subject to setpoint changes. Journal of Process Control. 21, 1164-1171 (2011).
7. Ang, K.H., Chong, G., Li, Y.: PID control system analysis, design, and technology. IEEE Trans. Control Systems Tec. 13, 559-576 (2005).

8. Bonissone, P., Badami, V., Chiang, K., Khedkar, P., Marcelle, K., Schutten, M.: Industrial applications of fuzzy logic at General Electric. Proc. IEEE. 83, 450-465 (1995).
9. Precup, R.E., Hellendoorn, H.: A survey of industrial applications of fuzzy control. Computers in Industry. 62, 213-226 (2011).
10. Lee, C.C.: Fuzzy logic in control systems: Fuzzy logic Controllers, Part I and II. IEEE Transactions on Syst, Man and Cyber. 20, 404-435 (1990).
11. Mann, G.K.I., Hu, B.G., Gosine, R.G.: Analysis of direct action fuzzy PID controller structures. IEEE Trans. Syst., Man, Cybern., Part B. 29, 371-388 (1999).
12. Li, H.X. and Tso, S.K.: Quantitative design and analysis of fuzzy proportional-integral-derivative control - a step towards autotuning. Int. J. Syst. Sci. 31, 545-553 (2000).
13. Woo, Z.W., Chung, H.Y., Lin, J.J.: A PID type fuzzy controller with self-tuning scaling factors. Fuzzy Sets and Systems. 115, 321-326 (2000).
14. Galichet, S., Foulloy, L.: Fuzzy controllers: synthesis and equivalences. IEEE Trans. Fuzzy Systems. 3, 140-148 (1995).
15. Xu, J.X., Hang, C.C., Liu, C.: Parallel structure and tuning of a fuzzy PID controller. Automatica. 36, 673-684 (2000).
16. Mann, G.K.I., Hu, B.G., Gosine, R.G.: Two-level tuning of fuzzy PID controllers. IEEE Trans. Syst., Man, Cybern., Part B. 31, 263-269 (2001).
17. Araki, M., Taguchi, H.: Two-degree-of-freedom PID controllers. Int. Journal of Control, Automation, and Systems. 1, 401-411 (2003).
18. Prashanti, G., Chidambaram, M.: Set-point weighted PID controllers for unstable systems. Journal of The Franklin Institute. 337, 201–215 (2000).
19. Visioli, A.: A new design for a PID plus feedforward controller. Journal of Process Control. 14, 457–463 (2004).
20. Barai, R.K., Nonami, K.: Optimal two-degree-of-freedom fuzzy control for locomotion control of a hydraulically actuated hexapod robot. Information Sciences. 177, 1892-1915 (2007).
21. Precup, R.E., Preitl, S., Petriu, E.M., Tar, J.K., Tomescu, M.L., Pozna, C.: Generic two-degree-of-freedom linear and fuzzy controllers for integral processes. Journal of The Franklin Institute. 346, 980-1003 (2009).
22. Panagopoulos, H., Astrom, K.J., Hagglund, T.: Design of PID controllers based on constrained optimisation. IEE Proc. Control Theory Appl. 149, 32-40 (2002).
23. Takagi, T., Sugeno, M.: Fuzzy identification of systems and its applications to modelling and control. IEEE Trans. Syst. Man and Cyber. 15, 116-132 (1985).
24. Gravel, A., Mackenberg, H.: Mathematical analysis of the Sugeno controller leading to general design rules. Fuzzy Sets and Systems. 85, 165-175 (1995).
25. Kosko, B.: Neural Networks and Fuzzy Systems: A dinamical Approach to Machine Intelligence. Prentice Hall, Englewood Cliffs (1992).
26. Astrom, K.J., Hagglund, T.: Automatic tuning of simple regulators with specifications on phase and amplitude margins. Automatica. 20, 645-651 (1984).
27. Astrom, K.J., Hang, C.C., Persson, P., Ho, W.K.: Towards intelligent PID control. Automatica. 28, 1-9 (1992).

Design of a Control and Acquisition System in an FPGA Platform for a Single Degree of Freedom of an Articulated Robot Via Wifi

Javier Ruiseco Lopez, Sergio Vergara Limón, M. A. Vargas Treviño, Fernando Reyes Cortés[1] y Amparo Palomino Merino, G. Humberto Bezares Colmenares

Benemérita Universidad Autónoma de Puebla, Maestría en Ciencias de la Electrónica opción Automatización, Puebla, México
javierruiseco_88@hotmail.com, svergara@ece.buap.mx, mavargas@ece.buap.mx, recf62@gmail.com, palomino@ece.buap.mx, theboy115@hotmail.com

Abstract. The Maestría en Ciencias de la Electrónica, opción en Automatización (MCEA) has been developing systems and control techniques for ROTRADI robots which it has built. With the purpose of improving this systems and techniques, a Fuzzy controller and WiFi communication is being implemented. Initially, ROTRADI robots were controlled by desktop computers via PCI cards and then a Field Programmable Gate Array platform was introduced. The advantage of an FPGA platform is that it allows building an embedded system that can manage all the needs of controlling a ROTRADI, discarding the use of a computer. A hyperbolic tangent controller was developed for the FPGA, but due to calculation timings and usage of logical elements a Fuzzy Controller was proposed in an attempt to reduce these aspects. On the other hand, WiFi was proposed to replace PCI communication in order to make use of a more innovative technique to manipulate the robot.

Keywords: Fuzzy control, robot, data acquisition system, WiFi.

1 Introduction

MCEA has managed to develop robot arm manipulators which are known as ROTRADI [1] (see figure 1) which initially were controlled using desktop computers running Windows 98 disk operating system in order to guarantee a real-time control. MCEA has been improving its control systems and Field Programmable Gate Array (FPGA) [2] control platforms were introduced, in which computers are no longer required because all control requirements have been implemented on an embedded system that has an FPGA as core of operation. The advantage of having an FPGA platform is to guarantee real-time control and simplify the elements that constitute the whole system. Giving this, a hyperbolic tangent controller was implemented in the FPGA. Due to the FPGA's logical elements limitations, the control of a single degree of freedom was proposed. In order to continue to improve the control system, a Fuzzy

© E. A. Santos, J. C. Chimal, L. Cabrera, E. Castillo.
Advances in Computer Science and Engineering
Research in Computing Science 67, 2013 pp. 93–103
Paper Recived 20-09-2013 and Acepted 21-10-2013

controller [3] is being developed in an attempt to reduce the use of FPGA's logical elements and reduce the clock cycles that hyperbolic tangent's calculations require. The objective of this improvement is to be able to add more capabilities in the FPGA in the future. On the other hand, current PCI data communication is intended to be replaced by IEEE802.11 [4] wireless protocol known as WiFi, whereby the user will be able to control the robot and analyze the controller's performance wirelessly. It is important to mention that this work is currently under development.

Fig. 1. ROTRADI robot.

Networking technologies have been applied in the area, for example with sensors [5]. This is due to the advances in microprocessors, memory, power consumption and cheaper technology in which networking with wireless technologies is becoming cheaper with and increasing market. On the other hand, robot related technologies have a broad area of application, from designing robots and control laws, through designing robots that are self-configurable [6] and therefore, can change their own shape.

2 System description

The system in general is constituted by software, firmware and hardware.

Software: The software that will be developed outside of the embedded system, whose function is to serve as a means of interaction between the user and the card controlling the robot.

Firmware: The FPGA programming, in which the control law resides, particularly a fuzzy controller.

Hardware: The electronics developed to implement the control and communication between the user and ROTRADI robot.

The system in development has he following block structure:

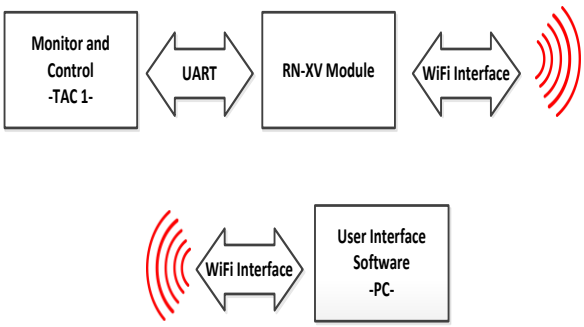

Fig. 2. General block diagram.

The proposed architecture for the system aims to create the embedded system which autonomously controls the robot, given the configurations of the user. The description for the block diagram is as follows.

User Interface: Is the software by which the user can perform the relevant configurations, such as the desired position of the degree of freedom, and to carry out the task of monitoring data from the robot. Particularly, the software will be developed in National Instruments Labview [7] which will also manage the Transport Control Protocol/Internet Protocol (TCP/IP) [8] communication to establish a WiFi connection.

RN-XV module [9]**:** Is by itself an embedded system which serves as a WiFi to serial converter. It will be integrated into the Tarjeta de Adquisición para Control 1(TAC1) to send and receive data wirelessly via the protocol IEE 802.11g, known as WiFi, "g" generation.

TAC1: Is the circuit board developed by the FCE MCEA in which the electronics regarding tasks of controlling the robot, reading motor encoders and controlling motor drivers reside.

ROTRADI robot: The ROTRADI robot (see figure 1) is an articulated robot with three degrees of freedom which first characteristic is that it is of direct transmission. This means that the motors of the joints are directly assembled to robot aluminum links, and therefore, no gearboxes are required. The motors have a linear response and they produce the necessary force to move the joints.

3 Acquisition system

3.1 TAC1 board

The main electronics hardware is the circuit board knows as TAC1 (see figure 3) developed by the MCEA. Initially the TAC1 was designed to function as data acquisition and send/receive data to the ROTRADI via the PCI bus. The TAC1 has been modified as a standalone embedded system which no longer requires a PC to control

the ROTRADI robot therefore, the PCI bus is only used to apply supply voltages to the card by an external power supply.

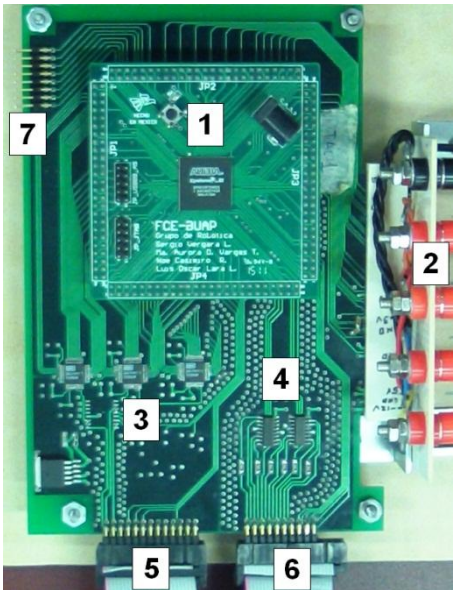

Fig. 3. TAC1 board.

1) FPGA Cyclone II EP2C8Q208C7: Is the core of the TAC1, in it resides the control law as well as the required firmware to acquire signals from the encoders and send the control data to the drivers.

2) Power supply bus: Voltages of 12V, 5V, 3.3V and -12V are applied.

3) Texas Instruments 7741Y DAC's: They translate the control law from the FPGA to voltage that serves as input to the motor drivers.

4) Differential filters SN65LVDT32B: They serve as filters for the incoming encoder signals.

5) Driver Bus: The voltage from the DAC's is sent to the driver via this bus.

6) Encoder Bus: The signals from the motors encoders are received via this bus.

7) H3 connector: A general purpose I/O bus with 3.3v and GND that has direct access to the FPGA.

3.2 RN-XV WiFi module

An important contribution of the present work is adding WiFi capabilities to the current TAC1 board. WiFi was chosen because of its increasing popularity and the innovation that a wireless robot control system represents. The core element of the WiFi interface is the RN-XV which will be integrated to the TAC1. The RN-XV module is based on the RN-171 module in which resides a firmware with the IEEE 802.11b/g TCP/IP protocol stack as well as the required electronics for the wireless transmis-

sion. It is a WiFi to serial converter and this is done via the serial protocol Universal Asynchronous Receiver Transmitter [10] [11]. The TCP/IP stack protocol [4] is a suite of protocols that has a layered architecture (see figure 4). It is formed by four layers; each one of them has its own protocols that work in order to establish a communication between TCP/IP. Particularly, WiFi resides in the bottom most layer, known as network access layer. Here resides the circuitry required to interpret the electric signals of the received/sent messages. The RN-XV has implemented in its firmware a mode of operation known as Access Point which is the one that will be used for this project. An access point is an infrastructure network that the user can connect to it and therefore control the robot. There are two protocols to use when sending data over TCP/IP, UDP and TCP. Due to the fact that TCP is a more reliable protocol to send data because it integrates means to determine if there was an error on the transmission, and on the other side UDP integrates rudimentary means to determine errors.

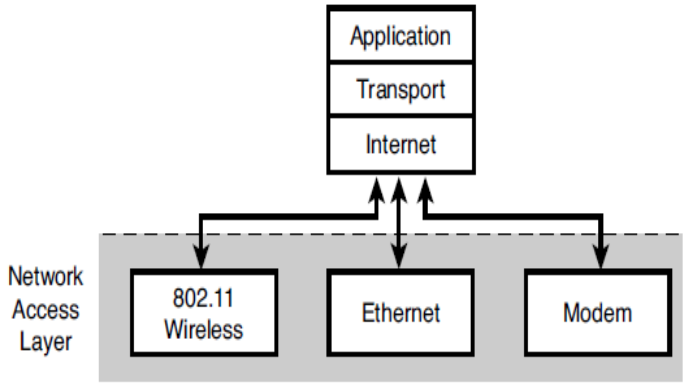

Fig. 4. TCP/IP stack.

When the module enters in Access Point mode in automatically broadcasts it's SSID which is the network's name and it will be ready to receive incoming connection on IP 1.2.3.4 and port 2000. The data is being sent over TCP with Labview, particularly in string type. As mentioned before, the module serializes the data received from WiFi via UART. In order to interface with the RN-XV's UART, a firmware in the FPGA has been implemented in order to establish communication between the FPGA and the WiFi module. The UART baudrate, network SSID, and other configurations where performed via a Telnet client, due to the fact that the module has implemented a Telnet server and therefore it can be configured wirelessly.

3.3 UART

The serial format of UART data may vary depending on whether it uses parity bits for error control. For this case, we will use 10 bits: 1 start bit + 8 data bits + 1 stop bit.

The signal is idle on logic "1" and activates at logic "0". In Figure 5 shows the format of the bit stream.

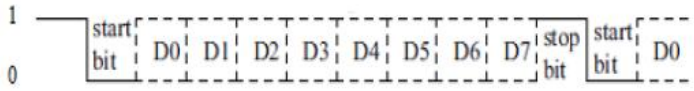

Fig. 5. UART bit transmission format.

The speed of bits is known as baudrate which is how many bits per second are being transmitted. The order of the data is from least significant to most significant. In the nomenclature of the UART, TX is for transition and RX is for receiving. It is important to establish a bit sampling at the middle of each bit transition, therefore, the RX sample rate is faster than the TX rate. The UART FPGA firmware was implemented in Altera Hardware Design Language (AHDL) based on state machines as can be seen in figure 6.

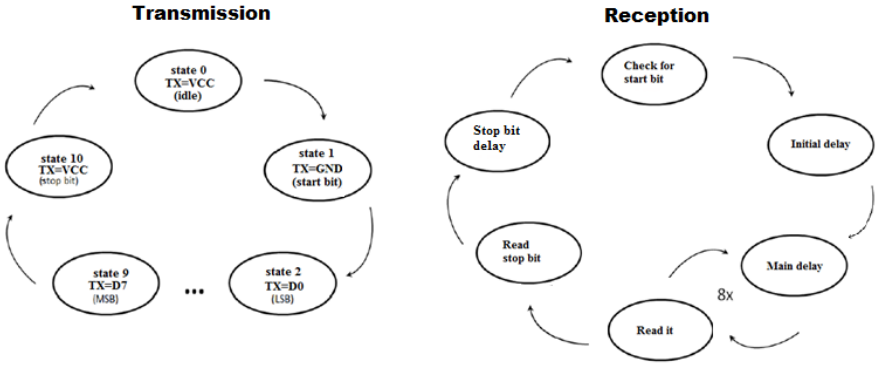

Fig. 6. UART Transmission and Reception state machines.

4 Control

The FPGA firmware currently has a hyperbolic tangent controller [1] with mechanical brake.

$$\tau = K_p \tanh \tilde{q} - K_v \tanh \dot{q} \tag{1}$$

Where $\tilde{q}$ is the position error, $\dot{q}$ is the velocity, K_p is the proportional gain and K_v is the derivative gain. The derivative section of the equation represents a brake to the control law. Since this controller uses floating-point units, the use of FPGA capacity is higher, at about 76% to control one degree of freedom. The reason that this work attempts to control one degree of freedom is due to the restriction of the amount of logical elements available on the FPGA, in addition, there must be logical elements left for the WiFi intercommunication, monitoring and user interface. In order to reduce the number of logic elements in use, and improve the clock cycles that hyperbolic tangent calculations require, it was proposed to implement a fuzzy controller as an alternative control law. The Fuzzy Controller has as input fuzzy variable the posi-

tion error and as output variable the torque, which establishes the membership functions of the position error which range varies between $\pm 360^{\circ}$ (see figure 7), due to the fact that the robot joints are rotational. The nomenclature of the membership functions is **E** for error, **T** for torque, **N** for negative, **P** for positive, **G** for large, **M** for medium, **EP** for small error and **MG** to very large.

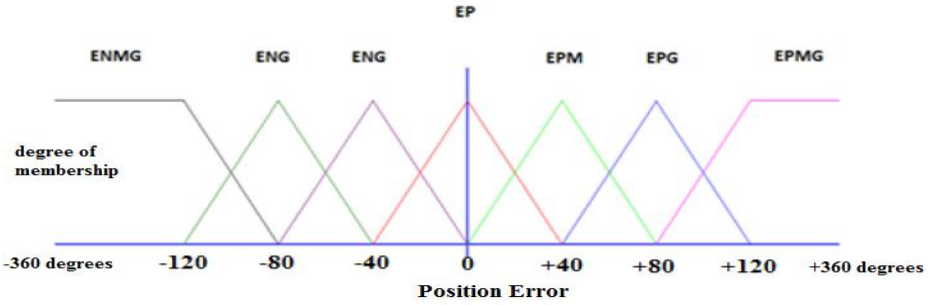

Fig. 7. Position Error membership function.

The rules were defined to be proportional to the error. Given a position error which magnitude is big, the output torque should be big. In contrast, if a position error is small, the output torque should be small. Having this, the fuzzy controller rules where defined as follows:

$$IF\ \mu ENMG, then\ \mu TNMG = \mu ENMG$$
$$IF\ \mu ENG, then\ \mu TNG = \mu ENG$$
$$IF\ \mu ENM, then\ \mu TNM = \mu ENM$$
$$IF\ \mu EP, then\ \mu TP = \mu EP$$
$$IF\ \mu EPM, then\ \mu TPM = \mu EPM$$
$$IF\ \mu EPG, then\ \mu TPG = \mu EPG$$
$$IF\ \mu EPMG, then\ \mu TPMG = \mu EPMG$$

Due to the fact that the output torque signal to the motor driver is a 16 bit number that represent a voltage range of $\pm 10\ volts$, the fuzzy output variable was defined as can be seen in figure 8.

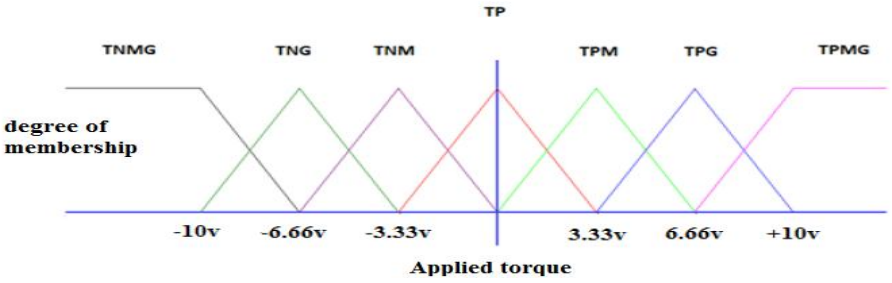

Fig. 8. Torque membership function.

The main state machines which constitute the fuzzy controller firmware are shown in figure 9, which also represent the fuzzy controller algorithm in use.

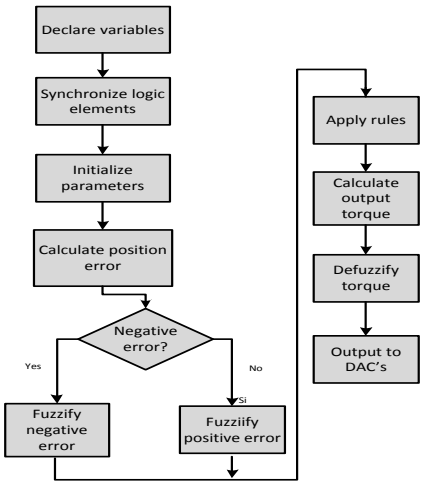

Fig. 9. Fuzzy controller algorithm.

5 Results

This work is in development and these are only preliminary results. The fuzzy controller implemented in AHDL code was able to reduce the number of logic elements in the FPGA compared with hyperbolic tangent. The fuzzy controller occupies about a ~ 62 % of logic elements in comparison to ~ 76 % of hyperbolic tangent. This is due largely to the operations with bit shifts. It is proposed as future work to optimize the firmware, particularly rethinking the architecture as the current one is optimized for speed and not for space. The response of the fuzzy controller is relatively fast, about 20 clock cycles to produce the result, which is about 0. 00000020 because the FPGA is clocked at 100Mhz. Due to the fact that an output gain adjusts were added to adjust the maximum torque that can be applied which the user can configure. Since the fuzzy controller delivers faster response than the hyperbolic tangent controller, in which a single Floating point operation takes about 11 to 14 clock cycles, it is intended that in the future the same fuzzy controller block originally designed to control one degree of freedom, can be used to control the three degrees of freedom of the ROTRADI robot by multiplexing data, since calculations are relatively fast. In order to ensure the proper functioning of the fuzzy controller firmware, a simulation of the firmware was performed (see fig. 10). First the theory of operation will be explained and then the results. In the first instance, the signals with which the motor operates will be explained. The controller takes the position of the encoder signals from the robot motor, which has a resolution of 0 to 655360 pulses per revolution, which equals the 0 to 360 degrees. As to the applied torque, the engine has a driver which converts a signal of $\pm$10 volts into torque. The controller has 16-bit, value that is converted to a voltage with the DAC's of the TAC1; -10 volts equals a value of 0, 0 volts to a value of 32767 and +10 volts to a value of 65535 binary.

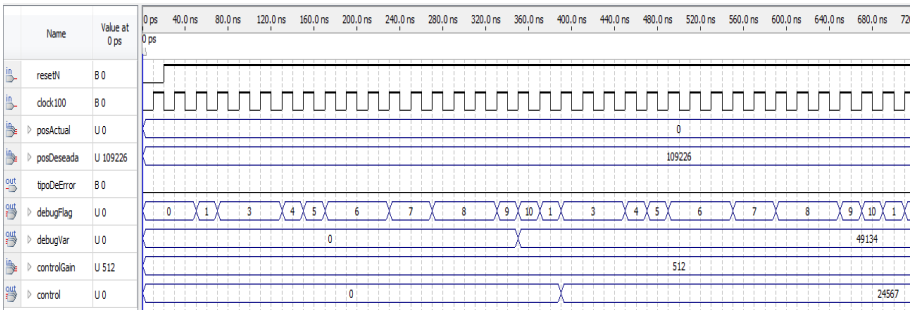

Fig. 10. Fuzzy Controller simulation.

Knowing these facts, the simulation will be then explained. Clock100 signal is the clock signal for the controller block , which operates at 100Mhz . For testing purposes, we assumed a current position of 0 degrees (home position) and a desired position of 60 degrees, which equals the 109226 if you were reading the encoder. It has an error signal "tipoDeError", which has a logical value of zero, if the error was positive and one if the error was negative. Since the error for the test values above is positive, "tipoDeError" has a logical value of zero. TorqueOut signal represents the output voltage to the motor driver (which will be converted from voltage to torque by the motor driver). TorqueOut has the value of 49134, a value that corresponds to 4.994 volts. This value was expected according to the rules applied, as it is expected to be applied half of the maximum torque by the controller in accordance with the output variable torque. Finally, there is a variable called debugFlag indicating the state machine in which is the FPGA firmware in order to monitor the proper functioning and the time it takes to process the information in each firmware's state machine.

As for WiFi communication, it was achieved to establish a bidirectional communication between Labview and the FPGA. Figure 11 shows values from a logic analyzer from an experiment where a data transfer over WiFi is being performed. In the RX (reception) test, the RN-XV module receives the data over WiFi and these are sent via UART to the FPGA. In the picture, number one indicates the pulses of when that data is read and number two indicates the actual bit being read. For this example the byte to read is AF hexadecimal. On the TX (transmission) test, transmission from the FPGA to the RN-XV module is shown in the following figure, where number one indicates the hexadecimal number 55 serialized. The RN-XV was configured to send data over WiFi each time is has a byte of data on its buffer.

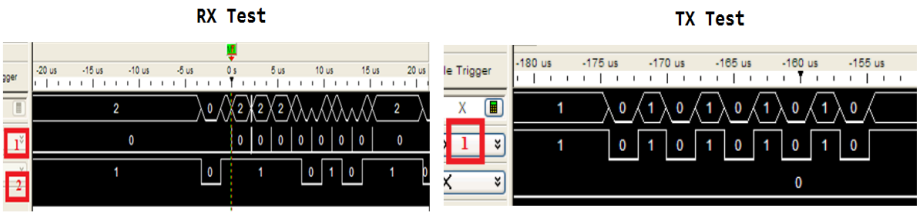

Fig. 11. Send/Receive data test.

6 Conclusions

Given the fact that the Fuzzy Controller has a faster response in comparison to the hyperbolic tangent, it is possible that in the future the same controller block can be used to control three degrees of freedom. The hyperbolic tangent uses floating point operations in which each ones requires an average of 11 clock cycles, and calculating the hyperbolic tangent requires considerable operations. In contrast, due to the simplicity of the Fuzzy controller and replacing floating point operation with bit shifts. Regarding the WiFi communication, sending commands to the FPGA and receiving data has been achieved.

References

1. F. Reyes Cortes, Robótica: Control de Robots Manipuladores, Primera Ed. Alfaomega, México D.F. Págs. 315,319. (2012).
2. I. Grout, Digital Systems Design with FPGAs and CPLDs, First Ed. Newnes, USA, Pág. 28. (2008)
3. V. Limón, Curso Lógica Difusa en la Vida Diaria, Facultad de Ciencias de la Electrónica, Benemérita Universidad Autónoma de Puebla, (2012).
4. J. Casad, Teach Yourself TCP/IP in 24 Hours, Fifth Ed. Sams, Págs. (20120).
5. Chalermek Intanagonwiwat, Ramesh Govindan, Deborah Estrin, John Heidemann, and Fabio Silva. Directed diffusion for wireless sensor networking. IEEE/ACM Trans. Netw., 11(1):2–16, (2003).
6. Distributed Control Diffusion: Towards a Flexible Programming Paradigm for Modular Robots. Ulrik P. Schultz Maersk Institute University of Southern Denmark.
7. National Instruments Labview, available at: http://www.ni.com/labview, [23 Septiembre 2012].
8. D. E. Comer, Internetworking with TCP/IP Vol I: Principles,Protocols and Architecture, Fourth Ed. Prentice Hall, Department of Computer Sciences, Purdue University, West Lafayette. (2000).
9. WiFly Command Reference, Advanced Features & Applications User's Guide. Roving Networks. USA. 2013. www.rovingnetworks.com. [Enero 9 del 2013].
10. R. Reese, Microprocessors from assembly language to C using the PIC18Fxx2, First Ed. Da Vinci Engineering Press, Págs. 259-263. (2005).
11. N. Laddha, A. Thakare, Implementation of serial communication using UART with configurable baud rate. International Journal on Recent and Innovation Trends in Computing and Communication. Volume: 1. Issue: 4. Pags. 263-268. (2013).

Simulation & Modeling

Modelado y Simulación Dinámica de los Efectos de los Tiempos de Demora en una Línea de Estampado Utilizando MATLAB

Lisaura Walkiria Rodríguez Alvarado, Eduardo Oliva López

Instituto Politécnico Nacional, Esime Zacatenco, Doctorado en ciencias de Ingeniería Mecánica, Distrito Federal, México
lrodrigueza1010@alumno.ipn.mx, eoliva@ipn.mx

Resumen. En esta publicación se presenta el desarrollo de un modelo computarizado de Dinámica de Sistemas (DS) y su aplicación en una empresa metal-mecánica. El modelo desarrollado se ha aplicado hasta ahora a una sección crítica de la planta de fabricación (línea de estampado) del ramo automotriz. Los resultados obtenidos muestran que: los tiempos de paros no programados (sin registro) ocasionan retrasos significativos en el flujo de producción, generando el incumplimiento de las órdenes de producción y de los tiempos de entrega. Ante el inconveniente de adquirir un software especializado para este tipo de simulación, se está desarrollando una nueva versión basada en MATLAB que se encuentra en un 50% de avance.

Palabras claves: Modelo computarizado, simulación, dinámica de sistema, proceso

1 Introducción

Al considerar un sistema de producción como un conjunto de variables interrelacionadas entre sí (información, insumos, costos, gastos, ingresos, tiempos de operación, niveles de inventarios entre otras), es posible analizarlo mediante la metodología de DS. Ya que esta permite el modelado, simulación y control de sistemas dinámicos complejos [1]. La aplicabilidad de la simulación digital en los sistemas de manufactura, ha estado dominada por la producción dinámica [2], la planificación y control de la producción [3], el análisis de capacidad de producción [4],[5]; los requerimientos de materiales [6] y las herramientas de la manufactura esbelta [7]. Es decir, la aplicación de la DS se ha enfocado al análisis de: comportamiento del sistema, análisis de escenarios de producción, evaluación de políticas administrativas y análisis de la capacidad de producción.

En este trabajo se describe un modelo de un sistema de producción enfocado al análisis de los efectos de las demoras o retrasos (delays). Estos efectos son ocasionados por los tiempos de paros no programados (sin registro) en el proceso de estampado de una empresa de autopartes. Para su simulación, se empleó la metodología de la

© E. A. Santos, J. C. Chimal, L. Cabrera, E. Castillo.
Advances in Computer Science and Engineering
Research in Computing Science 67, 2013 pp. 105–115
Paper Recived 09-08-2013 and Acepted 21-10-2013

DS, desarrollando una plataforma en el software MATLAB. La plataforma posee una interfaz gráfica, para lo cual se utilizó la herramienta GUIDE.

Este software fue seleccionado por las ventajas de su capacidad para resolver algoritmos numéricos y por sus herramientas de interfaz gráfica. Estas características responden a los requerimientos de simulación del objeto de estudio, permitiendo diseñar una plataforma de simulación personalizada (no adaptada). Otra de las razones por las cuales se optó por este software en lugar de usar uno de los disponibles comercialmente como Vensim o Powersim, es debido al alto costo de adquisición que representan estos software comerciales. Para indagar más en las diferentes herramientas de simulación especializadas en DS, se recomienda al lector leer el trabajo realizado por Andrade y otros [8].

2 Caso de estudio

El área de interés para este estudio es el área de estampados de una empresa de autopartes, dedicada a la fabricación de componentes automotrices de acero y sus aleaciones. Esta línea permite la continuidad del ciclo productivo generando producto semiterminado y producto final, y es la que presenta mayor oportunidad para mejorar la programación de la producción. La línea de estampados consta de 15 prensas, 8 de ellas trabajan de modo manual y 7 trabajan en forma progresiva, en la cual se fabrican alrededor de 700 números de parte en los procesos de corte, embutido o formado.

3 Problemática

El incumplimiento de las órdenes de producción se encuentra vinculado, además de la capacidad de producción de la línea, al aprovechamiento efectivo del tiempo y el desglose de actividades que debe realizar cada trabajador. En la tabla 1 se presentan las generalidades de la situación actual y los factores de interés que determinan la incidencia de los mismos en el comportamiento del proceso.

Tabla1. Generalidades de la situación actual y factores de interés.

Estándar	Capacidad	Paros	Programa
El estándar actual no corresponde al estándar de trabajo (pz/min) del proceso.	La capacidad de la línea no responde a la necesidad demandada.	Se registran una serie de tiempos de paros no contemplados dentro del proceso.	La secuencia del programa de producción y su planificación no corresponde a la situación actual de la línea.
-Tiempo real del ciclo de producción (pz/min). -Actividades anexas al proceso, no registradas.	-Capacidad necesaria para el cumplimiento del programa.	-Tiempo de montaje y desmontaje -Tiempo de proceso y preparación de la pieza -Factor de nivelación.	-Carga de trabajo. -Disponibilidad de material, herramental y equipo.

Los datos presentados anteriormente (que se derivan de los factores de interés) son los que caracterizan al sistema de producción (como fuente de información) y se generan del análisis de la problemática actual de la línea y determinan su comportamiento dinámico. A partir de esta información se desarrolla el modelo de DS mediante la plataforma desarrollada en el software MATLAB.

La metodología de la DS consta de las siguientes etapas: definición del sistema, conceptualización, formalización y comportamiento y evaluación, [9], [10]. El modelo de simulación diseñado en MATLAB, permitió integrar las bases de datos previamente creadas en Microsoft EXCEL. Para el diseño de la plataforma de simulación se utilizó el método en espiral propuesto por Barry Boehm [11].

4 Diseño del modelo

4.1 Conceptualización de las variables del sistema

Variable de Tipo Demora. Representa el tiempo que transcurre entre una causa y sus efectos, es decir, algunos eventos de los procesos se retrasan en su ocurrencia.

- Retraso en el flujo de producción (*RFp*). Esta variable corresponde al tiempo (minutos) destinado para realizar actividades anexas al proceso, las cuales no se registran actualmente: preparación de la pieza, limpieza por la rebaba generada, tiempo del proceso y acomodo de piezas.
- Ajuste para trabajo en proceso (*ATP*). Representa la demora que corresponde al tiempo (minutos) de los paros programados, como son el montaje, tiempo de limpieza, tiempo personal y desmontaje.

Variables de Tipo Flujo. Este tipo de variable simboliza el cambio de estado de las variables de nivel durante un periodo de tiempo.

- Flujo de entrada (*Fp*). Representa la entrada de datos proveniente de la demanda o pedido solicitado al ciclo de producción, influenciada por el valor de la variable de la primera demora *ATP*. Su ecuación está determinada por una función *Tren de Pulso*, es decir, que cada entrada representa una orden de pedido diferente.

$$Fp=\text{Pulse Train}\,(ATP, Pd, F, Fin) \tag{1}$$

Pd, corresponde a la variable: tiempo de producción en función de la cantidad demandada (uds).**F**, es la frecuencia, representada por la cantidad de carga de trabajo determinada por la producción deseada y su duración (min). **Fin**, Tiempo de culminación. Corresponde al tiempo de finalización de la última carga programada.

- Flujo de salida (*Fpt*). Este flujo de salida representa la salida del flujo productivo una vez que ha sido afectada por la demora *RFp*. La ecuación 2 representa el comportamiento del flujo de salida.

$$Fpt= Smooth (Fp, RFp) \quad (2)$$

Esta ecuación se traduce de la siguiente manera en el software Matlab.

$$Fpt_{t+1}=Fpt_t+(Fpt-Fpt_t)/RFp \quad (3)$$

Variables de Tipo Nivel. Son los recipientes, las variables que acumulan magnitudes con el tiempo. Estas definen la situación en que se encuentra el sistema.

- El nivel principal (*TP*). Representa la diferencia acumulada de los flujos de entrada y salida (*Fp, Fpt*) y corresponde a la variable principal. Este nivel representa la ecuación principal del sistema, ya que es donde se analiza la acumulación de piezas sin producir debido a los efectos de las demoras.

La ecuación 4 describe el comportamiento de la variable de nivel *TP*.

$$TP = INTEG(Fp-Fpt, TPinicial) \quad (4)$$

Donde, la constante *TP inicial* es el valor de la variable *TP* en el instante inicial de la simulación.

- Las variables de nivel *NFp*y *NFpt.* Representan la acumulación, en el tiempo, del comportamiento de los flujos de entrada y salida respectivamente. Las ecuaciones que definen estas variables de nivel son las siguientes, donde los valores *NFp inicial* y *NFpt inicial* son los valores de las variable *NFp* y *NFpt* en el instante inicial de la simulación.

$$NFp = INTEG(Fp,NFpinicial) \quad (5)$$

$$NFpt = INTEG(Fpt,NFptinicial) \quad (6)$$

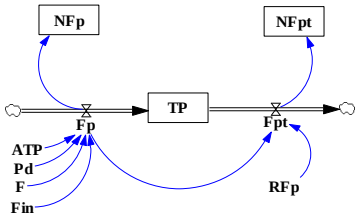

Fig. 1. Modelo dinámica del comportamiento de una prensa.

La interrelación de las variables explicadas anteriormente y el comportamiento dinámico de una prensa se resumen en la Figura 1. La secuencia se repite igual para las 15 prensas que integran el sistema. Se puede observar que la integración de los flujos afectan la variable principal *TP*, y las demoras el comportamiento de los flujos.

4.2 Desarrollo de la plataforma de simulación en el software matlab

Para el desarrollo del programa se recurrió a la herramienta de programación de ambiente gráfico de Matlab (GUI) y su plataforma de programación. El programa está estructurado en dos módulos, los cuales se dirigen desde la pantalla principal. A continuación se explica a detalle el desarrollo e integración de los módulos.

Módulo 1: Programa de Producción. Este módulo brinda un escenario real a ser evaluado mediante la programación de la producción. En la Figura 2, se muestra la pantalla principal que representa la interfaz entre el operador y el software creado, seguido del detalle de los elementos que integran dicha pantalla. Posteriormente se presenta el diagrama de flujo (ver Figura 3.) que integra la secuencia de programación realizada para obtener los resultados buscados. Cada etapa del diagrama está referenciada con cada uno de los elementos que se muestran en la pantalla principal de la interfaz, declaración de variables y origen de los datos de alimentación.

Fig. 2. Módulo 1: Programación de la Producción.

1. Información adicional. Registra el número de parte, la carga y la cantidad a producir. Es enviada a un archivo de Excel para procesar los demás datos.
2. Disponibilidad de prensas. Muestra la lista de prensas disponibles para procesar la pieza programada.
3. Requerimientos. Muestra los requerimientos necesarios para producción: herramental, tipo de herramental y estándar de producción y hora de inicio.
4. Paros programados. Estos corresponden a: preparación de la herramienta, desmontaje, complementos. La pausa para la comida, se calcula automáticamente.
5. Indicadores e información del proceso. El programa realiza el cálculo de indicadores, información adicional como paros no registrados. El programa realiza el cálculo de indicadores, información adicional como paros no registrados en el proceso, tiempo de producción, tiempo del proceso, paros no programados, hora de finalización y finalmente los indicadores de desempeño.
6. Registro de bases de datos. Esta etapa corresponde al envío de la información generada en el programa a una base de datos en Excel.

7. Gráficas. Consulta de cronograma, indicadores por prensa y total línea, paros registrados.

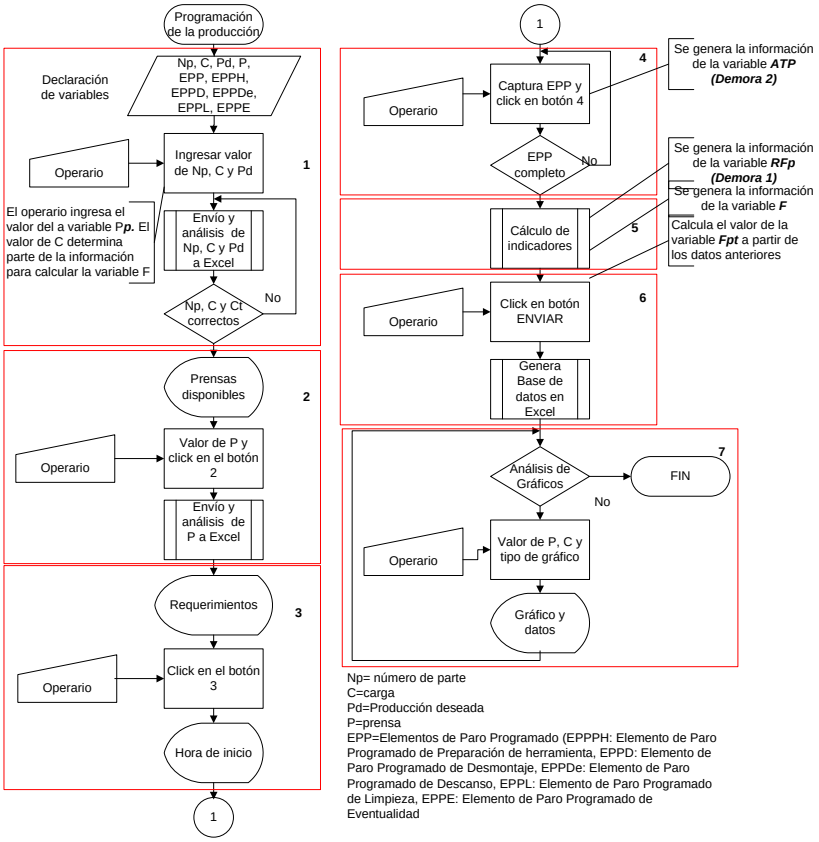

Fig. 3. Diagrama de flujo de la secuencia de programación del módulo 1.

Módulo 2: Simulación. El módulo 2 representa la plataforma de simulación, en el cual el usuario interactúa con los datos registrados en el módulo 1. En la Figura 4, se muestra la pantalla principal del programa y en la Figura 5 se muestra el diagrama de flujo de la secuencia de programación.

Tabla2. Elementos que integran la pantalla de interfaz

No.	Elemento	Descripción
1	Análisis del comportamiento de las demoras	El usuario puede interactuar con esta gráfica para realizar el análisis de la demora en el proceso de producción ocasionada por los diferentes tiempos de paros.
2	Análisis del comportamiento de los niveles	El usuario puede interactuar con el análisis de los niveles generados por los flujos de entrada y salida del proceso. De igual manera realizar el análisis de la cantidad de piezas que no se producen por los efectos de la demora.

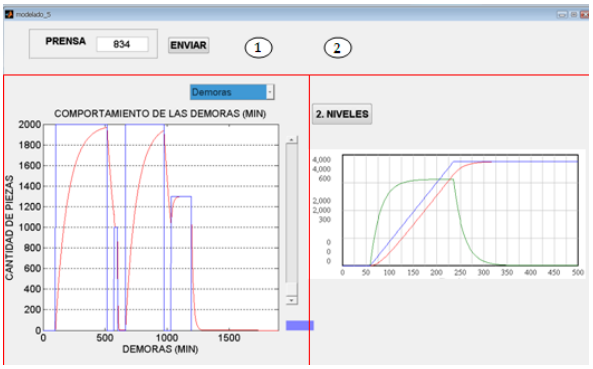

Fig. 4. Módulo 2: Simulación.

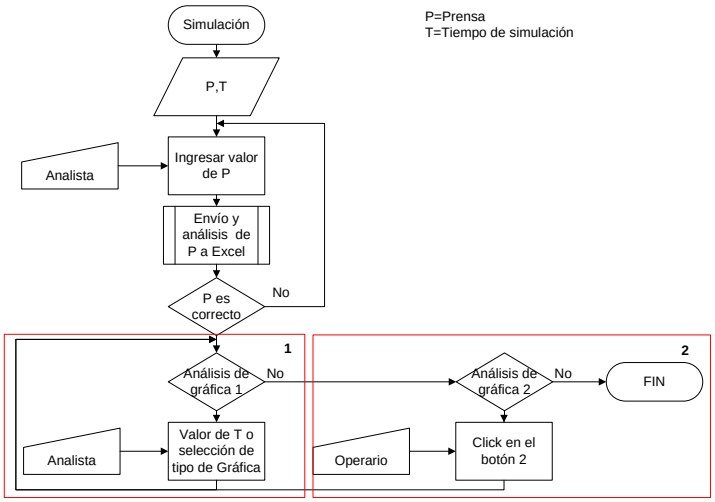

Fig. 5. Diagrama de flujo de la secuencia de programación del Módulo 2.

5 Simulación y evaluación

Los resultados de las *corridas* de simulación fueron validados contra datos reales de la producción en la línea de estampado, y también contra los resultados obtenidos con un demo del software especializado en DS, VENSIM, con el objetivo de verificar la validez de las ecuaciones y la veracidad de los resultados obtenidos. Se realizaron diferentes escenarios de simulación, con un universo amplio de situaciones posibles, con el proceso en operación de la línea de estampado. Se ilustra el caso más representativo. Para tal efecto se seleccionó el comportamiento de programación de la prensa

834 (prensa de 120 toneladas con procesamiento de piezas en forma automática y semiautomática).

Table3. Programación de la prensa 834

No. de Parte	Cantidad (uds/pza)	Tiempo de producción (min)	Paros programados (min)	Paros no programados (min)
Np	*Pd*	*C,F*	*RFp*	*ATP*
1ES9949 2p	2000	417	100	99
CM-3909 1P	1000	30	55	4
CM-3911 2P	2000	313	63	90
1ES1638 1P	1300	163	55	16

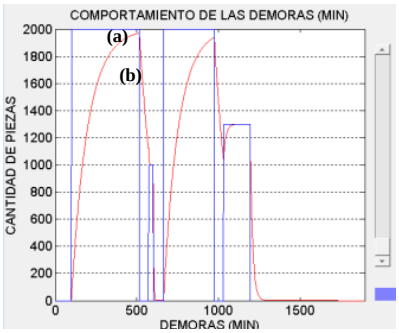

Fig. 6. Comportamiento de los flujos de entrada (a) y salida del sistema (b).

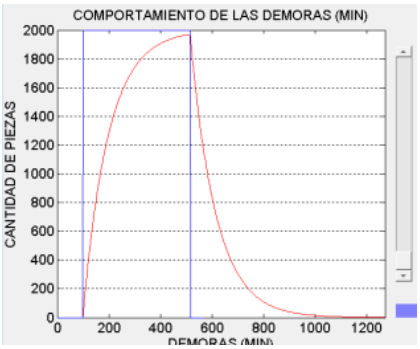

Fig. 7. Comportamiento del flujo de entrada y salida de la carga 1 de la prensa 834.

En la Figura 6, se puede ver la diferencia de flujos de entrada y salida. Se puede observar que en la demora ocasionada en la carga de trabajo 1, retrasa el flujo de producción de la siguiente carga, es decir, genera un incumplimiento en esa orden de producción. De acuerdo al comportamiento teórico, la programación realizada de la prensa 834 debería concluir en el minuto 1200 (20 horas después de iniciado el proceso). Sin embargo, las demoras ocasionan un retraso que extiende la producción hasta el minuto 1300, es decir casi dos horas de retraso. En la Figura 7, se observa el com-

portamiento de las demoras en el flujo de salida y entrada para la carga 1. En este caso, el ciclo debió concluirse en el minuto 500, sin embargo debido a las demoras, el proceso de producción de la pieza se extiende hasta el minuto 1100 aproximadamente.

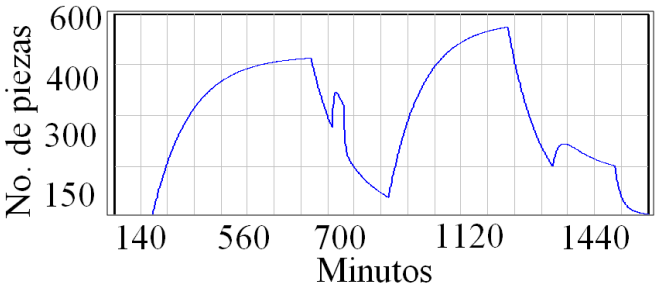

Fig. 8. Comportamiento de la variable de nivel TP.

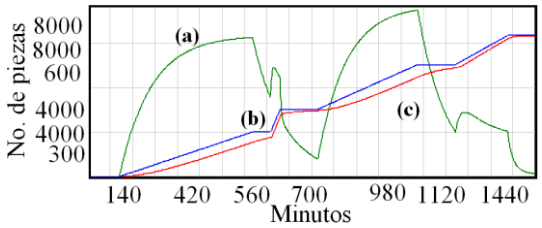

Fig. 9. Comportamiento de las variables de nivel (TP (a), NFp (b), NFpt (c)) en el tiempo.

La Figura 8, muestra el resultado de la simulación, que permite analizar la cantidad de piezas que se han dejado de hacer a consecuencia de las demoras registradas. Para la carga 1: 453 piezas, Carga 2: 400 piezas, Carga 3: 590 piezas y, finalmente, para la Carga 4: 170 piezas; aproximadamente. En la Figura 9, se observa el desfase en el tiempo de la variable *NFpt* con relación a la variable *NFp* en el tiempo, esto se debe a la influencia de los valores de las demoras explicadas anteriormente. La variable de nivel *TP*, representa la cantidad de piezas acumuladas retrasadas, es decir la diferencia entre la cantidad de las piezas teóricas a producir y las que realmente se producen. Esta diferencia de producción es el resultado de la producción con demoras.

6 Conclusiones

Los resultados obtenidos de las corridas de simulación del funcionamiento de la prensa 834, muestran que el modelo desarrollado representa satisfactoriamente la operación real de la prensa y también proporciona resultados muy aproximados a su funcionamiento actual. También se observa que el comportamiento de las demoras tiene gran incidencia en el comportamiento del proceso de producción de la línea de estampados. Se determinó que los tiempos de paros no registrados son la principal fuente de origen de las demoras del proceso que, al no ser considerados en programación normal, ocasionan que se retrase el flujo de materiales. El principal efecto de éste

se refleja en la cantidad de piezas que son dejadas de producir en el periodo. De igual manera las gráficas de Niveles presentadas en la Figura 9 permiten hacer un análisis más crítico de la situación, puesto que se visualizan las diferencias entre los flujos de producción real y la programada.

Este análisis fue realizado mediante un modelo computarizado desarrollado en el software Matlab, aplicando la metodología de DS. El diseño y construcción del modelo en este tipo de software presenta ventajas con relación a los softwares comerciales existentes, ya que se diseñó de acuerdo a las necesidades y requerimientos de la situación, es decir se creó un programa personalizado. La imposibilidad financiera de adquirir la licencia de los softwares especializados fue un obstáculo práctico. La integración de la metodología de la DS y el desarrollo de su modelo en Matlab, evidencian la efectividad de este modelo para el análisis del comportamiento dinámico de sistemas productivos. Actualmente se está desarrollando un modelo completo que incluye otras variables de interés, como análisis de las incidencias de las demoras en tiempos de entrega y retrasos en el flujo de comportamiento de materia prima, con un enfoque de rentabilidad sobre la inversión. Esto permitirá analizar la situación de la línea de producción para la toma de decisiones a nivel estratégico.

Referencias

1. Meyers, R. A.: Encyclopedia of Complexity and Systems Science.New York: Springerscience+Bussinesmedia, (2009).
2. Wiendahl, H.-P., & Breithaupt, J.-W.: Modelling and controlling the dynamics of production systems. Production Planning & Control: The Management of Operations , 389-401, (1999).
3. Georgiadis, P., & Michaloudis, C.: Real-time production planning and control system for job-shop manufacturing: A system dynamics analysis. European Journal of Operational Research. Volume 216, Issue 1, , 94-104, (2012).
4. Ruiz, U. R., Muñoz, M. A., Framian, J. M., Moreu, P., Leon, J. M., & Duran, M.: Modeling and Simulation of a Manufacturing Line in an Automotive Components Plant. 20 th International Conference of the System Dynamics Society, Palermo, Italy, (2002).
5. Towill, D.: Dynamic analysis of an inventory and order based production control system. International Journal of Production Research , 671-687, (1982).
6. Morecroft, J.: A SYSTEMS PERSPECTIVE ON MATERIAL REQUIREMENTS PLANNING. Decision Sciences. Volumen 14. Issue 1. , 1-18, (1983).
7. Deif, A.: Computer Simulation to Manage Lean Manufacturing Systems. 2nd International Conference on Computer Engineering and Technology. Vol 6 , 677-681, (2010).
8. Andrade Soza, H. H., Lince Mercado, E. d., Hernández Cuadrado, A. E., & Monsalve Quintero, A. J.: Evolución: Herramienta Software para Modelado y Simulación con Dinámica de Sistemas. Revista de Dinámica de Sistemas. Vol 4, (2010).
9. Martin, J.: Theory and Practical Exercises of System Dynamics.Barcelona: J.M. García, (2006).
10. Forrester, J. W.: Industrial Dynamics. New York: MIT Press and Wiley, (1961).
11. Boehm, B.W., C. Abts, A.W. Brown, S. Chulani, B.K.Clark, E. Horowitz, R. Madachy, D. Reifer, B. Steece.: Software Cost Estimation with COCOMO II, Prentice-Hall, Englewood Cliffs Boehm, Barry W., TRW Defense Systems Group (1988), A Spiral Model of Software Development and Enhancement, (2000).

Surfaces of the Reconstruction Error of Gaussian Fields with Non-stationary Regions

Daniel Rodríguez-Saldaña[1], Vladimir Kazakov[1], Luis Alejandro Iturri-Hinojosa[2]

[1]Department of Telecommunications, SEPI - ESIME - Zacatenco, Instituto Politécnico Nacio-nal, Mexico City, Mexico
[2]Department of Communications, ESIME – Zacatenco, Instituto Politécnico Nacional, Mexico City, Mexico
{dannyrsan, vkaz41}@hotmail.com, alejandroiturri@yahoo.com.mx

Abstract. This paper considers the reconstruction error of Gaussian fields, when a non-stationary region is present. The non-stationary character is only given for spatial data but not for spatio-temporal ones. The reconstruction method is specified on the basis of the conditional mean rule when the quantity of samples is restricted. The method estimates the surface of the optimal reconstruction error functions in the whole space domain of fields. The ability of the method is demonstrated with a simple statistical description of fields on stationary or non-stationary regions. The Gaussian fields are mainly described by a spatial covariance function to describe the nature of Gaussian Markov fields.

Keywords: Gaussian markov fields, mean square reconstruction error surfaces, stationary and non-stationary fields.

1 Introduction

The description of the Sampling-Reconstruction Procedure (SRP) of random fields has been discussed in many publications [1-7]. It is noticed in the majority of the works [1-4] that the probability density function (pdf) of fields is not mentioned. Therefore, this situation is the source of many complexities and imprecision in many papers devoted to SRP of fields.

The problem of the estimation of the error reconstruction in the SRP of random fields has practically not been solved in two-dimensions yet. One can appreciate that the reconstruction error function has been determined in [3, 4] only for a one-dimensional case, hence the reconstruction error of random processes is defined instead of the reconstruction error of random fields; and only some bounds for the reconstruction error has been evaluated in [5, 6].

In the present paper, a generalization of the conditional mean rule [8] is proposed for the statistical description of SRP of Gaussian random fields. With this rule the estimation of an unknown random variable is specified by the conditional mathematical expectation. This method provides the minimum of the mean square reconstruc-

© E. A. Santos, J. C. Chimal, L. Cabrera, E. Castillo.
Advances in Computer Science and Engineering
Research in Computing Science 67, 2013 pp. 115–122
Paper Recived 16-08-2013 and Acepted 21-10-2013

tion error. The description of various kinds of random processes and some Gaussian fields has been determined by this rule in [9-11].

The reconstruction problem of continuous random fields is described, in this work, only in the non-stationary space, that is, when they do not depend on time. In order to describe the Gaussian fields completely we use the usual statistical characteristics – the spatial covariance function and the mathematical expectation. In this work, the Gaussian random fields are specifically defined by the non-stationary spatial exponential covariance function. Non-stationary random fields are required in modelling image with complex patterns, in geophysical and environmental applications. For these purposes is common to describe spatial data with non-stationary covariance structure.

There has been little progress in the problem of non-stationary fields. Some works have been focused to transform non-stationary fields into stationary ones [12, 13].

The central differences between our methodology and that presented by the previous literature are the following: a) the conditional mean rule is applied to describe the reconstruction procedure of random fields; b) the optimal SRP algorithms are analyzed with an arbitrary and limited number of samples; c) the nature of the multidimensional pdf of fields is determined by the Gaussian distribution; d) the stationary or non-stationary character of Gaussian fields is described in any spatial region with these properties; e) the minimum reconstruction error surfaces are evaluated on the whole space domain.

2 Description of method

Generally, random fields $F(x,y,t)$ are considered as a continuous three-dimensional stochastic process with space variables (x,y) and the time variable t. This field can be completely described by knowledge of its joint pdf

$$p(F_1, F_2, \ldots, F_N; x_1, y_1, t_1, x_2, y_2, t_2, \ldots, x_N, y_N, t_N), \tag{1}$$

for all sample points N, where (x_i,y_i,t_i) indicate space and time samples of random fields.

The field is represented by infinity of surfaces as separate realizations. Generally, it is difficult to know the high-order joint probability densities of the fields. But, in the Gaussian case they can be completely determined by its mathematical expectation $\langle F(x,y,t)\rangle = m(x,y,t)$ and its covariance function $K(x_2-x_1,\ y_2-y_1,\ t_2-t_1)$, where $\langle\cdot\rangle$ is the expectation operator.

When we fix an arbitrary set of N samples of the field $S=\{F(x_1,y_1,t_1),\ F(x_2,y_2,t_2), \ldots, F(x_N,y_N,t_N)\}$, the random field is considered as a conditional field where all its realizations pass through all fixed points of the set S. The general expressions for the conditional mean matrix and the conditional covariance matrix of Gaussian multidimensional random variable are known [8].

In a variety of systems, the spatial and time domains of the fields are separable so that the covariance function may be written as

$$K(x_2-x_1,\ y_2-y_1,\ t_2-t_1) = K_{xy}(x_2-x_1,\ y_2-y_1)\, K_t(t_2-t_1). \tag{2}$$

The non-stationary spatial covariance function is determined as a function of the fo-llowing parameters: the difference in each spatial coordinates, x_2-x_1 and y_2-y_1; and the variation of the inverse of covariance radius both on x-axis and y-axis, which are represented by ξ_x or ξ_y, correspondingly. Moreover, it is possible to define the beginning of the non–stationary region of the field on x-axis and y-axis by L_x and L_y.

With the above-mentioned information the non-stationary covariance function has the following representation:

$$K_{xy}(x_2-x_1,\ y_2-y_1,\ \xi_x,\ \xi_y)=K_{nstat}(x,\ y). \tag{3}$$

Hence, when we apply the conditional mean rule to two-dimensional Gaussian fields, we have the following expressions:

$$\begin{aligned}\tilde{m}(x,y) = m(x,y) + \sum_{i=1}^{N}\sum_{j=1}^{N} K_{xy}(x-x_i, y-y_i, \xi_x, \xi_y)\times \\ \times a_{ij}\left[F(x_j,y_j) - m(x_j,y_j)\right],\end{aligned} \tag{4}$$

$$\begin{aligned}\tilde{\sigma}^2(x,y) = \sigma^2(x,y) - \sum_{i=1}^{N}\sum_{j=1}^{N} K_{xy}(x-x_i, y-y_i, \xi_x, \xi_y)\times \\ \times a_{ij} K_{xy}(x_j-x, y_j-y, \xi_x, \xi_y),\end{aligned} \tag{5}$$

where $\sigma^2(x,y)$ is the unconditional variance of the initial field and a_{ij} represents to each element of the inverse non-stationary covariance matrix:

$$\mathbf{A} = \mathbf{K}_{xy}^{-1}(x_i - x_j, y_i - y_j, \xi_x, \xi_y). \tag{6}$$

With (4) and (5), we can characterize the surfaces of the optimal reconstruction function and the minimum reconstruction error function of the fields.

Equations (4) and (5) may be useful to analyse stationary and non-stationary random fields if the covariance function is characterized with these properties.

3 Results

Now we employ the expressions (4) and (5) for some examples, where the quantity of samples is sixteen and their Cartesian coordinates are fixed as follows: $x_1=y_1=-1.5$; $x_2=-1.5$, $y_2=-0.5$; $x_3=-1.5$, $y_3=0.5$; $x_4=-1.5$, $y_4=1.5$; $x_5=-0.5$, $y_5=-1.5$; $x_6=y_6=-0.5$; $x_7=-0.5$, $y_7=0.5$; $x_8=-0.5$, $y_8=1.5$; $x_9=0.5$, $y_9=-1.5$; $x_{10}=0.5$, $y_{10}=-0.5$; $x_{11}=0.5$, $y_{11}=0.5$; $x_{12}=0.5$, $y_{12}=1.5$; $x_{13}=1.5$, $y_{13}=-1.5$; $x_{14}=1.5$, $y_{14}=-0.5$; $x_{15}=1.5$, $y_{15}=0.5$; $x_{16}=1.5$ and $y_{16}=1.5$. These samples are arranged in a four by four grid.

In this case, the field is modelled by the exponential covariance function which describes the Markov Gaussian field. Its mathematical expression is:

$$K_{nstat}(x,y) = \sigma^2 \exp\left[-\xi_x \mid x_2 - x_1 \mid -\xi_y \mid y_2 - y_1 \mid\right], \tag{7}$$

In this paper, we consider that the exponential covariance function has the trend type of non-stationarity. Hence, the inverse of covariance radii is given by the following expressions:

$$\xi_x = \alpha_x + \gamma_x |x - L_x|, \text{ when } x \geq L_x, \tag{8}$$

$$\xi_y = \alpha_y + \gamma_y |y - L_y|, \text{ when } y \geq L_y, \tag{9}$$

where α_x and α_y are the initial values of the inverse of the covariance radius on *x*-axis and *y*-axis, respectively. In all examples we consider $\alpha_x = \alpha_y = 1$.

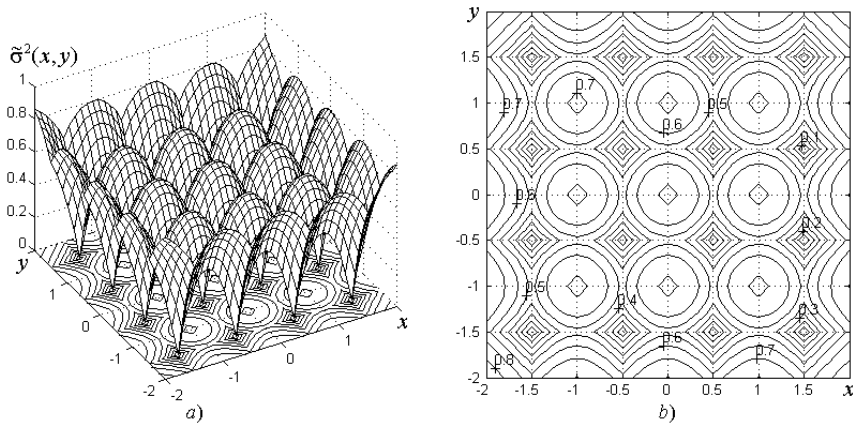

Fig. 1. Estimation of the reconstruction error of the stationary random field: *a*) the error reconstruction surface and *b*) its contour lines. Sixteen samples are spaced apart to an unitary distance.

The non-stationary character of the fields is limited by: $x \geq L_x$ and $y \geq L_y$. γ_x and γ_y are the variation factors of ξ_x and ξ_y on *x*-axis and *y*-axis. Therefore, the modified exponential covariance function is given by

$$K_{nstat}(x,y) = \sigma^2 \exp\Big[-\big(\alpha_x + \gamma_x |x - L_x|\big)|x_2 - x_1| - \big(\alpha_y + \gamma_y |y - L_y|\big)|y_2 - y_1|\Big]. \tag{10}$$

In the first example, the field is considered with a stationary character. For this case, the parameters γ_x and γ_y have the zero value in (9), and $m(x,y) = \langle F(x,y) \rangle = 0$ and the variance $\sigma^2(x,y) = \sigma^2 = 1$ in (4) and (5). The surface of the reconstruction error function $\tilde{\sigma}^2(x,y)$ of the field is shown in Fig. 1. In Fig. 1, we can observe that the reconstruction error function is zero at the location of spatial samples points (x_i, y_i), because in these locations we know the exact value of the field realization.

However, the reconstruction error function has maximum errors at the centre of the interval, that is, among neighbouring samples. These maxima raise if the coordinates of the current samples are locate at a bigger distance. Due to the field realization pre-

sents uniform sampling and has a Markovian property and a stationary character, all maximum errors are exactly the same.

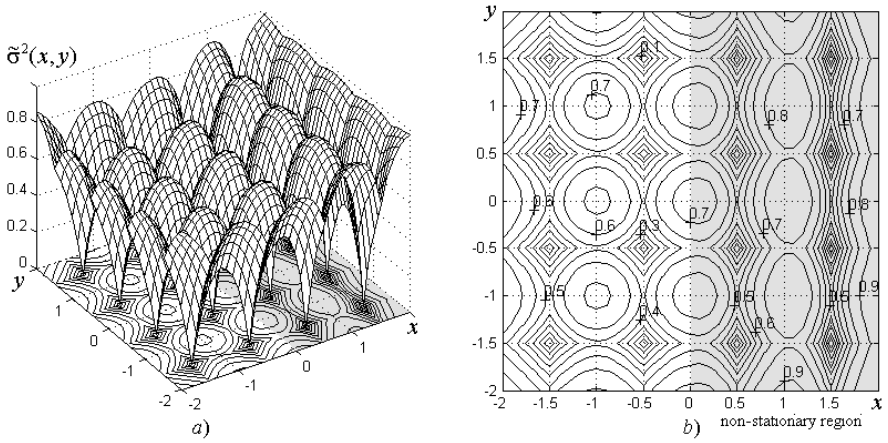

Fig. 2. Estimation of the reconstruction error of the random field when a non-stationary region is limited by the bound $x \geq L_x = 0$: *a*) the error reconstruction surface and *b*) its contour lines.

In the next instance, the field is considered as non-stationary on the *x*–axis and stationary on the *y*-axis. The variation factor γ_y defined here is zero, so the exponential covariance function depicted by (10) is reduced as follow

$$K_{nstat}(x,y) = \sigma^2 \exp\left[-\left(\alpha_x + \gamma_x \mid x - L_x \mid\right) \mid x_2 - x_1 \mid - \alpha_y \mid y_2 - y_1 \mid\right]. \tag{11}$$

The surface of the reconstruction error function $\tilde{\sigma}^2(x,y)$ of the field characterized by (11) is shown in Fig. 2. In this case, the field presents a non-stationary region in $x \geq L_x = 0$ and the variation factors are $\gamma_x = 0.25$ and $\gamma_y = 0$. We can notice that the maxima of the reconstruction error function increase when the value of the horizontal coordinate *x* tends to be far away of the limit L_x, due to the non-stationary behaviour of this region. However, if $x \leq L_x = 0$ the field maintains the stationary character.

In the last example, the non-stationary behaviour of the field affects the spatial structure of the field on the *x*-axis.

In Fig. 3 the surface of the reconstruction error function is given when the non-stationary region is contained into $x \geq L_x = -0.5$ and $y \geq L_y = -0.5$ and the variation factors of α_x and α_y have the same value: $\gamma_x = \gamma_y = 0.25$. It is important to notice that the maximum of the reconstruction error is bigger when the spatial coordinates of field are far away from the bounds L_x and L_y.

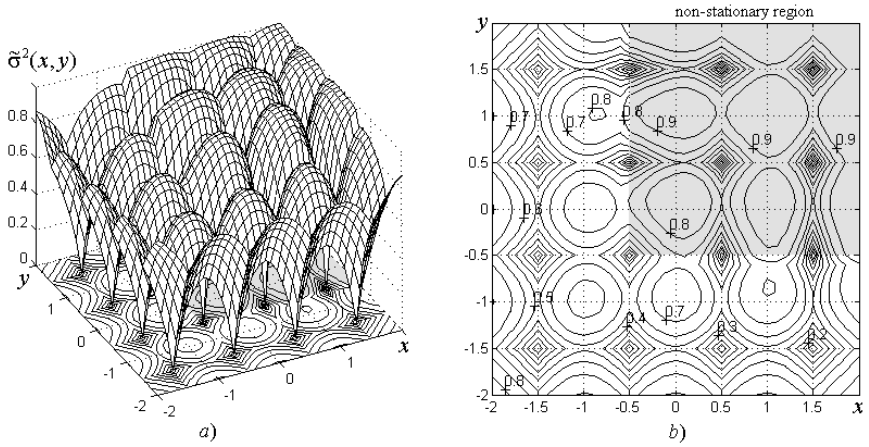

Fig. 3. Estimation of the reconstruction error of the random field when a non-stationary region is limited by $x \geq L_x = -0.5$ and $y \geq L_y = -0.5$: *a*) The error reconstruction surface and *b*) its contour lines.

4 Conclusions

This method provides directly the possibility to describe the stationary and non-stationary character of random fields when they are characterized by its spatial covariance function with stationary and non-stationary properties into any region of the field.

On the basis of this method, it is possible to evaluate the reconstruction error surfaces when the location of samples and the spatial covariance function of non-stationary regions are known.

This method presents some contributions to describe the sampling-reconstruction procedure of stationary or non-stationary random fields such as: images or surfaces with varying covariance structure, and the spatial distribution or concentration of substances in the subsurface. Moreover, it is possible to evaluate the error reconstruction of fields or estimate the number and distance of samples in order to provide the reconstruction of fields with a specific quality.

Acknowledgment

This research has been supported by the Instituto Politécnico Nacional through the project (SIP20131419).

References

1. Pogany, T.: On the sampling theorem for homogeneous random fields. Theor. Probab. and Mathem. Statist. 53, 153–159 (1995).

2. Van der Onderaa, E., Renneboog, J.: Some formulas and applications of nonuniform sampling of bandwidth-limited signals. IEEE Trans. on Instrum. Meas. 37(3), 353–357 (1998).
3. Petersen, D.P., Middleton, D.: Linear interpolation, extrapolation, and prediction of random space-time fields with a limited domain of measurement. IEEE Trans. on Information Theory 11(1), 18–30 (1965).
4. Petersen, D. P., Middleton, D.: Sampling and reconstruction of wave-number-limited function in n-dimensional Euclidean spaces. Inform. Control 5, 279–323 (1962).
5. Zeevi, Y. Y., Shlomot, E.:Nonuniform sampling and antialiasing in image representation. IEEE Trans. Signal Process. 41(3), 1223–1236 (1993).
6. Francos, J. M.: Cramer- Rae bound on the estimation accuracy of complex-valued homogeneus Gaussian random fields. IEEE Trans. Signal Process. 50(3), 710–724 (2002).
7. Klesov, O. I.: The restoration of a Gaussian random field with finite spectrum by readings on a lattice. Kibernetika 4, 41–46 (1985).
8. Pfeiffer, P. E.: Probability for Applications, Springer Verlag (1990).
9. Kazakov V., Belyaev, M.: Sampling reconstruction procedure for non-stationary Gaussian processses based on conditional mean rule. Sampling Theory in Signal and Image Processing. 1(2), 135–153 (2002).
10. Kazakov V., Rodríguez, D.: Sampling-reconstruction procedure of Gaussian processes with jitter characterized by the Beta-distribution. IEEE Trans. on Instrum. and Measur. 56(5), 1814–1824 (2007).
11. Kazakov V., Afrikanov, S.: Sampling-reconstruction procedure of Gaussian fields. Computación y Sistemas 9(3), 227–242 (2006).
12. Ramamurthy, K. N., Thiagarajan, J. J., Spanias, A.: Fast image registration with non-stationary Gauss-Markov random field templates. In: 6th IEEE International Conference on Image Processing, pp. 185–188 (2009).
13. Anoop, K. P., Rajgopal, K.: A non-stationary time-series modeling approach for CT image reconstruction from truncated data. In: TENCON 2009 - IEEE Region 10 Conference, pp. 1–6 (2009).

Feature Extraction with Discrete Wavelet Transform and Mel Frequency Filters for Spoken Digit Recognition

Andrés Fleiz, Mauricio Martínez

Universidad la Salle, 06140 México City, México
{andresfleiz, mauricio.martinez}@lasallistas.org.mx

Abstract. In this paper we propose a new method for analysis of speech signals based on the discrete wavelet transform and a mel frequency filter bank, in order to extract representative features of a speech signal as one of the most important steps in a speech recognition system. The major issues concerning the design of the proposed system are selecting the optimal wavelets and decomposition level. A comparison of the proposed approach and classic methods as Mel Frequency Cepstral Coefficients (MFCC) and novel proposals that use wavelets shows that our system competes in term of recognition rate.

Keywords: Automatic speech recognition, feature extraction, wavelet transform, speech parameterization, discrete wavelet transform, mel frequency cepstral coefficients, pre-processing, classification.

1 Introduction

The feature extraction process consists in the transformation of a voice signal into a parameter representation. Probably one of the most important representations is the spectral envelop [1] achieved through analysis methods as Mel Frequency Cepstral Coefficients (MFCC) [2]. Ideally, the analysis method should preserve all the meaningful perceptual information in order to identify the phonetic differences; it also should be insensitive to irrelevant variations. Therefore, the meaningful information is given by three variables: amplitude, frequency and time.

Conventional techniques as MFCC make use of time-frequency analysis with fixed window size i.e. uniform resolution that decrease the performance of recognition systems due to unacceptable resolution in time or frequency depending the size of the window. A possible solution is finding an optimal resolution for time and frequency through a multiresolution technique for the analysis, such as wavelet transform.

In the existing work we can find multiple ways of using wavelet for speech recognition tasks, in [3] the speech signal is decomposed into various frequency channels, based on the time-frequency multiresolution property of wavelet transform; in [4] new methods for feature extraction based on wavelet decomposition and reduced order linear predictive coding are proposed for speech recognition; in [5] a sub-band feature extraction technique based on a wavelet transform is proposed for phoneme recognition; in [6] the speech signal is preprocessed by a wavelet transform

© E. A. Santos, J. C. Chimal, L. Cabrera, E. Castillo.
Advances in Computer Science and Engineering
Research in Computing Science 67, 2013 pp. 123–132
Paper Recived 16-08-2013 and Acepted 21-10-2013

to increase the accuracy of the recognition system; in [7] an hybrid system based in the discrete wavelet transform and linear predictive coding is proposed for recognition of isolated words; in [8] the performance of the discrete Fourier transform is compared against the discrete wavelet transform in the computation of MFCC in the feature extraction process for speaker recognition; in [9] and [13] the author proposes a new feature vector consisting of coefficients obtained by applying the discrete wavelet transform to the mel-scaled log filter bank energies of a speech frame; in [10] the wavelet transform is used as a part of the front-end processor for feature extraction process in phoneme recognition; in [11] a comparative analysis is performed between the traditional MFCC and a wavelet based feature extraction method for speech recognition; in [12] a speech recognition system is proposed using discrete wavelet transform and artificial neural networks for isolated spoken words; in [14] a system consisting of wavelet based features, linear discriminant analysis and principal component analysis is proposed for recognition of spoken digits; in [22] a method to address the issue of noise robustness using wavelet domain in the front end of an automatic speech recognition (ASR) system; in [23] a paradigm which combines the Wavelet Packet Transform with the MFCC for extraction of speech features is prosed. These approaches can be classified in phoneme recognition, word recognition and speaker recognition. After review each proposed method we found that the design of these systems obeys to an empirical process because several factors affect their performance. The main motivation of this work is to study the behavior of wavelets as multiresolution analysis technique inside of novel recognition system that allows us to identify the main factors that define its performance, this, after delimitating the search space to those values and parameters recommended or used in previous published papers. In order to attain an objective comparison between our technique and others previously proposed, we must modify the recognition systems designed by other authors standardizing the classification and pre-processing steps.

Section 2 of this paper presents the conceptual basis of the method followed for the spoken digit recognition system implementation, for instance the discrete wavelet transform and the mel frecuency cepstral coefficient approaches. The section 3 presents the specifications and details of the experimentation step, and also the main results are presented for discussion in the section 4, where a set of conclusions are obtained in favor of the performance achieved by the proposed system.

2 Method

There have been proved several new approaches to solve speech processing tasks, including new research on the combination of MFCC and wavelet transform, [8] showed that for speaker recognition the DWT outperforms the recognition rate achieved compared to DFT. In [6] the wavelet is used to preprocess the signal and extract features that increase the accuracy for recognition of isolated words.

2.1 Discrete wavelet transform

The wavelet transform is a non-parametric type of analysis which allows multiresolution, understood as localization in time and frequency. This kind of techniques has been used successfully for the analysis of aperiodic and non-stationary signals as speech [15].

The wavelet coefficients are obtained by computing the inner product between an input signal and a function of limited time that has an average value of zero and unit norm [16] so that

$$\int_{-\infty}^{+\infty} \psi(t)\mathrm{d}t = 0\,, \tag{1}$$

$$\|\psi(t)\| = 1\,. \tag{2}$$

Wavelet transform then decomposes the input signal into a set of basic functions called wavelets, which are scaled and translated versions of the mother wavelet ψ. Since the signals treated are discrete we used the Discrete Wavelet Transform (DWT).

DWT is a wavelet transform for which the wavelet is discretely sampled and gives us a compact representation of the signal in time and frequency. It can be computed by an efficient algorithm [16]. The DWT of a signal $s[n]$ is calculated as

$$W[j,k] = \sum_{j}\sum_{k} s[k]a^{-j/2}\,\psi(a^{-j}n - k)\,. \tag{3}$$

The DWT can be represented as a filtering process using a low pass filter (scaling) that gives the approximate representation of the signal and a high pass (wavelet) filter that gives the details or high frequency variations. This process is illustrated in the Figure 1.

The filtering process begins when the signal s passes through the first pair of filters producing two coefficients sets: approximation coefficients CA1 and detail coefficients CD1, after the convolution of the filters and a down sampling procedure. The next step or decomposition level splits the CA1 in two other sets CA2 and CD2, this cycle continues until the j-th desired level. We label each wavelet based on the family and decomposition level. We have chosen the wavelet families according to the existing attempts of using the wavelet transform for feature extraction of speech signals [6, 8, 14].

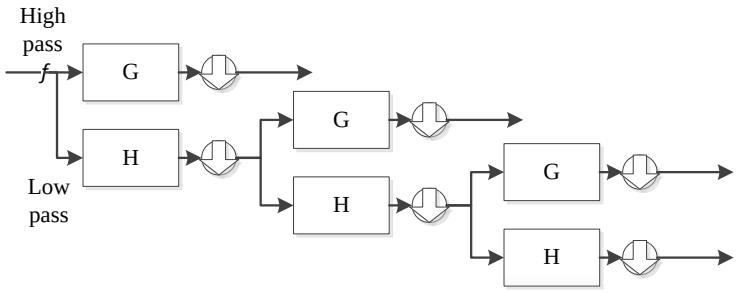

Fig. 1. Filtering representation of a 3 level Discrete Wavelet Transform (DWT) signal decomposition.

The DWT has the main advantage of applying varying widow size, broad for low frequencies and narrow for high frequencies this property allows good resolution in all the frequencies ranges. The coefficients that result of the transformation of the signal are obtained after the concatenation of the last level of the decomposition tree, beginning by the approximation coefficients CAj.

2.2 Mel frequency cepstral coefficients

MFCC's are one of the most popular and studied features used in speech processing applications [17]. MFCC technique obtains the cepstrum of a signal in a set of coefficients that model the human auditory perception through a scale called the mel scale which is linear before 1 kHz and logarithmic above this value. The frequency warping can be implemented through a filter bank of triangular bandpass filters which are centered in the mel scale.

Given the spectrum of a signal

$$S[w] = \sum_{k=0}^{N-1} s[k] e^{\frac{-j2\pi kw}{N}} . \quad (4)$$

The next step is to pass the data of the power spectrum through the mel filter bank, the output is the mel spectrum of the signal. In order to get the cesptrum the logarithmic of the mel spectrum is calculated. The final step involves converting the log mel spectrum back to "time". This could be done by taking the Discrete Cosine Tranform (DCT) of the mel-scaled log spectrum because it is real. The cepstral representation of the signal spectrum provides a good representation of the local spectral properties of the signal in the frame of analysis. This last procedure is represented by

$$c_n = \sum_{k=0}^{M} \log(S_k) \cos\left[\frac{n\left(k-\frac{1}{2}\right)\pi}{M}\right] \quad (5)$$

where $n = 1, 2, \ldots, k$ and S_k is the mel spectrum of the signal under analysis.

2.3 Feature extraction WMFC

In this paper, a multiresolution analysis is performed using the DWT replacing the traditional DFT used to obtain the cepstrum of a speech signal. To obtain a set of features first the signal is broken into 16 ms frames with 50% of overlap, and then is windowed with a hamming window.

$$w[n,\alpha] = (1-\alpha) - \alpha \cdot \cos\left(\frac{2\pi n}{N-1}\right) \tag{6}$$

where $\alpha = 0.46, 0 \leq n \leq N-1$ and N is the length of the window.

$$s_w[n] = s[n]w[n]\,. \tag{7}$$

The DWT of each windowed frame is computed until reach the level of decomposition chosen. The absolute value of the coefficients obtained at j level of decomposition is filtered by a mel scale filter bank and the logarithm of the output of these filters is computed.

$$Z_p = log\left(\sum_{k=0}^{N-1} H_p[k]D_j[k]\right) \tag{8}$$

where H_p is the p^{th} triangular mel filter and $k = 0,1,2,\ldots,N$.

Finally the DCT is applied to decorrelate the log-filter bank energies and a vector of features is obtained.

$$c_t = \sum_{p=1}^{P} Z_p \cdot \cos(\pi t(p-0.5)/P)\,. \tag{9}$$

The block diagram of the analysis system is represented by Figure 2.

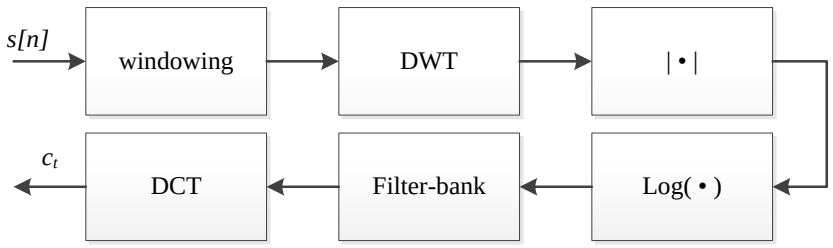

Fig. 2. Block diagram of the proposed analysis system.

3 Experiments and results

3.1 Experimental setup

Our experiments were conducted under ideal conditions, using the TI-46 Speaker Dependent Isolated Word Corpus [21], which consists of ten English digits “zero”

through “nine”, collected from several male and eight female speakers. We selected 360 speech samples from this database; from two male and two female speakers, each one repeating every digit ten times. The sample frequency rate is 11025 kHz, 12-bit PCM and mono channel.

The speech samples are pre-processed to remove the silence using energy threshold criteria, and then the corresponding feature extraction technique is applied. In all the cases the samples are windowed with 16 ms hamming window with 8 ms overlap.

After the preprocessing and windowing the feature vectors are obtained by the corresponding analysis technique. In the DWT case, selection of wavelet families and decomposition level is done accordingly to the conclusions and recommendations stated in [8] (db1, db4, db6, db8 and db10), [6] (db8), [14] (coif5), [18] (sym6)]. In MFCC with DFT and DWT, the number of mel filters in the filter bank is 20 and the number of MFCCs coefficients is 12, both values taken from [19].

The recognition task is achieved with a minimum Euclidian distance criteria based on the computation of the Frobenius norm of the test samples resulting feature vector. In the training phase the mean of 20 feature vectors of random samples is calculated to form the reference patterns for each digit.

The feature extraction techniques used for comparison are: a popular and well proved MFCC method, a new form of improved MFCC (Wavelet MFCC in [6]) and the method proposed in this paper. The comparison is done in term of the percentage accuracy achieved by each method in equal conditions.

In order to evaluate the robustness and performance of the proposed method in noisy environment and the known fact that wavelets performs better than Fourier in recognition tasks with noisy samples, the test patterns were contaminated with additive white Gaussian noise to various signals to noise ratios (SNR).

3.2 Results

To compare performance and robustness of the method here proposed with others (analysis technique in [6] and classic MFCC) experiments are conducted for various wavelets, level decomposition and SNR conditions. Table 1 show the recognition rate at given wavelet and decomposition level with clean speech.

Table 1. Best combination of parameters (wavelet family/order and decomposition level)

Parameter	Wavelet MFCC	WMFC
Wavelet	db1	db10
Decomposition level	4	3
Recognition Rate	83.6%	86.0%

Numerous experiments were conducted in the search of the best combination of wavelet and decomposition level for each of the feature extraction techniques, the result is shown in table 1.

After analyzing the performance of each system in terms of recognition accuracy at a given wavelet and decomposition level, we found that the best recognition rates were obtained with the 2^{nd}, 3^{th} and 4^{rh} level of decomposition with the Daubechies

and Coiflet families, particularly with db1, db10 and coif5. In Figure 3 shows the comparison of the Wavelet MFCC and the WMFC system performance.

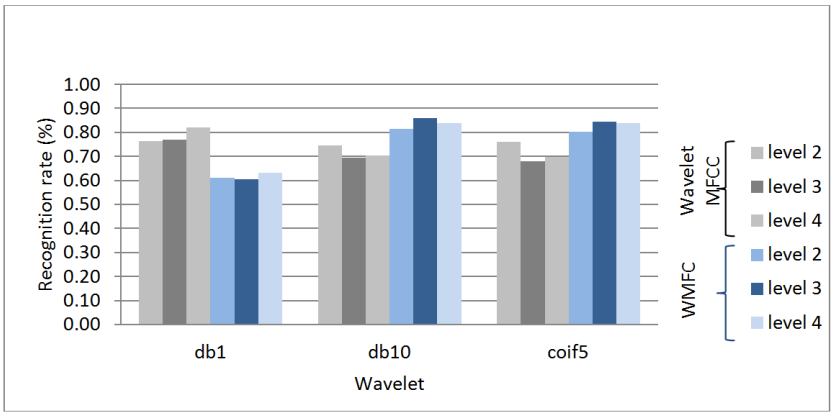

Fig. 3. Recognition rate of Wavelet MFCC system proposed in [6] and WMFC.

The behavior of the proposed system WMFC shows that the recognition accuracy is comparable with the performance of other systems proposed in the bibliography for clean speech.

In order to analyze the robustness of each technique against noisy conditions several experiments were conducted with different signal to noise ratio (SNR). As stated in [6] we found that wavelet techniques have better performance under non ideal conditions, nevertheless techniques that use Fourier as MFCC presented good performance with clean and less contaminated signals.

Table 2. Recognition rate per digit for WMFC in both clean and noisy environment.

Digits	Clean speech	SNR= 20dB	SNR= 10dB	SNR= 0dB
1	62.38	17.00	21.00	09.17
2	86.50	05.63	12.00	09.50
3	92.50	42.38	31.87	09.50
4	80.00	11.13	15.88	06.67
5	88.75	10.38	05.13	09.50
6	92.63	06.63	03.63	16.50
7	87.50	01.63	01.37	13.17
8	88.00	01.62	00.50	16.83
9	89.62	06.13	08.13	08.83
Average	85.32	11.39	11.06	11.07

After comparing Table 2 and Table 3, it is clear that the WMFC performs better with noisy signals in comparison with standard MFCC. Analyzing the recognition rates per digit results in Table 3, which shows an odd behavior as the noise increases, with clean signals having the lower performance for digit “one”, as shown in [20], strangely it improves as the noise increases, while the recognition in all the other digits decay abruptly. This is not the case in WMFC where the recognition rate for all the digits decays as the SNR decreases.

Table 3. Recognition rate per digit for MFCC in both clean and noisy environment.

Digits	Clean speech	SNR= 20dB	SNR= 10dB	SNR= 0dB
1	67.37	13.13	26.75	88.00
2	87.62	05.75	05.00	00.00
3	90.63	00.00	13.00	00.00
4	77.00	00.13	04.50	00.00
5	92.00	02.75	07.62	00.00
6	92.50	20.75	12.50	00.00
7	86.00	00.00	00.25	00.00
8	92.50	05.50	10.25	00.00
9	81.88	09.50	10.88	00.50
Average	85.28	06.39	10.08	09.83

A possible explanation could be that the Euclidian distance in high contaminated environments doesn't perform well for MFCC but still works with WMFC. This result is a clue that allows us to guess that with a more robust and complex classifier such a neural network the WMFC could outperform even more the recognition rate of MFCC.

4 Conclusion

The goal of this work is to develop a feature extraction system for spoken digits by using the multiresolution property of wavelets. The obtained results show that the proposed system WMFC is very competitive with previously published results [6] for different languages, data bases and [8] different tasks. An interesting result is the behavior of a conventional method such MFCC in noisy environments, as it is seen it gives less recognition accuracy as the noise increases, and the worst recognized digit (one) results in the best recognized digit; conversely, WMFC shows better recognition accuracy under noisy environments, and also coherent results.

To achieve a fair comparison of method and systems the conditions and parameters must be standardized, focusing the attention in the analysis method and establishing equal pre-processing and classification techniques. A formal analysis of the implication of using one or another wavelet family or one or another decomposition level is necessary to understand the sensitivity of the method to these factors.

References

1. Rabiner, L.R., Schafer, R.W.: Introduction to Digital Speech Processing. The Essence of Knowledge (2007).
2. Davis, S., Mermelstein, P.: Comparison of parametric representations for monosyllabic word recognition in continuously spoken sentences. In: IEEE Transactions of Acoustics, Speech and Signal Processing 28(4), 357-366 (1980).
3. Trivedi, N., et al.: Speech Recognition by Wavelet Analysis. International Journal of Computer Applications 15(8), 27-32 (2011).
4. Nehe, N. S., Holambe, R. S.: DWT and LPC based feature extraction methods for isolated word recognition. EURASIP Journal on Audio, Speech, and Music Processing, 1-7 (2012).

5. Datta, S., Farooq, O.: Wavelet Based Robust Sub-band Features for Phoneme Recognition. IEE Proceedings: Vision, Image and Signal Processing 151(3), 187–193 (2004).
6. Anusuya, M.A., Katti, S.K.: Comparison of different speech feature extraction techniques with and without wavelet transform to Kannada speech recognition, International Journal of Computer Applications 26(4), 19–23 (2011).
7. Ranjan, S.: A Discrete Wavelet Transform Based Approach to Hindi Speech Recognition. In: International Conference on Signal Acquisition and Processing, ICSAP 2010, pp.345-348 (2010).
8. Turner, C., Joseph, A., Aksu M., Langdon H.: The Wavelet and Fourier Transforms in Feature Extraction for Text-Dependent Filterbank Based Speaker Recognition. Complex Adaptive Systems, vol. 1, 124-129 (2011).
9. Tufekci, Z., Gowdy, J.N.: Feature extraction using discrete wavelet transform for speech recognition. In: Proc. of IEEE Southeast con 2000, pp. 116–123 (2000).
10. Tan, B.T., Fu, M., Spray, A., Dermody, P.: The Use of Wavelet Transforms in Phoneme Recognition. In: ICSLP 1996: Fourth International Conference on Spoken Language Processing, pp. 148–155 (1996).
11. Modic, R., Lindberg, B., Petek, B.: Comparative wavelet and mfcc speech recognition experiments on the slovenian and english speechdat2. In: Proc. Isca-ITRW NOLISP (2003).
12. Sunny, S., Peter, S., Poulose, J.: Discrete Wavelet Transforms and Artificial Neural Networks for Recognition of Isolated Spoken Words. International Journal of Computer Applications 38(9), 9-13 (2012).
13. Tavanaei, A., Manzuri, M.T., Sameti, H.: Mel-scaled discrete wavelet transform and dynamic features for the Persian phoneme recognition. In: Int. Symp. Artificial Intelligence and Signal Processing (AISP), Tehran, pp. 138–140 (2011).
14. Panwar, M., Sharma, R., Khan, I., Farooq, O.: Design of Wavelet Based Features for Recognition of Hindi Digits. In: Intl. Conference on Multimedia, Signal Processing and Communication Technologies (IMPACT 2011), pp. 232–235 (2011).
15. Strang, G., Nguyen, T.: Wavelets and Filter Banks. Wellesley, Cambridge (1996).
16. Mallat, S.: A Wavelet Tour of Signal Processing, 2nd edn. Academic Press, London (1999).
17. Anusuya, M.A., Katti, S.K.: Front end analysis of speech recognition: a review. International Journal of Speech Technology, vol. 14, 99-145 (2010).
18. Sanchez, F.L., et al.: Wavelet-Based Cepstrum Calculation. Journal of Computational and Applied Mathematics 227, 288-293 (2009).
19. Adam, T.B., Salam, M.D.: Spoken English Alphabet Recognition with Mel Frequency Cepstral Coefficients and Back Propagation Neural Networks. International Journal of Computer Applications 42(12), 21-27 (2012).
20. Martinez-Garcia, M.A.: Métodos de Reconocimiento de Palabras Aisladas Usando Segmentación Acústica y Cuantización Vectorial. M.S. Thesis, Faculty of Engineering, National Autonomous University of Mexico (1998).
21. TI 46 Word Speaker-Dependent Isolated Word Corpus, NIST Speech Disc 7-1.1 (1991).
22. Rajeswari, N. P., Sathyanarayana, V.: Robust Speech Recognition Using Wavelet Domain Front End and Hidden Markov Models. Emerging Research in Electronics, Computer Science and Technology, 435 (2014).
23. Srivastava, S., Bhardwaj, S., Bhandari, A., Gupta, K., Bahl, H., & Gupta, J. R. P.: Wavelet Packet Based Mel Frequency Cepstral Features for Text Independent Speaker Identification. In Intelligent Informatics, 237-247 (2013).

Modeling Chemical Reactions and Heat and Mass Transport in a Hydrating Cement Particle Using Comsol Multiphysics 3.5a

Emilio Hernández–Bautista, Sadoth Sandoval–Torres, Prisciliano Felipe de Jesús Cano–Barrita.
Instituto Politécnico Nacional, CIIDIR Oaxaca
Hornos No. 1003, Col. Noche Buena, Santa Cruz Xoxocotlan, Oaxaca, México
Bautistahe@gmail.com

Abstract. A model based on the continuum mechanics theory was developed to describe the hydration reactions occurring in a cement particle surrounded by water. The heat and mass transfer in the particle was described by a diffusion–based mechanism. To solve the model, we considered the chemical reaction stoichiometry, which was then written using a chemical reaction engineering approach. The hydration reactions of C_3S and C_3A are exothermic, therefore they significantly contribute to the amount of energy in the domain. The equation system was solved by coupling the Reaction Engineering Lab Module to Comsol Multiphysics 3.5a. The results correctly describe the products formation and reactants consumption, simulating the formation of a shell around the unreacted cement particle, as well as the temperature evolution in the material. Also the model is capable of simulating the temperature increase in the whole system caused by the exothermic reactions.

Keywords. PID control, Fuzzy control, 2DOF PID control

1 Introduction

The process of curing concrete is meant to provide a high relative humidity and a suitable temperature in order to promote the cement hydration reactions. Steam curing at atmospheric pressure is routinely used in precast concrete plants, because it accelerates the cement hydration compared to curing at ambient temperature.

The concrete curing process has a significant influence in the properties of hardened concrete [1]. Adequate curing increases its durability, water–tightness, volume stability, mechanical strength, abrasion, and freezing and thawing resistance. However, during the steam curing process undesirable effects also occur during the hydration of cement. These are mainly moisture and temperature gradients that may cause micro-cracking, reducing the durability of the concrete elements.

The development of mathematical models of heat and mass transport during cement hydration is an essential tool for the study, design and optimization of new equipment, improving energy efficiency in transformation processes and reducing concrete deterioration by making it more impervious to aggressive agents.

For instance, various models have been developed to study the hydration of cement at a microscopic scale, such as the models developed by Bentz [2] and Van Breugel [3]. These models are capable of simulating the hydration of Portland cement

© E. A. Santos, J. C. Chimal, L. Cabrera, E. Castillo.
Advances in Computer Science and Engineering
Research in Computing Science 67, 2013 pp. 133–145
Paper Recived 16-08-2013 and Acepted 21-10-2013

particles. Other models incorporating heat and mass transport have been developed by [4] and [5].

The aim of this work is to develop a mathematical model that describes the transport mechanisms of moisture, heat transport and chemical reaction during curing of concrete with water vapor at atmospheric pressure. The focus of the model is a continuous type model to explain the transport phenomena occurring in the material thickness. The prediction of those variables will help us understand various phenomena occurring during hydration at the particle level, and then transferred to the material level. Moreover, the model proposed in this work will help understand the phenomena involving the differences in temperature and humidity profiles in concrete and propose steam curing procedures that minimize temperature and humidity gradients to prevent micro-cracking.

The first part of this paper presents the chemical engineering reaction for the hydration of cement without any spatial variation, the second part describes how the reactions are coupled to a 2-D model, showing its geometry, mass and energy balances, the constitutive equations, initial and boundary conditions, and the solution implementation by finite element in Comsol Multiphysics. The third part presents the simulation results for the species' concentration, the heat generated by hydration reactions and temperature evolution.

2 Development of the mechanistic model

The continuous medium is a physical description of the matter in which the domain can be described by a set of differential equations. The scale of the material can be represented from a set of molecules to volume scale of meters depending on the desired precision. Since the material is never continuous, the continuous medium approach is always an approximation to the actual phenomena.

A continuous type model is composed of a geometry, general balance equations of mass, energy or momentum, equations of state, boundary conditions and initial conditions of the system, and a set of assumptions that are necessary for the model development [6].

2.1 Chemical reaction engineering

The unreacted-core model for spherical particles of constant size was developed by Yagi and Kunii Paor [7], which consists of five phases. In cement hydration reactions only three of them occur: 1) Diffusion of water on the solid particles forming a thin film around the particle; 2) Diffusion and penetration of water through the reaction products on the surface of the particle; 3) reaction of water with the solid. The other two stages occur when the reaction products are in gaseous phase, but in this case we only have solid products. The reaction rate can be determined by any of these stages, so it is important to identify which of these control the process.

Stoichiometry of the chemical reaction in the hydration of cement: The cement phases generating hydration products upon contact with water that give early and subsequent compressive strength, and also generate most of the heat of reaction are:

3CaO SiO_2 (C_3S), 2CaO SiO_2 (C_2S) and 3CaO · Al_2O_3 (C_3A). Furthermore, these reagents comprise more than 80% of non-hydrated cement, and react according to the following stoichiometric equations:

$$2(3CaO{\cdot}SiO_2)+7H_2O=3CaO{\cdot}SiO_2{\cdot}3H_2O+3Ca(OH)_2 \quad (1)$$

$$2(2CaO{\cdot}SiO_2)+5H_2O=3CaO{\cdot}SiO_2{\cdot}3H_2O+Ca(OH)_2 \quad (2)$$

$$3CaO{\cdot}Al_2O_3+6H_2O=3CaO{\cdot}Al_2O_3{\cdot}6H_2O \quad (3)$$

Equations 1, 2 and 3 are modeled in the COMSOL Reaction Engineering Lab module to describe the disappearance of reactants and the appearance of hydrated products. This depends on the reaction stoichiometry and is described by Equation 4.

$$\frac{d(c_i V_r)}{dt} = V_r R_i \quad (4)$$

where c_i is the molar concentration of species i (mol/m^3), V_r is the reactor volume (m^3), t is time, and R_i is the rate of reaction (mol/m^3s), and i = C_3S, C_2S, C_3A, H, CSH, and C_3AH_6 COH. The above equation is a mass balance for each one of the species participating in the chemical reaction.

Note that this module does not model particle reaction, instead data related to reaction engineering and kinetics such as reaction time and heat generated as a function of time are obtained by considering that reactions are held in a $1m^3$ batch reactor, perfectly mixed at 300 K.

Reactants: Equation 4 gives the material balance for the reactants in the mixed reactor. In this case the balance has a negative sign because of the decrease in concentration of these reactants during the course of the reaction (Equations 5-8).

$$\frac{d(c_{C3S})}{dt} = -2r_1 \quad (5)$$

$$\frac{d(c_{C3A})}{dt} = -r_3 \quad (6)$$

$$\frac{d(c_{C2S})}{dt} = -2r_2 \quad (7)$$

$$\frac{d(c_H)}{dt} = -7r_1 - 5r_2 - 6r_3 \quad (8)$$

Products: The balance of products has a positive sign because of its formation within the stirred reactor during the hydration (Equations 9-11).

$$\frac{d(c_{CSH})}{dt} = r_1 + r_2 \quad (9)$$

$$\frac{d(c_{COH})}{dt} = 3r_1 + r_2 \quad (10)$$

$$\frac{d(c_{C3AH6})}{dt} = r_3 \quad (11)$$

The reaction time depends on the reaction constant, which in turn depends primarily on the process conditions. In this case, the reaction conditions depend on the temperature, which is taken into account by the Arrhenius equation and is calculated with the rate constant *k (*Equation 12).

$$k = AT^n \exp(\frac{E}{R_g T}) \quad (12)$$

where A denotes the frequency factor, n is the temperature exponent, E is the activation energy (J / mol) and R_g is the ideal gas constant, 8.314J / (mol K). The value of the frequency factor for the reaction of tricalcium aluminate is $A = 1x10^{-5}$ [4], the exponent of the temperature is zero for $n = 0$ and the activation energy for the three reactions are: $E = 100$ J/mol, 155 J/mol, and 88 J/mol, for $C_3$2, C_2S, and C_3A, respectively.

Once the rate constant is expressed as a function of temperature, the reaction rate is obtained as a function of the constant of reaction and concentration of the reactants. Equations 13-15 show that the reaction of C_3S is ninth order, c_C_3S is the concentration of tricalcium silicate and c_H_2O is the concentration of water. The concentration units are specified in moles. C_2S and C_3A reactions are seventh order.

$$r_1 = \text{kf\_1*c\_C}_3\text{S}^2\text{*c\_H}^7 \quad (13)$$

$$r_2 = \text{kf\_2*c\_C}_2\text{S}^2\text{*c\_H}^5 \quad (14)$$

$$r_3 = \text{kf\_3*c\_C}_3\text{A*c\_H}^6 \quad (15)$$

In order to get the heat of reaction, it is necessary to establish the thermochemical of the reaction, by calculating the reaction enthalpy from each of the reactions, obtained by subtracting the enthalpy of the less reactive products. Equation 16-18.

$$H_{reaccionC3S} = \text{-2h\_C3S + h\_CSH + 3h\_COH - 7h\_H} \quad (16)$$

$$H_{reaccionC2S} = \text{h\_CSH + h\_COH - 2h\_C2S - 5h\_H} \quad (17)$$

$$H_{reaccionC3A} = \text{-h\_C3A - 6h\_H + h\_C3AH6} \quad (18)$$

The maximum heat generated during these reactions is thus calculated. If negative, we refer to an exothermic reaction [7], which releases heat to the outside.

Then the heat generated is calculated and will depend on the reaction rate *r* of each chemical reaction and the concentration of each of the reactants. Heat generated by chemical reactions is expressed by equation 19.

$$Q = -V_r \sum_j H_j r_j \quad (19)$$

Substituting equations 16 to 18 in equation 19 would provide the heat generated by the reaction.

$$Q = -V_r \left(H_{reaccionC3S} r_1 + H_{reaccionC2S} r_2 + H_{reaccionC3A} r_3 \right) \quad (20)$$

2.2 Model geometry

Model geometry is shown in Figure 1. It consists of one cement particle having a 0.005 m diameter and surrounded by water in a closed system represented by a square of 0.01 m. Therefore, the domain Ω of the system is composed of two subdomains

(subdomain Ω1 for water and subdomain Ω2 for cement) and 4 external boundaries δΩ, 3 internal borders δΩ and 10 points $\delta^2\Omega$.

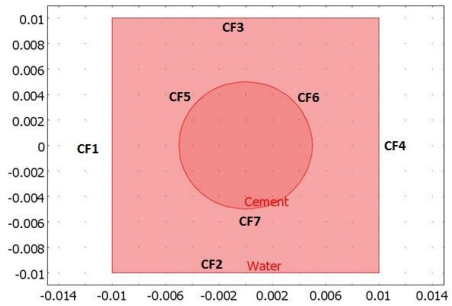

Fig. 1. Cement particle geometry.

The hydration chemical reactions of C_3S, C_2S and C_3A occur only in the domain of the particle.

2.3 Mass and energy balances

Mass transfer in the geometry shown in Figure 1 occurs primarily by diffusion of the species participating in the chemical reaction. The equation describing the transport of all species in the model is as follows (Equation 21):

$$\delta_{ts}\frac{\partial c_i}{\partial t}+\nabla\left(-D_i\nabla c_i\right)=R_j \tag{21}$$

where c is the concentration of species *i* participating in the reaction either as a product or as a reactant, D_i is the diffusion coefficient for each species i, and j is the reaction rate j = 1, 2 and 3 for C_3S, C_2S and C_3A, respectively. The process can be anisotropic and in this case, ***D*** has to be considered as a tensor. However this model only considers the medium as isotropic because of the domain size. In our model we have seven equations that correspond to the number of chemical species in the system domain.

Regarding the heat equation (Eq. 22), it is considered that the energy is transported mainly by conduction in both the domain of the particle and the domain of water.

$$\delta\rho C_p\frac{\partial T}{\partial t}+\nabla\left(-k\nabla T\right)=Q \tag{22}$$

where δ is a temporal scaling coefficient (dimensionless), ρ is the density of the cement paste and hardened cement kg/m^3, C_p is the specific heat capacity at constant pressure (J/kgK), k is the thermal conductivity (W/mK), and Q (W/m^3) contains the heat source due to the chemical reaction of C_3S, C_2S and C_3A, Eq. 20. The thermal conductivity may be anisotropic, however in this model it is considered to be isotropic in the direction of heat flow.

2.4 Equations of state

As a first approximation the diffusion coefficients in the cement paste were considered constant and are given in Table 1.

Table 1. Density and diffusion coefficient of the phases in the cement paste

Phase	Density (kg/m^3)	Diffusion coefficient (m/s^2)
C_3S	3150	$1X10^{-20}$
C_2S	3310	$1X10^{-20}$
C_3A	3030	$1X10^{-20}$
H	1000	$1X10^{-5}*(r_1+r_2+r_3)$
CSH	2350	$1X10^{-20}$
COH	2240	$1X10^{-20}$
C_3AH_6	2520	$1X10^{-20}$

Diffusion coefficient: The diffusion coefficients of the chemical species in the cement are from $1.0E^{-20}$ to $1.0E^{-5}$ m^2/s [6]. The diffusion coefficient of water in the domain is described as a function of reaction rates as shown in Table 1. The reaction rate decreases during the hydration process because the products such as CSH, COH and C_3AH_6 cover the cement particle surface and prevents water from penetrating and reaching the unreacted cement.

Thermal conductivity and specific heat: The thermal conductivity of concrete is considered constant, with a value of 3 W / (m · K) and densities of water and cement are 1000 kg/m^3 and 3000 kg/m^3 respectively. The heat capacity of water and cement are 4200 J/kgK and 2000 J/kg K, respectively.

2.5 Boundary and initial conditions

The system begins with initial conditions of a concentration of 6 mol/m^3 H_2O and a concentration of 3 mol/m^3 C_3S at a temperature of 300 K. In Figure 1 we show the geometry of the model, consisting of two subdomains, the domain of water and the domain of cement where reactions, heat and mass transport occur. In the domain of water heating only occurs by the release of energy from the particle.

Table 2. Initial conditions for subdomains

Phase	Initial concentration mol/m^3 ($\delta\Omega 1$)	Initial concentration mol/m^3 ($\delta\Omega 2$)
C_3S	0	3
C_2S	0	2
C_3A	0	1
H	6	0
CSH	0	0
COH	0	0
C_3AH_6	0	0

The initial concentrations in the two subdomains of the model are shown in Table 2. It can be observed that the concentrations of the products are zero at the start of the

reaction at time zero. The C_3S, C_2S, and C_3A contents for the cement used were calculated according to the Bogue equations [1].

The system has four internal and three external contours as shown in Figure 1. The boundary conditions of each of the diffusion equations for the species *i*, are expressed in equations 23 to 26 as follows:

External border conditions for species, i = C_3S, C_2S, C_3A, H_2O, CSH, COH and C_3AH_6 are insulated and no exchange of matter with the environment occurs. In Figure 1, these boundaries are marked as CF1, CF2, CF3 and CF4, and the conditions are expressed for each compound *i*, as follows.

$$\mathbf{n}\cdot\left(-D_i\nabla c_i\right)=0 \quad \text{Over } \delta\Omega 1 \tag{23}$$

For internal boundary conditions CF5, CF6 and CF7, boundary conditions depend on the concentration of reactants and products in the subdomain Ω1 (water) and in the subdomain Ω2 (cement). Because the concentrations are an extension of the interaction of the two domains is said to be a continuous boundary condition.

$$\mathbf{n}\cdot\left[\left(-D_i\nabla c_i\right)_{\Omega 1}-\left(-D_i\nabla c\right)_{\Omega 2}\right]=0 \quad \text{Over } \delta\Omega 2 \tag{24}$$

For the energy balance, boundary conditions are similar to the conditions used in the mass transport equations (23–24). The boundary conditions for exterior boundaries are thermal insulation and conditions for internal contours are continuous type boundary conditions, and they are given in equations 25 and 26.

$$\mathbf{n}\cdot\left(K\nabla T\right)=0 \quad \text{Over } \delta\Omega 1 \tag{25}$$

$$\mathbf{n}\cdot\left[\left(K\nabla T\right)_{\Omega 1}-\left(K\nabla T\right)_{\Omega 2}\right]=0 \quad \text{Over } \delta\Omega 2 \tag{26}$$

2.5 Solution

COMSOL Multiphysics 3.5a, which has methods based on finite element solution, was used to solve the partial differential equations system in the domain. The solution was obtained by the following steps [8, 9].

- Discretization of continuous media: The geometry was divided into 989 elements and set a time step of 1 s, and started from 0 to 1000s. The computation time was 54.84s
- Selecting an interpolation function: The preset interpolation function in Comsol Multiphysics 3.5a is a function for two-dimensional triangular quadratic polynomial represented by a LaGrange polynomial.

$$T=\alpha_1+\alpha_2 x+\alpha_3 y+\alpha_4 x^2+\alpha_5 y^2+\alpha_6 xy \tag{27}$$

- Establishing the mathematical formulation of the partial differential equations in matrix form.
- Assembling the basic equations for a system of simultaneous equations.

- Solving the system of equations: Using UMFPACK code incorporated into COMSOL Multiphysics 3.5a, which is the code for sparse nonlinear systems.
- Calculating secondary quantities such as space heat fluxes, space concentration fluxes, etc.

3 Simulation results from the hydration of a cement particle

3.1 Chemical reactions

We obtained the main reaction kinetics in the module Reaction Engineering Lab, shown in Figure 2. This plot shows the evolution of the concentration of reactants in a batch reactor of 1 m^3 of volume.

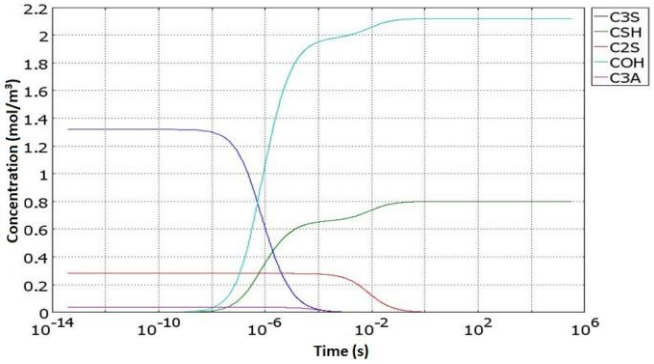

Fig. 2. Reaction kinetics of the species modeled in COMSOL Multiphysics 3.5a.

The graph shows the evolution of reactants C_3S, C_2S, C_3A and the products CSH, COH, and C_3AH_6. As can be observed the product formation does not contemplate the dormant period [10], because having the assumption of a continuous stirred reactor, products react within seconds when they reach the last part of kinetics. Generating calcium silicate hydrate and calcium hydroxide consists of two phases: first when it is generated due to the reaction of tricalcium silicate, and the second due to the reaction of dicalcium silicate. In water there are also different stages in the reaction kinetics (not shown in Figure 2.), which are the result of the C_3S, C_3A and C_2S reactions.

3.2 Evolution of reactants in the cement particle

We simulated the hydration reaction in a cement particle, from 0 s to 1000s, using the kinetic data obtained in the Reaction Engineering Lab Module, as mentioned above. Figure 3 shows that the concentration of reactants is high only in the core after 100 s (Figure 3 left) and is represented by red color. The concentration decreases with respect to time. In a time of 1000s the C_3S concentration in the core starts to decrease.

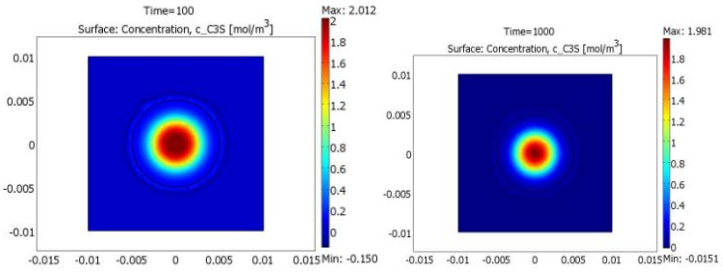

Fig. 3. Spatial evolution of the concentration of C_3S of during hydration of a particle (left 100s, 1000s right).

In the case of the reaction of C_2S, Figure 4, the reaction occurs slower due to the low activation energy involved in the chemical reaction.

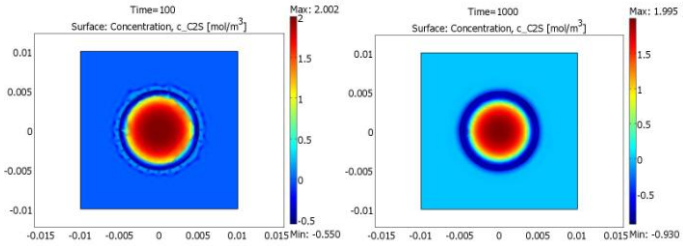

Fig. 4. Spatial evolution of the concentration of C_2S of during hydration of a particle (left 100s, 1000s right).

The C_3A is at lower concentration in the reactions, but the reaction rate in the particle is faster than the C_2S and C_3S reactions (Figure 5).

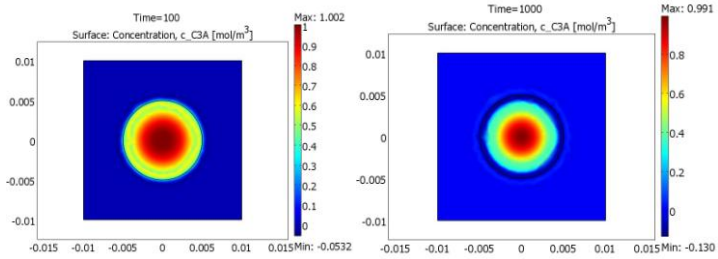

Fig. 5. Spatial evolution of the concentration of C_3A of during hydration of a particle (left 100s, 1000s right)

3.3 Evolution of products in the cement particle

Regarding the evolution of products, it can be observed that the calcium silicate hydrate increases the particle surface rapidly since it is occurring in two reactions of Equation 1 and Equation 2. Thus, molar concentration of CSH increases by the contribution of C_3S and C_2S reactions Figure 6.

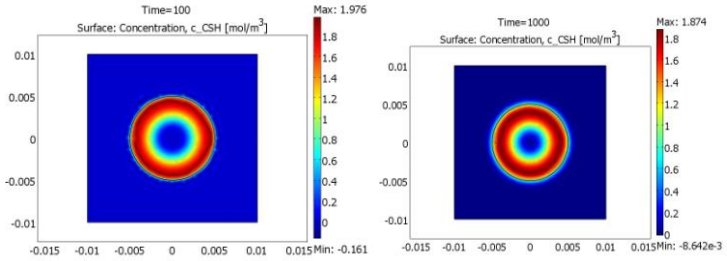

Fig. 6. Spatial evolution of the concentration of CSH of during hydration of a particle (left 100s, 1000s right).

The concentration of calcium hydroxide (COH) will increase twice compared to the concentration of calcium silicate hydrate Figure 7. However, this increase is only in concentration because the amount of calcium silicate hydrate is in higher proportion, since the molecular weight is much larger than C_3S.

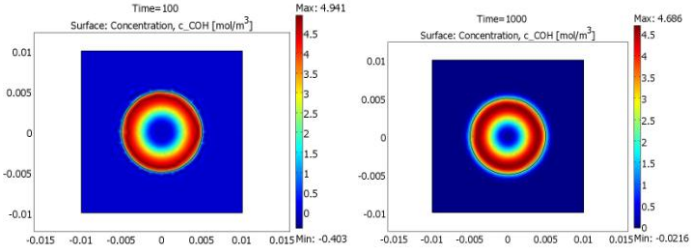

Fig. 7. Spatial evolution of the concentration of COH of during hydration of a particle (left 100s, 1000s right)

The concentration of tricalcium aluminate hydrated products C_3AH_6, Figure 8, will have a slow increase in the border of the particles, due to the low reactant concentration, and at 1000s just begins to react around the core.

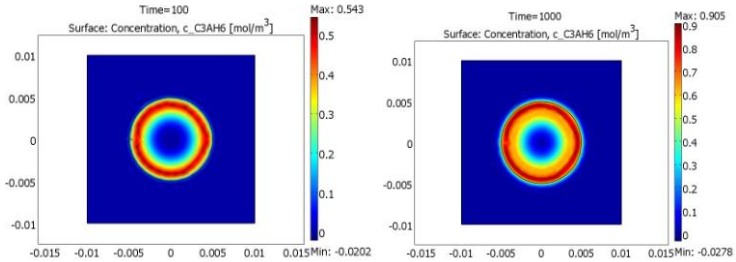

Fig. 8. Spatial evolution of the concentration of C_3AH_6 of during hydration of a particle (left 100s, 1000s right).

3.4 Temperature

Due to heat generation by the exothermic reactions at the surface of the particle, the water domain starts a heating period at approximately 100s. Figure 9 shows the

direction of heat flux (red lines). It is important to see that the heat flux is increased in the surface, as shown by larger arrows in the surface. These arrows are moved to the center, which indicates that heat flow after 1000s is mainly inside the particle.

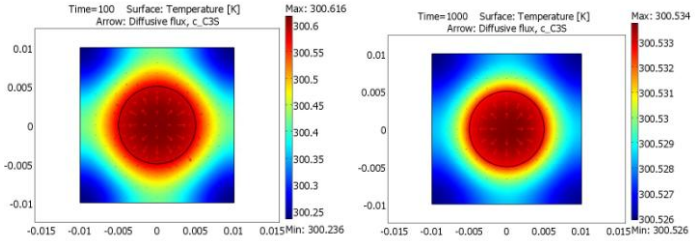

Fig. 9. Spatial evolution of the temperature and heat flow during hydration of a particle (left 100s, 1000s right)

Figure 10 shows the increase in temperature at different points of the radius of the particle, $1.25x10^{-3}$ $2.5\ x10^{-3}$ $3.7\ x10^{-3}$, at the surface 0.005m and at the water domain. It is observed that the temperature changes rapidly from 300 K to 301.2 K, due to heat generation on the surface. This flow of heat generated is conducted to the water, because of the continuity conditions shown in Equation 26. Since concrete is a self–heating material, the heat generation rate is much larger than the rate of heat loss at the boundaries. This happens due to the particular thermal conductivity and specific heat capacity, therefore heat generation occurs at the surface, where there is a loss of heat in the medium. The surface reaches 301.2 K ($5x10^{-3}$m), and as we approach the core, the temperature begins to decrease because the nucleus reactions have not been carried out or not completed ($1.25x10^{-3}$m).

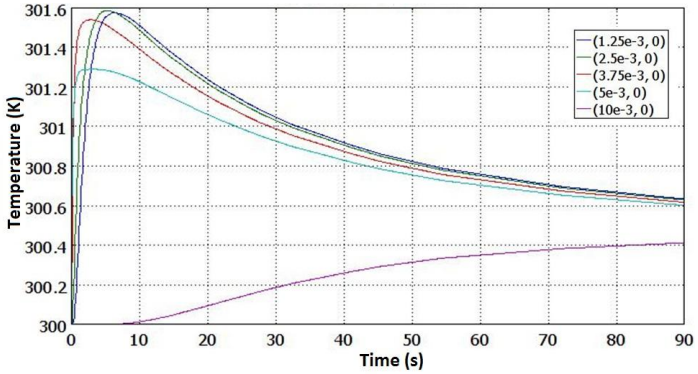

Fig. 10. Evolution of temperature during the time in four points on the radius of the particle.

Now if we compare the external boundary of the domain of water ($10x10^{-3}$), we see that there is a temperature increase. We should clarify that the heat transfer at the cement particle-water interface, and at the water domain the heat transfer occurs by conduction, so it is considered that there is no water movement (buoyancy effect)[11].

4 Conclusion

A model for hydration of a cement particle, transport of matter and energy has been developed based on an approximation of the continuous type. This model describes the hydration of a particle with a radius of 0.01m, which is surrounded by water.

The model describes the chemical reactions, evolution of heat, diffusion of chemical species in a circular geometry. The model involves the reaction of C_3S, C_2S, and C_3A.When considering these reactions a higher rate is shown, resulting in a rapid generation of heat, which propagates into the medium. The incorporation of the three species mainly contributes to the generation of CSH and COH, as C_3S and C_2S contributes to an increase in the generation of this products. In addition, the incorporation of the C_3A leads to increased heat generation.

Acknowledgments

Emilio Hernández Bautista acknowledges Conacyt for the PhD scholarship and to the Instituto Politecnico Nacional for the PIFI scholarship.

References

1. Mehta, P. K. , and Monteiro, P. J. M: Concrete Microestructure, properties, and Materials, Third Edit. New York USA (2006) p. 644.
2. Bentz, D. P.: CEMHYD3D: A Three-Dimensional Cement Hydration and Microstructure Development Modeling Package . Version 3 . 0, Nist (2005) p. 234.
3. Chen, W.: Hydration of slag cement Theory, Modeling and Application, (2006) p. 223.
4. Zhang, B. , and Yu, X. : Multiphysics for Early Stage Cement Hydration: Theoretical Framework. Advanced Materials Research (2011) p 4247.
5. Maekawa, K., and Ishida,: Multi-scale Modeling of Concrete Performance Integrated Material and Structural Mechanics. Journal of Advanced Concrete Technology (2003) p 670.
6. Bear, J., Cheng, H. D.: Modeling Groundwater Flow and Contaminant Transport. Springer (2010) p 834.
7. Levenspiel, O.: Ingenieria de las Reacciones Quìmicas. Limusa Wiley, third edition (2002) p. 638.
8. Baker, A. J. : Finite Elements Computational Engineering Sciences. Wiley, first edition (2012) p 873.
9. Battaglia, J.-L.: Heat Transfer in Materials Forming Processes. University of Bordeaux, France (2008), p. 358.
10. Smilauer, V., Krejci, T.: Multiscale model for temperature distribution in hydrating concrete. International Journal for Multiscale Computational Engineering (2009) p 135.
11. Tritt, T. M.: Thermal conductivity, First edition. United States (2005) p. 153.

Detección de Estacionalidad en Series de Tiempo

E. A. Santos-Camacho, J. G. Figueroa-Nazuno

Centro de Investigación en Computación (CIC)
araceli.libelula@gmail.com,jfn@cic.ipn.mx

Resumen. El análisis de series de tiempo tiene como objetivo investigar el comportamiento de una o más variables $t(x)$. Los ejemplos de su aplicación son muchos y muy variados como tasa de inflación, índice de precios, meteorología, contaminación, tasa de natalidad y el efecto de El Niño, por mencionar algunos. Usando técnicas modernas en el análisis de series de tempo se pueden detectar patrones en su comportamiento, pero en muchos casos una de las técnicas más usadas es la Transformada Rápida de Fourier (FFT por sus siglas en ingles); esta técnica es muy rígida y hace inadecuado su uso en series de tiempo naturales. En este trabajo se presenta una técnica que nos permite aportar un mayor conocimiento sobre la estacionalidad en los fenómenos naturales. Los resultados experimentales indican que la técnica de Lomb-Scargle es una alternativa para detectar estacionalidad empleando criterios matemáticos y estadísticos.

Palabras clave: Estacionalidad, serie de tiempo, periodograma Lomb-Scargle, Transformada Rápida de Fourier.

1 Introducción

Una forma de representar fenómenos naturales es mediante una serie numérica de tiempo, la cual puede verse como un conjunto de valores en forma consecutiva en el tiempo. Empleando diferentes técnicas de análisis de señales podemos describir el comportamiento del fenómeno a corto y mediano plazo. Sin embargo, es muy difícil determinar las diferentes características que pueden presentar [1] debido a que comúnmente las series de tiempo no presentan un muestreo regular y/o no son uniformes, lo cual genera problemas en la búsqueda de características, en especial la búsqueda de estacionalidad, limitando el uso de técnicas como FFT, ya que el uso de este tipo de técnicas son muy estrictas.

La estacionalidad es una característica o patrón repetitivo en los fenómenos y puede presentarse en períodos anuales, mensuales, semanales y otros diarios; pero en muchas ocasiones estos patrones se presentan en forma irregular para el mismo fenóme-

© E. A. Santos, J. C. Chimal, L. Cabrera, E. Castillo.
Advances in Computer Science and Engineering
Research in Computing Science 67, 2013 pp. 145–155
Paper Recived 02-09-2013 and Acepted 21-10-2013

no por lo que esto complica su estudio. Como una alternativa se ha propuesto la técnica de Lomb-Scargle (1976 y 1982), el cual es un método de estimación de espectro de frecuencias, sobre la base de mínimos cuadrados ajustando ondas sinusoides a muestras de datos, en donde se toma primero un retardo de tiempo τ, logrando obtener senusoides mutuamente ortogonales en tiempos de muestreo t_i, para obtener la mejor estimación en la frecuencia de poder [2,3], y posteriormente usar técnicas estadísticas, para la obtención de estacionalidad en series de tiempo.

2 Serie de tiempo

Una serie de tiempo, es un conjunto de datos numéricos obtenidos a partir de una observación experimental de algún sistema o mediante el cálculo numérico de ecuaciones, es decir, una serie de tiempo es un conjunto de tipo:

$$ST = \{x_1, x_2, \ldots\ldots, x_t, \ldots\ldots x_N\}$$

Una serie de tiempo por lo general consta de diferentes oscilaciones de valores, sin embargo, las series de tiempo naturales raramente tienen oscilaciones tan simples como las que se muestran en la figura 1, por lo que tienden a ser más complejas, como se muestra en la figura 2 [4].

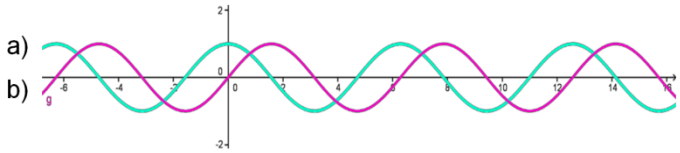

Fig. 1. Ejemplo de a) serie de tiempo seno y b) serie de tiempo coseno

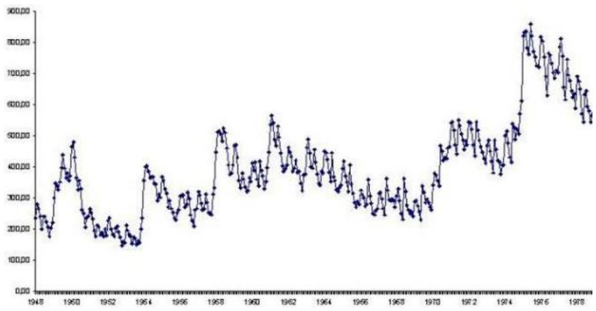

Fig. 2. Ejemplo de serie de tiempo natural.

3 Técnica lomb-scargle

Un método para extraer y evaluar una serie de tiempo periódica y obtener de forma significativa estacionalidad en el sentido estadístico con datos irregularmente espa-

ciados, es la técnica Lomb-Scargle [5], la cual evalúa los datos como senos y cosenos solo en el tiempo t_i que se está midiendo en ese momento, como se describe a continuación:

Dados N mediciones $h_i \equiv h(t_i)$ para $i = 0$ hasta $N - 1$, se puede calcular el periodograma mediante la ecuación (1) [6].

$$\boldsymbol{P_\omega(f)} = \frac{\mathbf{1}}{\mathbf{2\sigma^2}}\left\{\frac{\left[\sum(\boldsymbol{h_i}-\bar{\boldsymbol{h}})\boldsymbol{cos\omega(t_i-\tau)}\right]^2}{\sum \boldsymbol{cos^2\omega(t_i-\tau)}} + \frac{\left[\sum(\boldsymbol{h_i}-\bar{\boldsymbol{h}})\boldsymbol{sin\omega(t_i-\tau)}\right]^2}{\sum \boldsymbol{sin^2\omega(t_i-\tau)}}\right\} \quad (1)$$

donde $\bar{h} = \frac{1}{N}\sum_{i=0}^{N-1} h_i$, $\sigma^2 \equiv \frac{1}{N-1}\sum_{i=0}^{N-1}\left(h_i - \bar{h}\right)^2$, $\omega \equiv 2\pi f > 0$ y τ es definida por la relación $tan(2\omega\tau) = \frac{\sum sin2\omega t_j}{\sum cos2\omega t_j}$.

La distribución de probabilidad para datos aleatorios (no periódicos) es $exp(-P_\omega)$. Si $P \cong 3$, existe $\sim 5\%$ de probabilidad de que el componente sea aleatorio. Por otro lado si la prueba se realiza en muchas frecuencias, la probabilidad "máxima" aleatoria se expresa en la ecuación (2):

$$P_\omega \equiv 1 - (1 - e^{P_\omega})^M \quad (2)$$

Donde M es el número de frecuencias, $\sim 1.2x$ el número de observaciones.

3.1 Pseudocódigo

A continuación se presenta el pseudocódigo, para calcular estacionalidad estadística con la técnica de Lomb- Scargle para datos irregularmente espaciados:

Entradas: ***N*** (serie de tiempo), ***T*** (intervalos de tiempo), $\boldsymbol{hifac} \geq \mathbf{1}$ y $\boldsymbol{ofac} \geq \mathbf{4}$.

```
Inicio
   inicializar N ← longitud de h;
   inicializar m1 ← el máximo valor de t;
   inicializar m2 ←el mínimo valor de t;
   inicializar Suma ← 0;
   asignar T ← m1 - m2;
   para i=0 hasta N-1
      asignar suma ← suma + h(i);
   fin
   asignar media ← suma / N;
   asignar suma ← 0;
   para i=0 hasta N-1
      asignar suma ← suma + (h(i) - media) ^ 2;
   fin
```

asignar varianza ← suma / (N – 1);
asignar j ← 0;
para i←1/(T*ofac) hasta hifac*N/(2*T)), en incrementos de 1/(T*ofac)
asignar f[j] ← i;
asignar j ← j+1;
fin
para i←0 hasta longitude de f-1
asignar w[i] ← f[i] * 2 * $\boldsymbol{\pi}$;
fin
para i=0 hasta longitude de w-1
asignar tau[i]← $arcotang\ \left(\frac{\boldsymbol{seno}(\mathbf{2}*\boldsymbol{w}[\mathbf{1}]*\boldsymbol{t}[\mathbf{1}])}{\mathbf{2}*\boldsymbol{w}[\boldsymbol{i}]}\right),\left(\frac{\boldsymbol{coseno}(\mathbf{2}*\boldsymbol{w}[\mathbf{1}]*\boldsymbol{t}[\mathbf{1}])}{\mathbf{2}*\boldsymbol{w}[\boldsymbol{i}]}\right)$
fin
para i←0 hasta longitude de w -1
asignar Asin[i] ←$coseno\big(w[i]*t[i]-repmat(w[1]*tau[1],longitud\ de\ t)\big)$;
asignar Bcos[i]← $seno\big(w[i]*t[i]-repmat(w[1]*tau[1],longitud\ de\ t)\big)$;
fin
para
asignar P ← $sumar\big(Bcos*diagonal(h-mu)\big)$
fin
asignar M ←$(2*longitud\ de\ f)/ofac$
asignar prob← $M+exp(-P)$;
asignar inds ← prob>0.01;
asignar prob(inds)← $1-\big(1-exp\big(-P(inds)\big)\big)^{\wedge}M$;
Fin

4 Metodología

Dado las bases de datos con series de tempo naturales y artificiales se les aplica la técnica de Lomb-Scargle empleando la ecuación 1, para calcular el periodograma y posteriormente se hace el análisis estadístico, obteniendo como resultado dos graficas; en la figura 3, se presenta esta descripción de forma visual.

En la figura 4, se presenta una grafica en la cual el eje de las "x" representa la frecuencia. Para la figura izquierda se presenta la frecuencia de la serie de tiempo obtenida a partir de la técnica Lomb-Scargle. En la figura derecha el eje de las "y" representa el grado de significancia. En este ejemplo todas las frecuencias que sobrepasan el umbral de significancia marcado con el numero 1 en la grafica izquierda, se filtran para obtener la grafica derecha como se muestra en el numero 2.

1. Se obtiene el conjunto de datos.
2. Se aplica la ecuación (1) perteneciente a la técnica de Lomb-Scargle.
3. Se obtiene la estacionalidad estadística.

Nota. La significancia es un parámetro.

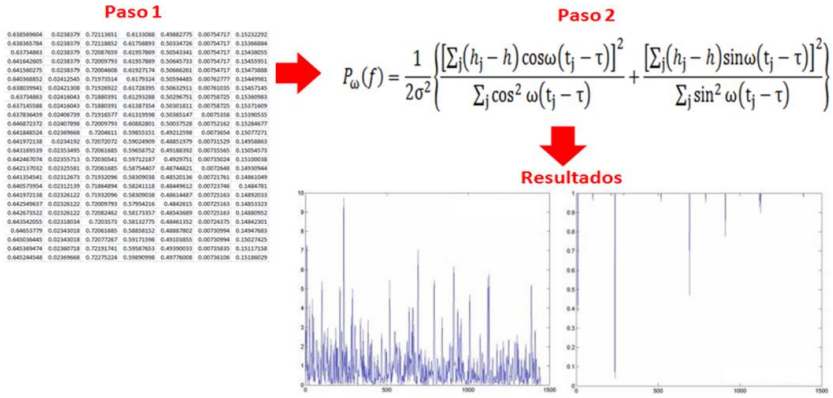

Fig. 3. Metodología para la extracción de estacionalidad empleando la técnica Lomb-Scargle.

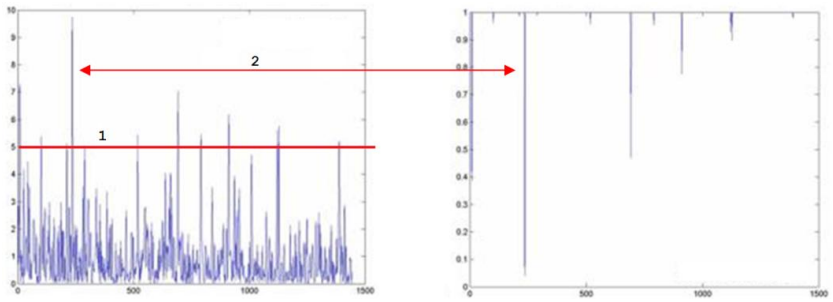

Fig. 4. En la parte izquierda se presenta la frecuencia obtenida a partir de una serie de tiempo, y en la parte derecha se presenta la frecuencia significativa, la cual sobrepasa el umbral marcado con la línea numero 1.

5 Conjuntos de datos

Para el análisis experimental se tomaron dos conjuntos de datos, el conjunto A contiene series de tiempo naturales, las cuales han sido muy estudiadas y se sabe que presentan estacionalidad [7]. El segundo conjunto B, contiene series artificiales en los cuales no se sabe si presentan o no estacionalidad.

5.1 Conjunto de datos A (datos naturales)

Para el análisis experimental con series naturales, se tomaron los datos de 8 índices de teleconexión [8, 9], cuyas mediciones fueron tomadas desde 1950 hasta 2010, para cada uno. A estos datos se les realizó una transformación lineal [10]. En la tabla 1, se muestran las siglas utilizadas para identificar los en la descripción de resultados.

Table 1. Índices de teleconexión.

Siglas	Índices de teleconexión	Siglas	Índices de teleconexión
NOA	North Atlantic Pattern	PNA	Pacific North American Pattern
EA	East Pacific Pattern	EA/WR	East Atlantic/West Russia Pattern
WP	West Pasific Pattern	SCA	Scandinavia Pattern
EP/NP	East Pasific/North Pacifica Pattern	POL	Polar Eurasia Pattern

5.2 Conjunto de datos B (datos sintéticos)

Se tomaron 30 series de tiempo obtenidas a partir de ecuaciones y análisis experimental, en la tabla 2 se enlista el nombre de cada una de ellas.

Table 2. Series sintéticas.

Santa Fe	DownJones	HIVDNA	Logistic	Primos	Sine
SCII	ECG	HumanDNA	Lorenz	QP2	Star
BrownMotion	EEG	IKEDA	Lovaina	QP3	Tent
Cantor	El Niño	Kobe	Mackey-Glass	Rossier	Vaderpol
D1	Hennon	Laser	Plasma	S&P500	White Noise

6 Análisis experimental

A cada serie de tiempo de ambos conjuntos de datos se les aplicó la técnica de Lomb-Scargle y la FFT, para obtener el periodograma de cada una de ella, algunos de los resultados muestran a continuación.

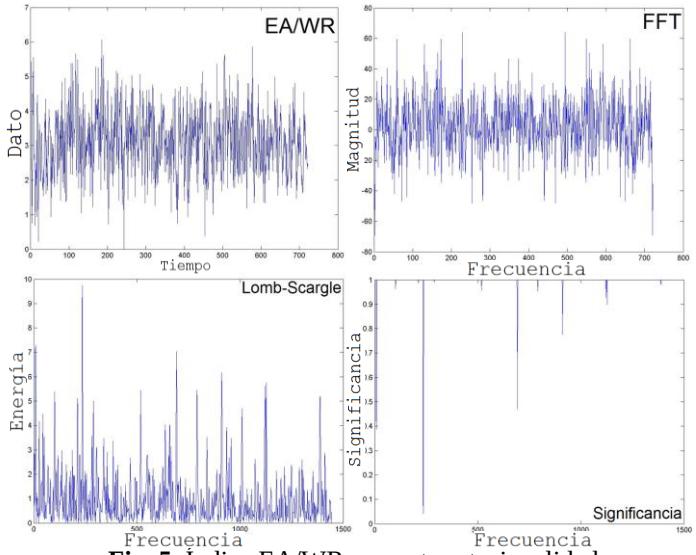

Fig. 5. Índice EA/WR presenta estacionalidad.

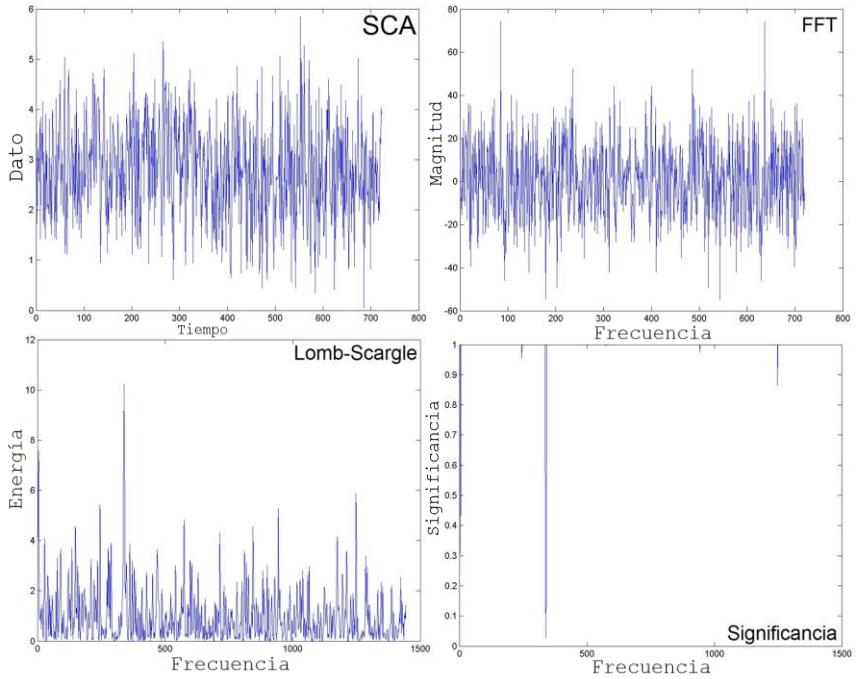

Fig. 6. Índice SCA, presenta estacionalidad.

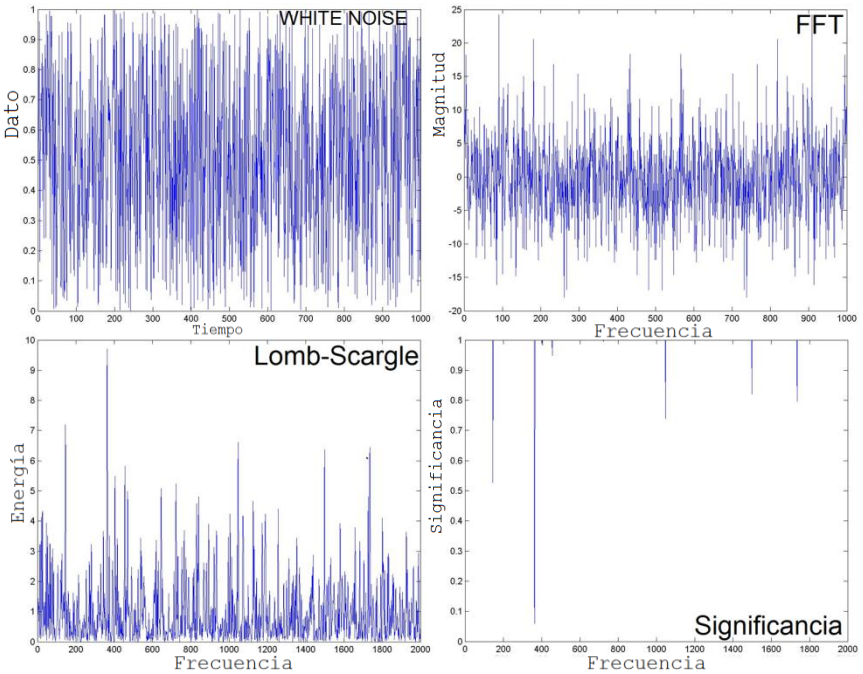

Fig. 7. Serie White Noise, presenta estacionalidad.

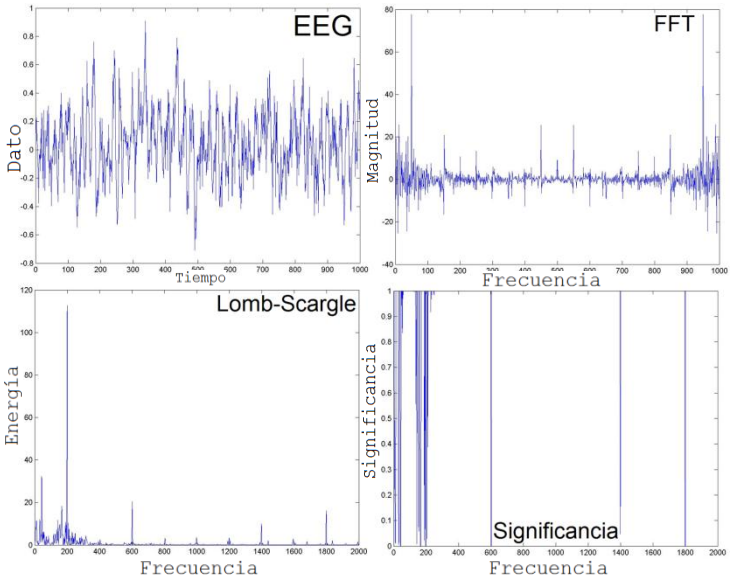

Fig. 8. Serie EEG, presenta estacionalidad.

Como se puede observar en los diferentes ejemplos mostrados en las figuras 4 - 8, las series presentan estacionalidad observada a través de la técnica de Lomb-Scargle, además de obtener la estacionalidad significativa. Por otra parte, las series de la figuras 9 y 10 para el conjunto de índices y el conjunto B respectivamente no presentan estacionalidad, por lo que el comportamiento que presentan las series de tiempo es complejo.

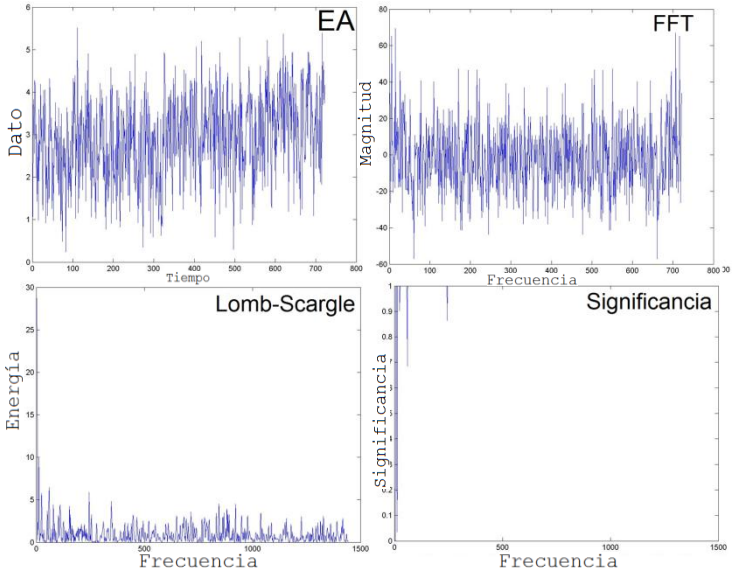

Fig. 9. Índice EA, no presenta estacionalidad.

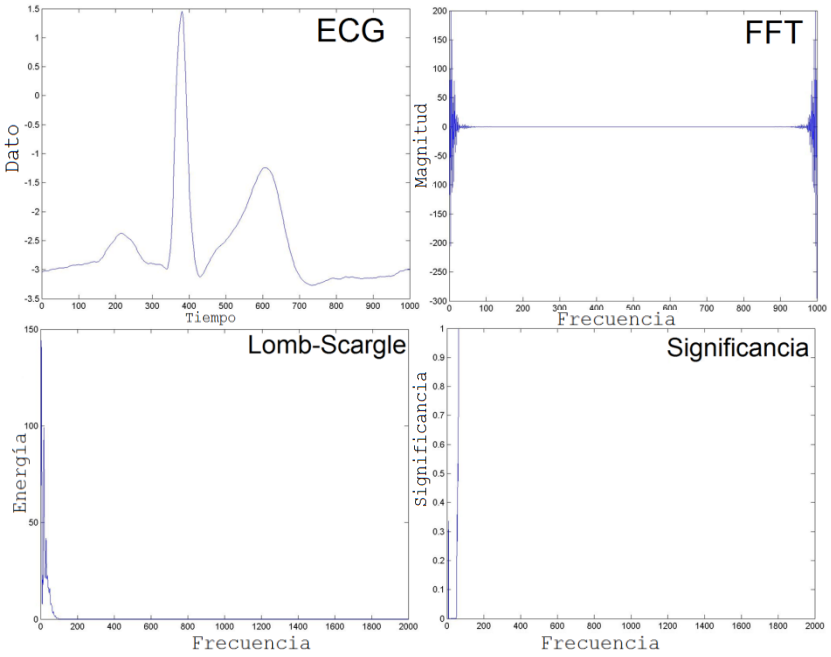

Fig. 10. Serie ECG, no presenta estacionalidad.

7 Conclusiones

Uno de los paradigmas que está latente y sigue siendo un reto en diferentes áreas es predecir fenómenos naturales, por lo que una forma de atacarlo es conociendo el comportamiento de las series de tiempo, actualmente una de las características más significativas es la estacionalidad, pero la mayor parte de las series presentan un grado de dispersión variable, es decir, se presenta el mismo fenómeno pero no con el mismo rango de tiempo por lo que al manifestarse de esta forma no es claro conocer su dinámica, sin embargo, existen técnicas que pueden mitigar esta condición.

En este trabajo se presento el análisis de series naturales y artificiales, en los que se presenta estacionalidad estadísticamente significativa, sin embargo, empleando la técnica FFT, no es claro detectarla como se puede observar en los diferentes ejemplos debido al funcionamiento de técnica de FFT, ya que para su análisis requiere que sean acotadas, infinitas, por mencionar algunas características y esto no es posible encontrarlo en series naturales, por lo que al aplicar FFT se puede llegar a tener resultados erróneos. Los resultados obtenidos muestran el potencial de la técnica Lonm-Scargle, para la obtención de estacionalidad en las series de tiempo natural y artificial, empleando métodos estadísticos que con otras técnicas no se puede hacer.

Referencias

1. E. F. Bautista Thompson, “Medición de la predictibilidad de series de tiempo: un estudio experimental, “Tesis de Doctorado en Ciencias de la Computación del Centro de Investigación en Computación del Instituto Politécnico Nacional, México, 2005.
2. Press, “Numerical Recipes”, Cambridge University Press, 3rd ed., 2007.
3. J. D. Scargle, "Studies in astronomical time series analysis. II – Statistical aspects of spectral analysis of unevenly spaced data", Astrophysical Journal 263: 835, 1982.
4. G. P. Weedon, "Time-Series Analysis and Cyclostratigraphy", Cambridge University Press, 2003.
5. R. H. D. Townsend, “Fast Calculation of the Lomb–Scargle Periodogram ysing Graphics Processing Units”, The Astrophysical Journal Supplement Series, 191:247– 253, The American Astronomical Society, 2010.
6. N. Lomb, “Least-Squares Frequency Analysis of Unqually Spaced Data”, Astrophysics and Space Science, 39:447-462, 1975.
7. E. Bautista-Thompson, E. Guzmán-Ramírez y J. Figueroa-Nazuno, "Predicción de Múltiples Puntos de Series de Tiempo Utilizando Support Vector Machines", Computación y Sistemas, vol. 7 No. 3 pp. 148-155, México 2004.
8. J. W. Hurrell, Y. Kushnir, G. Ottersen, M. Visbeck, “The North Atlantic Oscillation: climatic significance and environmental impact.”, Geophysical Monograph Series. Washington, DC: American Geophysical Union, 2003.
9. J. W. Hurrell, “Decadal trends in the North Atlantic Oscillation: regional temperatures and presipitation”, Science, vol. 169, pp. 676-679, 1995.
10. E. A. Santos-Camacho & J. Figueroa-Nazuno, “Clasificación de Series de Tiempo Mediante una Comparación Elástica”, Tesis que para obtener el grado de Licenciatura, Universidad Autónoma del Estado de México, 2012.

Voronoi Diagrams - a Survey

Netz Romero, Ricardo Barrón

Center for Computing Research of the National Polytechnic Institute, México
jromero_a13@sagitario.cic.ipn.mx, rbarron@cic.ipn.mx

Abstract. The Voronoi diagrams have had a considerable effect on different areas of interest for the development of engineering, geography, mathematics, systems and others. In this document we present a description from their beginnings, showing the formality of their properties, explaining construction algorithms and finally mentioning their relation with other technologies such as the parallel computing, the GPU's and other areas of interest. The Voronoi diagrams present a structure apparently simple at first glance that we may even observe in different phenomenon of the nature but it is important to understand the duality through other structure called Delaunay triangulation.

Keywords. Convex hull, delanuay triangulation, graphic processing unit, natural neighbor interpolation, voronoi diagrams.

1 Introduction

The human mind has forged space domination during the evolution of its being, for us it is important to understand and delimit spatial areas, either for knowledge of territorial areas, shorter searches for resources or even for the visual esthetics. Step by step, a great variety of cases with limited scope are being presented but with the passage of the time it calls the attention of specialists and results in different studies and applications until forming a research area.

The Voronoi diagrams help us to form an organized decomposition of a determined space and according to a set of point elements (Voronoi sites). This concept was used in order to provide one of the solutions for the Kaplan conjecture on the optimum packaging of spheres and Decartes employs it in the book Principles of Philosophy published in 1644 to apply the vortex theory to the functioning of the universe, where the stars would be the center of celestial vortices and at the same time the Sun would be one of them that would drag the planets through an invisible fluid. In the year of 1854 in London during a cholera outbreak, John Snow performed geographical methods in order to identify the origin of the epidemics, where the faucets represented the sites of a Voronoi diagram. However, formally those who introduce an adequate definition of this spatial structure are the mathematics Gustav Dirichlet and Georges Voronoi, who name them as Dirichlet tessellation [1] in 1850 and Voronoi diagrams [2] in 1908 respectively. Georges Voronoi discovers the duality of this structure when connecting two sites that have a common border, but it is Boris Delone in 1934 who defined this property as the Delaunay triangulation, employing the empty sphere method [3].

© E. A. Santos, J. C. Chimal, L. Cabrera, E. Castillo.
Advances in Computer Science and Engineering
Research in Computing Science 67, 2013 pp. 155–166
Paper Recived 02-09-2013 and Acepted 21-10-2013

The first applications go back to 1911 when Alfred Thiessen performs meteorological studies in the calculation of precipitations and in 1927 Paul Niggli reports research in crystallography. Subsequently until the present, the Voronoi diagrams and the Delanuay triangulation are employed in different areas, to mention some of them we have: astronomy, geometric calculation, construction of models, architectonic design, geology, meteorology, optimization, robotics and geographic information systems [4].

2 Definition and properties

2.1 Voronoi diagrams

We will express the Euclidean distance between two points as $p = (p_1, p_2, \dots, p_n)$ and $q = (q_1, q_2, \dots, q_n)$ as $dist(p, q)$, defined as

$$dist(p,q) = ((p_1 - q_1)^2 + (p_2 - q_2)^2 + \cdots + (p_n - q_n)^2)^{1/2} \quad (1)$$

The perpendicular line that divides the segment $\overline{pq}$ in two equal parts (perpendicular bisector) is expressed as $B(p, q)$ and defined as

$$B(p,q) = \{x \in \mathbb{R}^n \mid dist(x,p) = dist(x,q)\} \quad (2)$$

$P = \{p_1, p_2, \dots, p_m\}$ being a set of m different points on the plane (these points are called sites). We will define the Voronoi diagram of first order of P as a subdivision of the plane in m regions (see figure 1), where each region T_i is associated to a site p_i, such that any point T_i is close to p_i, the above mentioned is defined as:

$$T_i = \{x \in \mathbb{R}^n \mid dist(x,p_i) < dist(x,p_j), \forall\, i \neq j\} \quad (3)$$

The geometric structure of the diagram is formed by semi-circles and Voronoi vertices. Some important properties of the Voronoi diagram in two dimensions are listed below:

- A Voronoi edge is defined as a perpendicular bisector of the two closest sites p_i and p_j, see figure 2. The condition of the circle that contains two close sites and the edge that passes through its center should comply with the condition that no other site should be in its interior.
- A Voronoi vertex is the intersection of three edges of the diagram, the vertex also represents the center of a circle defined by three sites p_i, p_j and p_k, as long as the Voronoi diagram is regular or grade three, see figure 3. As condition of the circle generated by the three sites, it should not contain other sites in its interior.
- The regions formed by the diagram are convex polygons or non-enclosed regions.

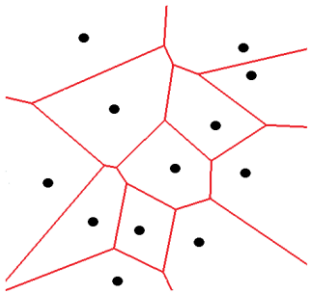

Fig. 1. Voronoi diagram in two dimensions.

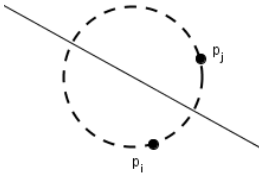

Fig. 2. Two sites.

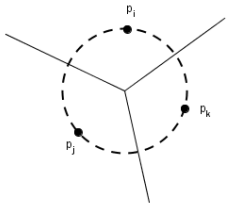

Fig. 3. Three sites.

2.2 Delaunay triangulation

The Delaunay triangulation is a graphic that presents the dual characteristic of the Voronoi diagram, it is only needed to unite the sites that share a common edge and complement with a convex cover where applicable. But to construct a Delaunay triangulation from the Voronoi diagram is costly which is why other techniques are used to generate it. In the figure 4 a triangulation is shown following the properties of the work of Boris Delone and the figure 5 shows the duality of both structures.

The Delaunay triangulation is used for the generation of nets, defining a method to connect an arbitrary set of points in a manner that they form a topologically valid set of triangles that does not intercept [5].

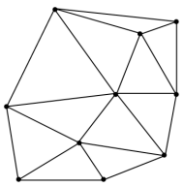

Fig. 4. Delaunay triangulation.

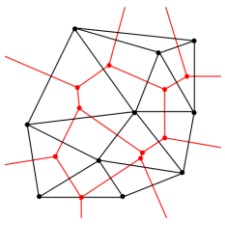

Fig. 5. The duality of both structures.

The main properties of the Delaunay triangulation in two dimensions are:

- For a set of points $P = \{p_1, p_2, \dots, p_m\}$, where D is a Delaunay triangulation of P if and only if no point P is in the interior of a circle formed by the circumscribed circumference of any triangle of D, see figure 6 and 7.
- A convex cover is formed in the border points of the Delaunay triangulation.
- A Delaunay triangulation is unique.

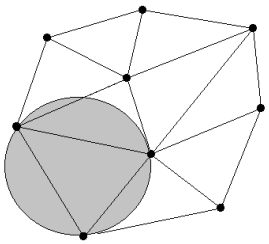

Fig. 6. Legal triangulation.

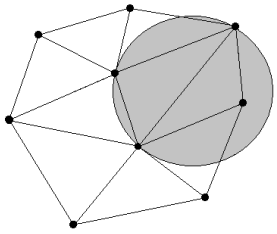

Fig. 7. Illegal triangulation.

3 Construction algorithms

Due to the extensiveness of the algorithms to generate the Voronoi diagrams the two most classic from its history will be mentioned and explained in a brief but concise manner.

3.1 Incremental algorithm

This algorithm can be considered as one of the simplest and most intuitive procedures, one of the first works where the incremental method is used in the Voronoi diagrams was studied by Green and Sibson [6]. The idea that implements the present algorithm consists in adding one site at a time from the set of point sites P (a complexity $O(n^2)$), the figure 8 illustrates an example of the addition of a new site to the Voronoi diagram, the shaded area indicates the space occupied by the added site. For each one of the insertions the diagram is modified and the problem resolved in iterative manner. The technique of natural neighbor interpolation introduced by Sibson will be used that makes reference to the use of the second order Voronoi diagram. The cloud of sites P is subdivided in regions called T_{ij}, and now each region T_{ij} defines the geometric place of the site p_i as the closest one and the site p_j as the second closest, this is presented in the following manner:

$$T_{ij} = \{x \in \mathbb{R}^n \mid dist(x, p_i) < dist(x, p_j) < dist(x, p_k), \forall\, i \neq j \neq k\} \qquad (4)$$

The inserted site will generate a new region which is why the Voronoi diagram will have to be modified; this new space is formed with perpendicular bisectors between the close neighbor sites and creates areas proportional to the recently created site.

Sibson established that the coordinates of a natural neighbor of a point x generate a weight that is proportional to each one of their natural neighbors, generating a section of T_{xi} region. The figure 9 establishes an example, the added point x generates the area understood as T_{x1} (shaded area) formed by the closed polygon for the site 1. We also observe in the figure 8 that x has four natural neighbors (sites 1, 2, 3 and 4) and each one generates a section of region around and within x, the sum of these regions corresponds to T_x (shaded area in the figure 8).

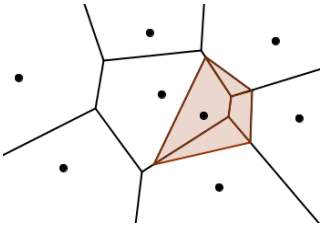

Fig. 8. A new site added.

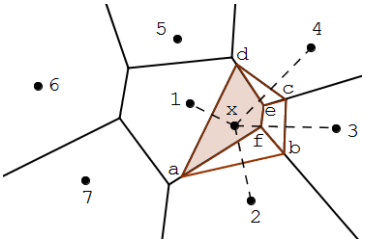

Fig. 9. There are four natural neighbours.

From other point of view, this method of insertion can be better implemented through its dual modality and it is called the incremental flipping algorithm. In the same manner, when a site is added, the triangulation should be reconstructed complying with the properties of the empty sphere. During the insertion a new net is generated around the new site, which is why the illegal edges have to be legalized and every new generated triangle is traversed, validating it with regards to its property of circumscribed circle. In the event that it does not comply we proceed to exchange the edge with the neighbor triangle, the procedure is illustrated in the figure 10.

Let us try to solve a real life problem, we have several post office locations in a city, see figure 11a (the small circles are the post offices). For each location we have the coordinates and we can represent them in a Euclidean space. Then the problem is visualize and find the closest post office to a given house by proximity. In the figure 11b the dots represent the post offices.

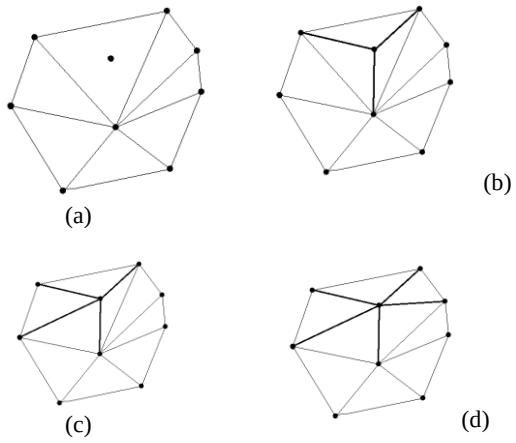

Fig. 10. a) Added a new point b) General triangulation c) First flip d) Second flip.

Now the postman must go out and make a delivery, but it would be wasteful if another post office is closer (we need a region optimal for the postman). The service region for a postman is a cell of Voronoi diagram. We know the algorithm to how construct a Voronoi diagram with a set of points in the plane. The figure 11c show us this construction and finally the figure 11d we can see the application about in the map.

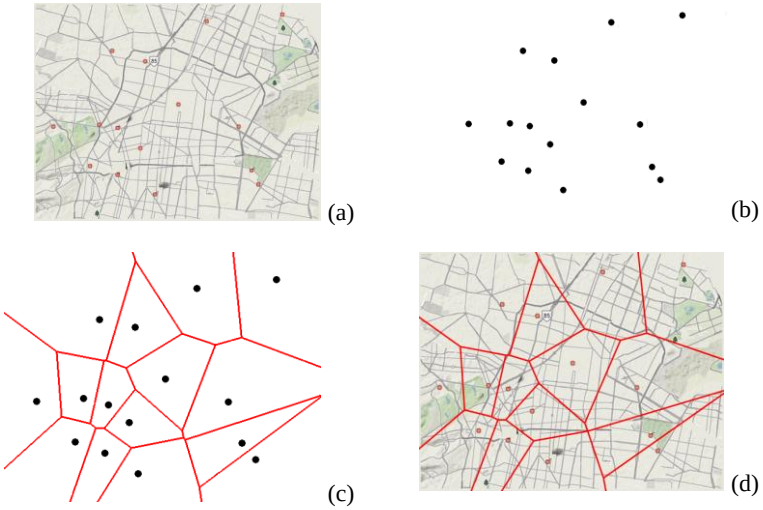

Fig. 11. a) Post offices in the map b) Sites represent the post offices c) Construction of Voronoi diagram d) Voronoi diagram in the map.

3.2 Divide and conquer algorithm

The method divide and conquer is one of the fundamental paradigms in the design of algorithms, where the idea is to divide the main problem in various simpler problems in order to subsequently find a solution based on them.

The first ones to use this technique were Shamos and Hoey [7] with a complexity O(n logn) to construct the Voronoi diagram with an optimum computer cost in the worst case scenario. The process starts with a subdivision of the set of sites of P, either horizontal or vertical, we will have two halves with approximately the same quantity of sites to which a convex hull is applied, see figure 12a. Subsequently the Voronoi diagram is constructed in a recursive manner for each subset of sites, see figure 12b.

The most important procedure is to construct a polygonal open line that would be dividing into two subsets where each straight segment represents a bisector between two points from different subsets, points that have the characteristic of forming part of the convex cover, they are border of the subsets to be united and form close neighbors. The straight segment changes trajectory each time that it intersects with a Voronoi diagram edge entering other region generated by other site and other bisector is constructed complying with the above mentioned characteristics, see figure 12c.

The Voronoi diagrams are constructed recursively in order to perform afterwards the corresponding unions of each pair of subsets until including all the sites of P.

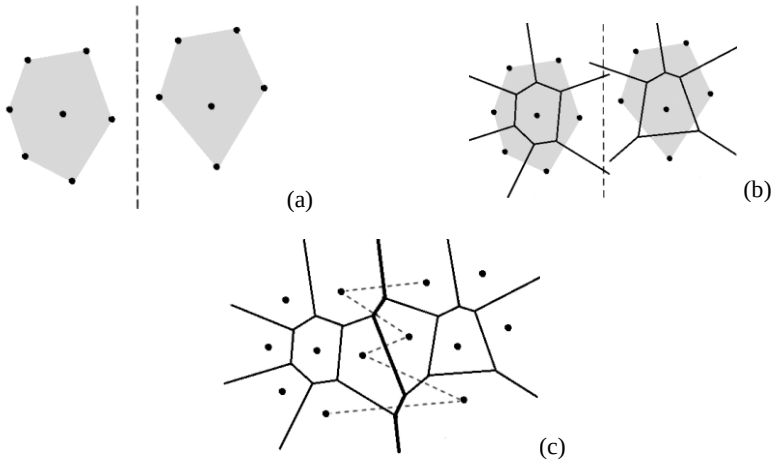

Fig. 12. Divide and conquer algorithm for Voronoi diagram.

The divide and conquer algorithm also applies to the Delaunay triangulation, in the same manner as to the Voronoi diagram, the set of points is divided in two subsets of the same size, each Delaunay triangulation is calculated separately and finally the two triangulations are united complying with the established criteria. This implementation was elaborated by Guibas and Stolfi [8], see figure 13.

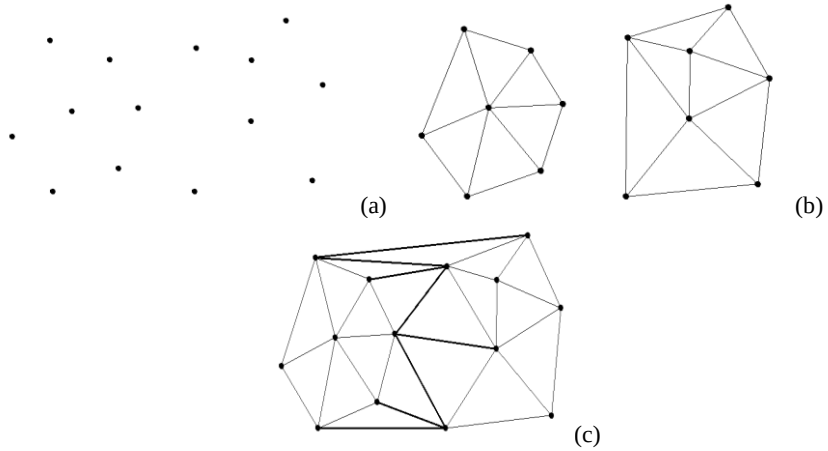

Fig. 13. Technique divide and conquer for Delaunay triangulation.

The above mentioned techniques were shown in a 2D space, even though many important applications in different disciplines require greater dimensionality, the Voronoi diagrams are also elaborated in a 3D environment. Deok-Soo Kim and his colleagues worked in 2005 on an algorithm for construction of the Voronoi diagrams

in an Euclidean space using spheres in 2D, the complexity of its algorithm is of O(m n) in the worst case scenario, where m is the number of the Voronoi diagram edges and n is the number of spheres [9].

4 Voronoi diagrams in other areas

4.1 Parallel computing in voronoi diagrams

In the applications of the Voronoi diagrams where multiple calculations or operations have to be performed in real time, the need has been observed to address the analysis, design and implementation of parallel algorithms. Sequential algorithms had been developed since 1975 for the geometric computing problems but since 1980 a noticeable contribution has been presented by Chown [10] in the parallel computing for geometric problems. The work performed by Aggarwal et al in 1985 should be noted [11], where they present an efficient parallel algorithm in order to construct the Voronoi diagrams among other geometric applications.

A parallel algorithm primarily needs parallel computing in order for different parts of the algorithm to be executed by various processors in simultaneous manner and to finally unite them to obtain the desired result. The technological progress has produced machines that have become more and more powerful and generally work with more than one processor; fortunately the cost of hardware is not so elevated, which allows for the parallel processing applications to be used with greater frequency. A technology has been introduced recently that releases the load of operations of the central processing unit (CPU) and also the memory depending on the applications, these are sent to a graphic processing unit (GPU) that were used primarily for the use of videogames and graphic operations. Thanks to the great capacity of operations that the GPU's are able to perform, due to the considerable quantity of processors that they contain, they have been employed in different areas of science and engineering to accelerate the involved calculations. The concept of construction of the Voronoi diagram used with GPU was employed by Rong and Zhan Yuan in the works [12] y [13].

4.2 Parallel algorithm

The divide-and-conquer is a variant of the more general top-down programming strategy and is one of the first optimal solution allowing for efficient parallelization for constructing Voronoi diagram or the Delaunay triangulation. This structures have been proposed for computing in parallel in computational geometry. The technique divide-and-conquer try to work out a problem into two or more subproblems, every subproblem can be solve recursively in parallel. The crux is solved through a series of merges for every subproblem.

We going to speak about the Delaunay triangulation for use to give a parallelism with the divide-and-conquer strategy. In the figure 14 we appreciate the algorithm when the cloud of points is divided in two groups, every group is solve with a compute process independent (we can see the illustration of the procedure in the figure 13).

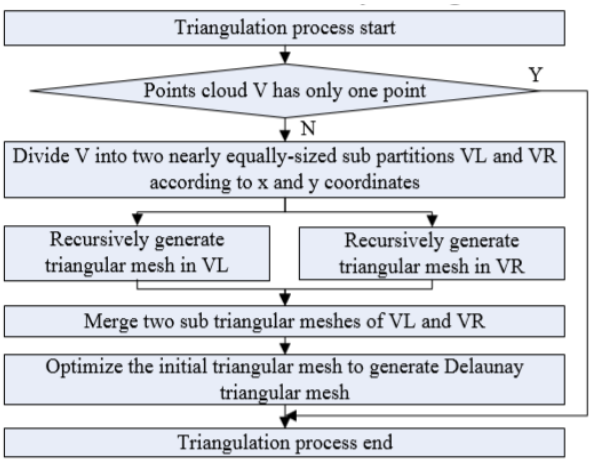

Fig. 14. Divide and conquer algorithm for Delaunay triangulation [14]

If we have computers with large numbers of process unit are capabilities to run multiple processes that solve everyone of block of triangulation, see figure 14 a and b. Merging the blocks is the critical step and this procedure can used parallel scheme for the merging phase, in the figure 13 b and c we can see the merger of two triangulation.

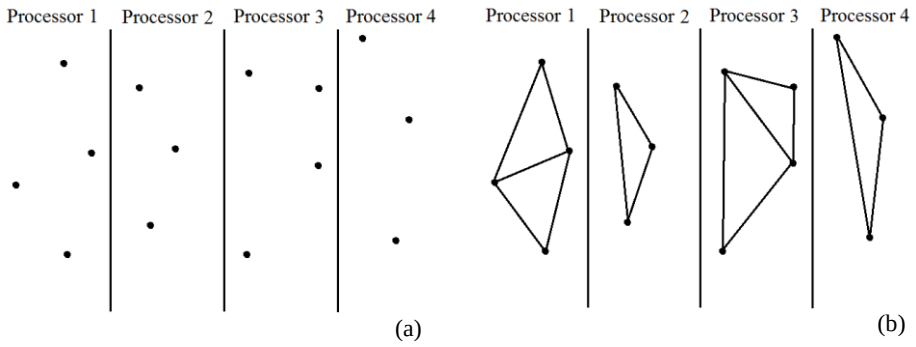

Fig. 15. A set of point going to be worked for four processors.

4.3 Voronoi diagrams and other applications

In the robotics area we have various applications such as the planning of routes of robot using Voronoi diagrams or when the robot should move avoiding collisions, which is why the trajectory of the robot should be designed. In 2007 Bhattacharya and Gavrilova worked on the planning of optimum routes using Voronoi diagrams [15]. Working with the same idea of the robots, M. Gold in 2006 proposes the use in the field of the GIS (Geographic Information Systems from its English initials) in order to

avoid collisions with geographic accidents [16]. Within the GIS, the number of applications is considerable when trying to adjust the Voronoi diagrams to the geographic characteristics of the different regions of the planet. The use of classifiers in pattern recognition using the Voronoi diagrams is employed in techniques of minimum distance or the closest neighbor (that are non-parametrical rules for techniques), as used in the work of Narendra Ahuja [17]. This tool provides countless applications such as those used in image recognition and an example is the one used by Abbas Cheddad in order to obtain the extraction of characteristics of human face [18].

5 Conclusions

The Voronoi diagram is a fundamental structure in many applications of technology and is relatively simple concept with a wide gamma of applications in science and engineering. We observe a promising future in Voronoi diagram applications, through unprecedented development when use computing parallel and graphic processing unit.

Acknowledgements

This work was realized with support of CONACyT, SIP-IPN and COFAA-IPN.

References

1. Dirichlet, G.: Uber die Reduction der positiven quadratischen Formen mit drei unbestimmten ganzen Zahlen, Journal fur die reine und angewandte Mathematik 40, no. 3, 209-227 (1850).
2. Voronoi, G.: Nouvelles applications des parametres continus a la theorie des formes quadratiques, Journal fur die reine und angewandte Mathematik 134, no. 4, 198-287 (1908).
3. Delone , B. N.: Sur la sphere vide, Bulletin of the Academy of Sciences of the U. S. S. R., no. 6, 793-800 (1934).
4. http://www.voronoi.com
5. Cofre, R.: http://cybertesis.ubiobio.cl/tesis/2003/cofre_r/html/index-frames.html
6. Green, P. J., Sibson, R. R.: Computing Dirichlet tessellations in the plane. Comput. J., 21:168–173 (1978).
7. Shamos, M. I., Hoey, D.: Closest-point problems. In Proc. 16th Annu. IEEE Sympos. Found. Comput. Sci., pages 151–162 (1975).
8. Guibas, L. J., Stolfi, J.: Primitives for the manipulation of general subdivisions and the computation of Voronoi diagrams. ACM Trans. Graph., 4(2):74– 123, Apr. (1985).
9. Kim D., Cho Y., Kim D.: Euclidean Voronoi diagram of 3D balls and its computation via tracing edges, Computer-Aided Design, Vol. 37, No. 13, pp. 1412-1424, (2005).

10. Chow, A.: Parallel algorithms for geometric problems. Ph.D. Dissertation, Computer Science Department, University of Illinois at Urbana-Champaign, (1980).
11. Aggarwal, A., Chazelle, B., Guibas, L., O'Dunlaing, C., Yap, C. K.: Parallel computational geometry, Algorithmica 3, 293-327, preliminary version in FOCS 1985, pp. 468-477 (1988).
12. Rong, G., Tan, T.: Jump Flooding in GPU with Applications to Voronoi Diagram and Distance Transform, ACM Article. Bibliometrics Data, pp 109 - 116 (2006)
13. Yuan, Z., Rong, G., Guo, X.: Generalized Voronoi Diagram Computation on GPU, Eighth International Symposium on Voronoi Diagrams in Science and Engineering, pp 75 - 82, (2011).
14. Zhe, W., Sanhong, G., Lichun, L.,: A Parallel Delaunay Algorithm Applied in Lunar Rover Stereo Vision System, Proceedings of the 2nd International Conference on Computer Science and Electronics Engineering (2013).
15. Bhattacharya, P., Gavrilova, M.: Voronoi Diagram in Optimal Path Planning, ISVD 2007, IEEE Proceedings, pp. 38-47 (2007).
16. Gold, C. M.: What is GIS and what is not? Transactions in GIS, 10(4), (2006)
17. Narendra, Ahuja: Dot Pattern Processing Using Voronoi Neighborhoods, IEEE Transactions on Pattern Analysis and Machine Intelligence, vol. 4, no. 3, pp. 336-343 (1982).
18. Abbas, C., Dzulkifli, M., Azizah, M.: Exploiting Voronoi Diagram Properties in Face Segmentation and Features Extraction. Pattern Recognition 41 (12) 3842-3859, Elsevier Science (2008).

Review Committee
Comité revisor

Altamirano Álvaro
Argüelles Cruz Amadeo José
Bonilla Licea Daniel
Chimal Eguía Juan Carlos
Dean León Emmanuel Carlos
Delgado Hernández Julio Carlos
Díaz de León Santiago Juan Luis
Felipe Riverón Edgardo Manuel
Figueroa Nazuno Jesús Guillermo
Gelbukh Alexander
Guzmán Lugo José Giovanni
Iliac Huerta Trujillo
Landassuri Moreno Victor Manuel
Lazcano Salas Saul
Ledeneva Yulia
Martínez Luna Gilberto Lorenzo
Menchaca Méndez Rolando
Morales Escobar Saturnino Job
Moreno Armendáriz Marco Antonio
Moreno Ibarra Marco Antonio
Orantes Jiménez Sandra Dinora
Orozco Aguirre Héctor Rafael
Quintana López Maricela
Ramírez Amaro Karinne
Rendón Morales Elizabeth
Ricardo Barrón Fernández
Salinas Rosales Moisés
Sánchez Fernández Luis Pastor
Santos Camacho Evelia Araceli
Sidorov Grigori Olegovich
Sossa Azuela Juan Humberto
Suárez Guerra Sergio
Tamariz Flores Edna Iliana
Téllez Castillo Germán
Torrealba Meléndez Richard
Xicoténcatl Pérez Juan Manuel
Yáñez Márquez Cornelio

Impreso en los Talleres Gráficos
de la Dirección de Publicaciones
del Instituto Politécnico Nacional
Tresguerras 27, Centro Histórico, México, D.F.
noviembre de 2013
Printing 500 / Edición 500 ejemplares

www.ipn.mx
www.cic.ipn.mx

ISSN: 1870-4069